

***A novel core factor for unconventional
secretion in Ustilago maydis***

Inaugural-Dissertation

Zur Erlangung des Doktorgrades der
Mathematisch-Naturwissenschaftlichen Fakultät der
Heinrich-Heine-Universität Düsseldorf

vorgelegt von

Michèle Reindl

aus Königs Wusterhausen

Düsseldorf, Mai 2020

aus dem Institut für Mikrobiologie
der Heinrich-Heine-Universität Düsseldorf

Gedruckt mit der Genehmigung
der Mathematisch-Naturwissenschaftlichen Fakultät
der Heinrich-Heine-Universität Düsseldorf

Erstgutachter: Prof. Dr. Michael Feldbrügge

Zweitgutachter: Prof. Dr. Lutz Schmitt

Tag der mündlichen Prüfung: 19. Juni 2020

Eidesstattliche Erklärung

Hiermit versichere ich, Michèle Sophie Reindl, an Eides statt, dass ich die vorliegende Dissertation selbständig und ohne unzulässige fremde Hilfe unter Beachtung der „Grundsätze zur Sicherung der guten wissenschaftlichen Praxis an der Heinrich-Heine-Universität Düsseldorf“ erstellt worden ist. Die Dissertation wurde in ihrer jetzigen oder einer ähnlichen Form bei keiner anderen Hochschule eingereicht. Ich habe zuvor keine erfolglosen Promotionsversuche unternommen.

Ort, Datum

Unterschrift

Die Untersuchungen zur vorliegenden Arbeit wurden von April 2016 bis Januar 2020 in Düsseldorf an der Heinrich-Heine-Universität im Institut für Mikrobiologie unter der Betreuung von Herrn Prof. Dr. Michael Feldbrügge durchgeführt.

Teile dieser Arbeit wurden veröffentlicht in:

Reindl, M.; Hänsch, S.; Weidtkamp-Peters, S. und Schipper, K. (2019). A potential lock-type mechanism for unconventional secretion in fungi. *Int. J. Mol. Sci.* (20), 460; doi:10.3390/ijms20030460

Reindl*, M.; Stock*, J.; Hussnaetter, K.P.; Genc, A.; Brachmann, A. and Schipper, K. (submitted to *Frontiers in Microbiology*). A novel factor essential for unconventional secretion of chitinase Cts1.

*geteilte Erstautorenschaft

Weiterer wissenschaftlicher Beitrag:

Terfrüchte, M.; **Reindl, M.;** Jankowski, S.; Sarkari, P.; Feldbrügge, M. und Schipper, K. (2017). Applying unconventional secretion in *Ustilago maydis* for the export of functional nanobodies. *Int. J. Mol. Sci.* (18), 937; doi:10.3390/ijms18050937

Für Mama und Opa.

Summary

The secretion of proteins by the conventional machinery is described as the most abundant export process in eukaryotic cells. However, in the past years more and more examples have been described in literature in which proteins do not follow the classical ER-Golgi route. Among those, factors for cell survival, tumour markers and viral effector proteins have been identified. Hence, it is of great interest to unravel the cellular machineries involved in these secretory processes.

In yeast cells of the smut fungus *U. maydis* a novel lock-type mechanism for unconventional protein secretion has been identified. It was first described for the chitinase Cts1 which does not harbour an N-terminal signal peptide. In the late stage of cytokinesis, Cts1 is targeted into a compartment formed between mother and daughter cell. After the sequential formation of a primary septum by the mother and a secondary septum by the daughter cell, Cts1 is released from the so-called fragmentation zone. In a screening approach, the gene *umag_03776* and its corresponding gene product Jps1 was identified as a key player of the novel secretion process.

In this work, the protein Jps1 was initially characterized. Analyses revealed a strict dependency of Cts1 secretion on Jps1. Interestingly, Jps1 and Cts1 co-localize in the fragmentation zone, though Jps1 can already be detected at the future division zone during early stages of the cell cycle. Moreover, Jps1 is secreted unconventionally. According to predictions, orthologues of Jps1 are present in close relatives of *U. maydis*. However, neither functional domains nor other characteristics could be assigned yet. Studies of truncated Jps1 protein versions allowed to identify an N-terminally located domain, the so called Cts1 Localization Domain (CLD). The CLD is not only important for the localization and secretion of Cts1 but also for the intracellular targeting of Jps1 to the future division zone. Since the localization of the truncated protein version in the fragmentation zone was rescued by additional expression of a Jps1 full-length protein, a dimerization of Jps1 monomers was hypothesized. Biochemical analyses using size exclusion chromatography and multi angle light scattering verified dimerization and indicated the additional formation of higher oligomeric complexes. Additionally, lipid binding studies with giant unilamellar vesicles revealed affinity of Jps1 to the plasma membrane marker lipid phosphoinositol-(4,5)-

bisphosphate. This might represent a putative mechanism for the early localization of Jps1 to the zone of bud emerge.

Hence, results obtained in this thesis imply that Jps1 might resemble a membrane-associated anchoring factor involved in recruiting Cts1 to the zone of cell division and hence constitutes a core factor for unconventional secretion.

Zusammenfassung

Der Mechanismus der konventionellen Proteinsekretion wurde lange als der in eukaryotischen Zellen vorherrschende Sekretionsweg beschrieben. Jedoch häufen sich in den letzten Jahren die Beispiele an Proteinen, die die Zelle nicht über den klassischen ER-Golgi Weg verlassen. Darunter befinden sich wichtige Proteine wie Zellwachstumsfaktoren, Tumormarker, aber auch eine Reihe viraler Effektorproteine. Es ist daher von großem Interesse, die diversen Mechanismen dieser unkonventionellen Sekretionswege zu entschlüsseln.

Hefezellen des Brandpilzes *U. maydis* besitzen einen neuartigen unkonventionellen Sekretionsweg, der ähnlich einer Schleuse funktioniert. Die Chitinase Cts1 wurde als erstes Protein identifiziert, das diesen Sekretionsweg durchläuft. Cts1 besitzt kein konventionelles N-terminales Signalpeptid. Im späten Stadium der Cytokinese lokalisiert die Chitinase in einem Kompartiment zwischen Mutter- und Tochterzelle, der sogenannten Fragmentierungszone. Da Cts1 wahrscheinlich von dort freigesetzt wird und die begrenzenden Septen sequenziell von Mutter- und Tochterzelle eingezogen werden, ähnelt der Vorgang einem Schleusenmechanismus. Das Gen *umag_03776* und sein resultierendes Proteinprodukt Jps1 wurde in einem genetischen Screen als maßgebliche Komponente dieses neuartigen Sekretionsmechanismus identifiziert.

In der vorliegenden Arbeit wurde Jps1 initial charakterisiert. Analysen zeigten eine strikte Abhängigkeit der Cts1 Sekretion von Jps1. Interessanterweise ko-lokalisieren Jps1 und Cts1 in der Fragmentierungszone, Jps1 ist jedoch bereits in früheren Stadien des Zellzyklus im Knospungsbereich präsent. Darüber hinaus gelangt auch Jps1 über unkonventionelle Sekretion in das extrazelluläre Medium. Laut bioinformatischer Vorhersage, exprimieren nahverwandte Basidiomyceten ebenfalls Orthologe von Jps1. Jedoch besitzt keines der Proteine beschriebene funktionelle Domänen oder andere Merkmale, anhand derer man auf eine potenzielle Funktion schließen könnte. Die Untersuchung verschiedener Jps1-Verkürzungsvarianten ermöglichte die Identifizierung einer ersten Domäne am N-Terminus des Proteins, der sogenannten „Cts1-Lokalisierungsdomäne“. Diese ist nicht nur entscheidend für die Cts1 Lokalisierung und Sekretion, sondern auch für die intrazelluläre Rekrutierung von Jps1 zur zukünftigen Teilungszone. Da die Lokalisierung der verkürzten Jps1 Variante durch die zusätzliche Expression eines Volllängenproteins wiederhergestellt werden konnte,

wurde eine Dimerisierung angenommen. Biochemische Analysen mittels Größenausschlusschromatographie und „Multi Angle Light Scattering“ bestätigten die Dimerisierung von Jps1 und deuteten sogar auf die Bildung oligomerer Komplexe hin. Lipidbindestudien mit großen unilamellaren Vesikeln (GUV) zeigten eine Affinität von Jps1 zu dem Plasmamembran-spezifischen Markerlipid Phosphoinositol-(4,5)-bisphosphat und lieferten somit eine mögliche Erklärung für die frühe Rekrutierung und membranständige Lokalisierung von Jps1 in der Knospungszone.

Somit weisen die in dieser Arbeit gewonnenen Ergebnisse darauf hin, dass Jps1 ein Membran-assoziiertes Ankerprotein darstellen könnte, welches unter anderem Cts1 zur Zellteilungszone rekrutiert. Es stellt daher eine Kernkomponente der unkonventionellen Sekretion dar.

Abbreviations

Abbreviation	Meaning
(v/v)	volume per volume
(w/v)	weight per volume
μl	microliter
μM	micrometer
α	anti
aa	amino acid
Afu	arabinofuranosidase
Amp	ampicillin
BiP	binding immunoglobulin protein
BNP	blue native PAGE
bp	base pair
BSA	bovine serum albumin
Cbx	carboxin
CD	circular dichroism
CLD	Cts1 localization domain
CM	complete medium
COP	coat protein complex
C-terminal	carboxyterminal
DAB	3,3'-Diaminobenzidine
ddH ₂ O	double distilled water
DF	downstream flank
DHFR	dihydrofolate reductase
DIG	digoxigenin
DNA	desoxyribonucleic acid
et al.	and other
EtOH	ethanol
ER	endoplasmic reticulum
FGF-2	fibroblast growth factor 2
FITC	fluorescein
G418	geneticin

gDNA	genomic DNA
GEF	guanine exchange factor
eGfp	enhanced green fluorescent protein
Glc	glucose
Gus	β -glucuronidase
GUV	giant unilamellar vesicle
h	hour
HF	high fidelity
HA	hemagglutinin
His	histidin
HRP	horseradish peroxidase
Hyg	hygromycin
IL-1 β	interleukin-1-beta
IMAC	immobilized metal-chelate chromatography
Jps1	jammed in protein secretion screen 1
kb	kilobase
kDA	kilo dalton
M	molar (mol/l)
mA	milliampere
MALS	multi angle light scattering
MAPS	misfolding-associated protein secretion
mb	megabase
MeOH	methanol
mM	millimolar
mRNA	messenger RNA
mut	mutant
MUC	4-methylumbelliferyl- β -D-N, N', N''- triacetylchitotrioside
MUG	4-methylumbelliferyl- β -D-glucuronide
4-MU	4-methylumbelliferon
MVB	multi vesicular body
nm	nanometer
Nat	nourseothricin
NEB	New England Biolabs

nosT	nos terminator
N-terminal	aminoterminal
OD	optical density
PAGE	polyacrylamide gel electrophoresis
PBS	phosphate buffered saline
PCR	polymerase chain reaction
PS	primary septum
PtdInsP	phosphatidyl-inositol-phosphate
RFP	red fluorescent protein
RNA	ribonucleic acid
RRM	RNA recognition motif
RT	room temperature
SAXS	small angle X-ray scattering
SDS	sodium dodecyl sulfate
Sec	second
SEC	size exclusion chromatography
SHH	streptavidin-histidin-haemagglutinin
SP	signal peptide
SS	secondary septum
TBS	Tris buffered saline
TexRed	Texas red
U	unit (enzyme activity)
UF	upstream flank
UPR	unfolded protein response
UV	ultra violette
V	volt
WT	wild type
X-Gal	5-bromo-4-chloro-3-indolyl-beta-D-galactopyranosid
X-Gluc	5-bromo-4-chloro-3-indolyl-beta-D-glucuronic acid, cyclohexylammonium salt
YL	yeps light
Δ	deletion

Table of content

Summary	VI
Zusammenfassung	VIII
Abbreviations	X
1. Introduction	15
1.1 The smut fungus <i>Ustilago maydis</i>	15
1.2 Mechanisms of protein secretion in eukaryotic cells	17
1.3 Cytokinesis-dependent unconventional secretion in yeast-like cells of <i>U. maydis</i> ...	21
1.4 The machinery for cell polarization and cytokinesis in yeast cells of <i>U. maydis</i> and <i>S. cerevisiae</i>	25
1.5 Aim of this thesis	30
2. Results	31
2.1 <i>In silico</i> analysis of Jps1	31
2.1.1 Jps1 is conserved among basidiomycetes and does not harbour known domains or motifs	31
2.2 <i>In vivo</i> analysis of Jps1	32
2.2.1 Deletion of <i>jps1</i> does not alter growth or phenotype of yeast-like cells	32
2.2.2 Cts1 secretion and localization is impaired in absence of <i>jps1</i>	34
2.2.3 Jps1 and Cts1 co-localize during the late stage of cytokinesis	36
2.2.4 Jps1 is recruited to the zone of bud emerge during early cytokinesis	39
2.2.5 Applying the Gus reporter assay to analyse potential secretion of Jps1	40
2.2.6 N-terminal truncation of Jps1 impairs localization and unconventional secretion of Cts1	43
2.2.7 Jps1 ^{ΔCLD} does not localize to the fragmentation zone during late cytokinesis	47
2.2.8 Bioinformatic predictions suggest the formation of amphipathic helices by the CLD	50
2.3 <i>In vitro</i> analysis of Jps1	51
2.3.1 Biochemical analysis of Jps1	51
2.3.2 Recombinant Jps1 forms a homo dimer	51
2.3.3 Recombinant Jps1 ^{ΔCLD} forms a homo dimer	55
2.3.4 Blue Native PAGE confirms homo-dimerization of Jps1 and Jps1 ^{ΔCLD}	57
2.3.5 Jps1 binds to phosphatidyl-inositol-phosphates on lipid strips via the CLD domain	58
2.3.6 Jps1 binds PtdIns(4,5)P ₂ but not PtdIns(3,4,5)P ₃ containing GUVs	60
2.4 Interaction studies	63
2.4.1 Pull-down analysis of Jps1G from cell extracts identifies putative interaction partners	63
3. Discussion	65
3.1 Jps1 resembles a novel protein crucial for unconventional secretion of Cts1	65
3.2 Jps1 might resemble an accessory factor for cell polarization	66
3.3 The CLD is crucial for unconventional secretion but not for dimerization of Jps1	68
3.4 The CLD is involved in lipid binding of Jps1	69

3.5	The characteristics discovered for Jps1 reveal similarity to the annexin family	70
3.6	Conclusion and current model for unconventional secretion of Cts1	73
3.7	Future perspectives	75
4.	Material and Methods.....	78
4.1	Material.....	78
4.1.1	Chemicals.....	78
4.1.2	Media and solutions.....	78
4.1.3	Plasmids.....	86
4.1.4	<i>U. maydis</i> expression strains	90
4.1.5	<i>E. coli</i> expression strains	92
4.1.6	Enzymes.....	93
4.1.7	Kits and substrates for detection purposes	93
4.1.8	Bioinformatic tools and computer programs.....	94
4.2	Methods.....	96
4.2.1	Molecular biology methods	96
4.2.2	Microbiological methods for <i>E. coli</i>	103
4.2.3	Microbiological methods for <i>U. maydis</i>	105
4.2.4	Protein biochemical methods.....	108
4.2.5	Biochemical characterization of Jps1	117
4.2.6	Lipid biochemical methods.....	120
4.2.7	Microscopy	123
4.2.8	Determination of enzyme activities	124
4.2.9	Interactome studies	126
5.	Supplementary Material	127
	References	132
	Author contributions.....	147
	Danksagung	148

1. Introduction

1.1 The smut fungus *Ustilago maydis*

Ustilago maydis is a hemi-basidiomycete fungus causing corn-smut disease. Only infecting *Zea mays*, the fungus has a very narrow host range and is innocuous to humans (Bölker, 2001; White and Doebley, 1998). In the past decades *U. maydis* was established as a model organism for studies on cell biology and biotrophic development (Banuett et al., 2008; Bölker, 2001; Sánchez-Martínez and Pérez-Martín, 2001). The genome of *U. maydis* is fully sequenced and annotated (Kämper et al., 2006). Accompanied by a couple of established methods for targeted genome modifications, generation of new or improved strain variants is fast and handy (Brachmann et al., 2004; Terfrüchte et al., 2014).

U. maydis is a dimorphic fungus. The yeast-like state resembles its non-pathogenic growth form (Figure 1.1). Similar to *Saccharomyces cerevisiae*, cells divide by budding. In contrast, a morphological switch to its filamentous growth form is a prerequisite for plant infection and biotrophic development. Therefore, two yeast-like cells of compatible mating type need to mate on the plant cell surface (Bölker, 2001; Spellig et al., 1994; Szabó et al., 2002).

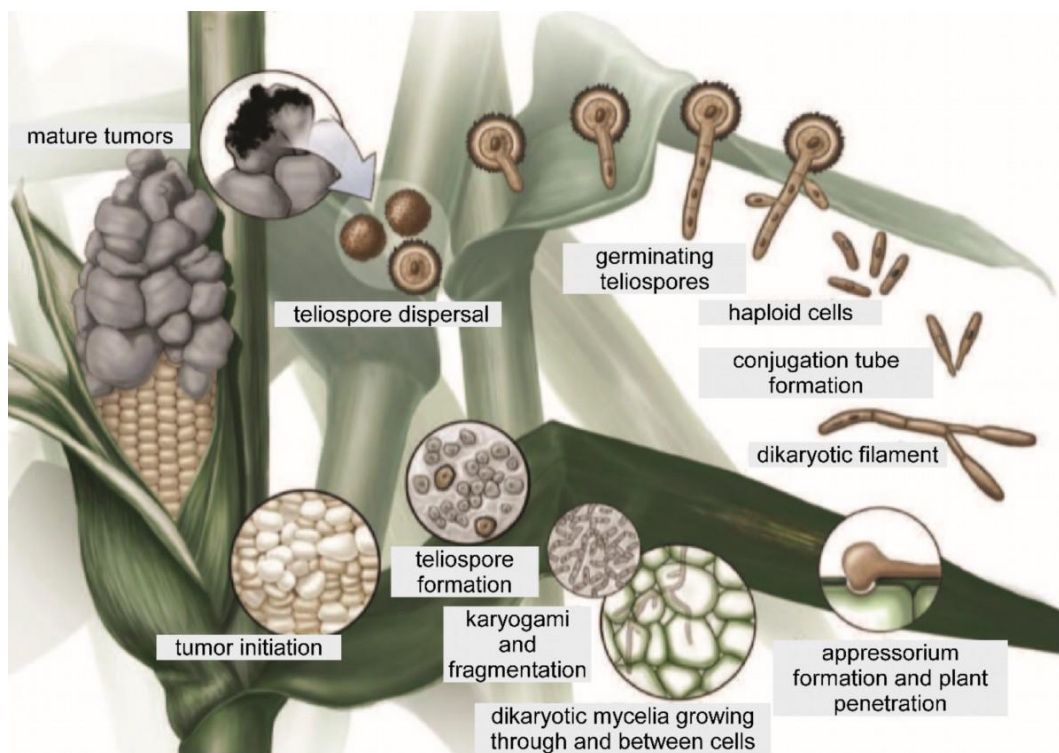


Figure 1.1: Lifecycle of *U. maydis*. If two haploid cells of different mating type recognize each other on the plant surface, conjugation tubes are formed along a pheromone gradient. Pheromones and pheromone receptors are encoded by the biallelic *a* locus. The conjugation tubes finally fuse at their extending tips. Plasmogamy leads to the formation of a dikaryotic filament and activation of the heterodimeric transcription factor *bE/bW* in cells with compatible *b* alleles. The transcription factor now initiates the expression of genes required for the pathogenic life phase of the fungus. Formation of an appressorium-like structure allows penetration of the plant and ongoing proliferation of the fungus within the plant tissue. The massive proliferation finally results in the formation of tumours and karyogamy. Diploid teliospores are released into the environment upon hyphal fragmentation, entering the saprotrophic phase of the life cycle. Modified from Saville et al., 2012.

A conserved pheromone/pheromone-receptor system, encoded by the biallelic *a*-locus (*a1/a2*), is crucial for recognition of the mating partners (Begerow et al., 2011; Casselton and Feldbrügge, 2010). Conjugation tubes are formed along a pheromone gradient finally resulting in plasmogamy and formation of a dikaryotic filament (Snetselaar et al., 1996). The mating process is only continued if also alleles of the partners *b*-loci are compatible. The multi-allelic *b*-locus (*b1-b20+*) encodes subunits of the heterodimeric transcription factor *bE/bW*. Successful formation of *bE/bW* is important for the transcription of genes involved in pathogenicity and biotrophic development (Kämper et al., 1995; Banuett, 1991; Schulz et al., 1990).

After mating the diploid filaments extend at their apical ends. Empty sections are inserted in regular intervals allowing a tip-directed migration of the cytoplasm (Lehmler et al., 1997; Steinberg et al., 1998). For plant penetration, an appressorium-like structure develops at the apical end of the filament. Ongoing proliferation of the fungus within the plant tissue is leading to tumour formation, followed by karyogamy. Diploid teliospores result from hyphal fragmentation inside the tumour structures. They are released into the environment to re-start the saprotrophic phase (Doehlemann et al., 2008; Feldbrügge et al., 2006; Vollmeister et al., 2012).

For research purposes, laboratory strains have been established forming filaments without prior mating. In the strain AB33 (Brachmann et al., 2004) a switch of the nitrogen source activates the *nar* promoter controlling transcription of *bE/bW*. Thus, filament formation can be induced in liquid culture or on plates. In addition, also the yeast-like form of AB33 is used for basic research and the preferred for biotechnological applications.

Besides fundamental research, *U. maydis* offers great biotechnological potential for the production of industrially-relevant products (Feldbrügge et al., 2013). During plant infection, the fungus produces a native repertoire of biomass-degrading enzymes. Uncoupling the production of these carbohydrate-active enzymes (CAZymes) from the

biotrophic phase allowed degradation of lignocellulose-derived substrates (e.g. cellulose, xylan) by the yeast form of the fungus and the concomitant synthesis of important platform chemicals like itaconic acid (Geiser et al., 2016). Additionally, co-expression of heterologous endo- and exo-polygalacturonases further extended the capability of *U. maydis* for the valorisation of pectin-rich biomass, a main side-stream of sugar production from sugar beet (Müller et al., 2018). Other secondary metabolites produced by *U. maydis* include mannosylerythritol- and cellobiose lipids which might serve as biosurfactants in industry (Feldbrügge et al., 2013). Additional biotechnological applications focus on the establishment of *U. maydis* as protein expression platform (Stock et al., 2012; Sarkari et al., 2014; Terfrüchte et al., 2018).

1.2 Mechanisms of protein secretion in eukaryotic cells

The majority of mRNAs coding for secreted proteins are translated by Endoplasmic Reticulum (ER)-resident ribosomes and get co-translationally imported into the lumen of the ER (Blobel and Dobberstein, 1981; Palade, 1975). The entry into the conventional secretion pathway is mediated by the encoded hydrophobic N-terminal signal peptide (SP). Its recognized by ER-resident signal recognition particles (SRPs) which bind to the hydrophobic SP of the nascent polypeptide chain. Next, the SP is cleaved by SP peptidases and the polypeptide is delivered to the heterodimeric Sec61 complex (Ast et al., 2013; Chirico et al., 1988). Sec61 is composed of three subunits: alpha, beta and gamma. They are forming an aqueous channel, allowing the passage of polypeptides into the ER-lumen (Deshaies et al., 1991; Rédei, 2008). Here, the pH is favourable for the formation of disulphide bridges between side chains of intramolecular cysteines. Moreover, readily folded proteins can be modified by *N*-glycosylation. The ER resembles a checkpoint for quality control. The best characterized quality control mechanisms are the unfolded protein response (UPR) and the ER-associated protein degradation (ERAD) (Bertolotti et al., 2000). Key player of the UPR is the Hsp70 protein BiP. Like a chaperone, BiP binds to hydrophobic regions within the protein to prevent aggregation of the polypeptide chain (Ellgaard and Ruddock, 2005). Furthermore, the protein disulphate isomerase (PDI) and calnexin support folding of the polypeptide chain thus inhibiting degradation by the ERAD machinery (Braakman and Bulleid, 2011; Tatu and Helenius, 1997). After being folded into a catalytically active state, proteins are translocated to the Golgi apparatus. Therefore, proteins need to be incorporated into vesicles that bud off from exit sites of

the ER. These vesicles are covered by the coat protein complex II (COPII) and allow the anterograde transport to the *cis*-face of the Golgi apparatus (Malkus et al., 2002). The compartments of the Golgi apparatus resemble layered cisternae, called Golgi stacks (Nakamura et al., 2012). Arriving secretory proteins are transported onwards vertically through the stack. Stack-resident enzymes further modify the proteins by attaching glycan residues (Guo et al., 2014; Stanley, 2011). When proteins approach the *trans*-Golgi site, they are sorted into trafficking intermediates. This allows further distribution into endosomes, secretory vesicles or to the plasma membrane (Witkos and Lowe, 2017).

In addition to this evolutionary strongly conserved mechanism, unconventional protein secretion is spread throughout eukaryotic organisms from protists to multicellular organisms. Proteins secreted unconventionally, do neither carry a SP at their very N- terminus, nor are they transported through the endomembrane system (Figure 1.2). Hence, proteins evade the ER quality control machinery and do not get post-translationally modified by *N*- or *O*-glycosylation. Especially avoiding the attachment of glycan-residues is beneficial for some proteins, since it might impair folding and activity. In the case of lectins like FGF-2, bypassing the ER seems to prohibit binding to glycoproteins within the ER lumen and thus, protein aggregation (Nickel, 2010). Interestingly, glycosylated and non-glycosylated forms of single protein can co-exist within the cell (Radisky et al., 2009). This seems to allow a double life with divergent functions as observed for Annexin A2. First it was described to function in intracellular vesicle trafficking and cytokinesis (Jacob et al., 2004). Later on, a function as cell surface receptor promoting angiogenesis could be attributed to the protein as well (Maji et al., 2017).

Currently described unconventional mechanisms for protein secretion comprise self-mediated translocation across the plasma membrane or export via ABC-transporters (Figure 1.2). Furthermore, proteins can hitchhike autophago- and autolysosomes to be transported to and across the membrane. Some of these proteins are inflicted with important cellular processes thereby contributing to cell survival and immune surveillance (Rabouille et al., 2012).

A prominent example for a self-mediated translocation mechanism is the fibroblast growth factor 2 (FGF-2) (Schäfer et al., 2004). FGF-2 is recruited to the plasma membrane by interaction with phosphoinositol (4,5) bisphosphate (PtdIns(4,5)P₂).

Pores in the lipid bilayer, formed by oligomerization of FGF-2, allow secretion of FGF-2 into the extracellular space where it interacts with heparan sulfate. Insertion into the membrane is stimulated upon phosphorylation by the membrane-resident Tec kinase (Ebert et al., 2010). Also, the yeast mating factor MAT α is recruited to the plasma membrane by PtdIns(4,5)P₂. In contrast to FGF-2, release into the extracellular space is dependent on the ABC transporter Ste6. Both FGF-2 and MAT α are secreted in their folded conformation (Ding et al., 2012; Schäfer et al., 2004).

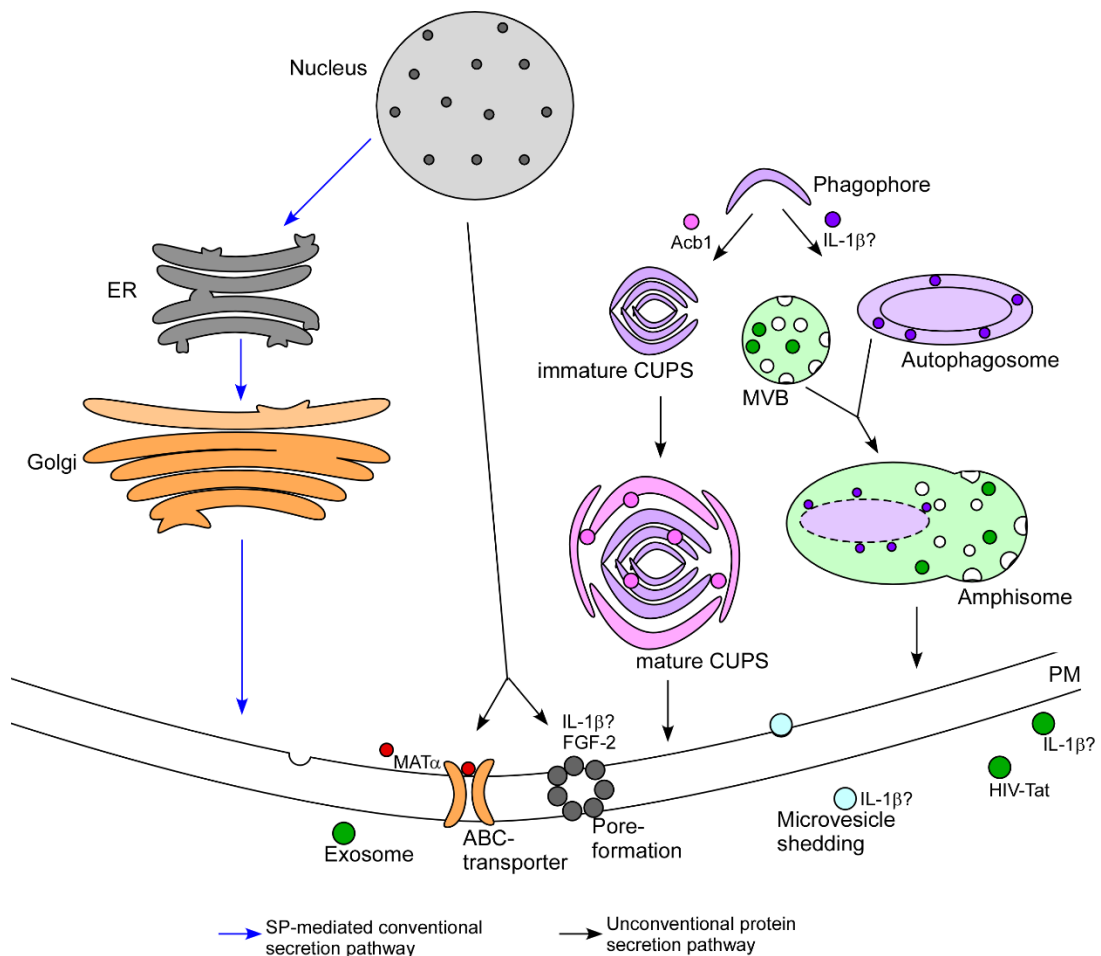


Figure 1.2: Conventional vs. unconventional secretion in eukaryotic cells. Conventional secretion of proteins is directed by an N-terminal SP. The SP mediates co-translational import into the ER where post-translational modifications take place. Readily folded proteins are incorporated into vesicles and further transported into the Golgi apparatus. Here, the proteins are modified and sorted into trafficking intermediates for their transport to the plasma membrane. By contrast, unconventional secretion pathways do not involve transport through the endomembrane system of ER and Golgi apparatus. Proteins can be secreted via vesicular and non-vesicular mechanisms. Secretion of Acb1 from *S. cerevisiae* is for example mediated by phagophore-derived CUPS, whereas the mating factor Mat α is translocated across the plasma membrane via ABC transporters. FGF-2 reaches the extracellular space by forming pores into the lipid bilayer of the membrane. For other proteins like IL-1 β the mechanism of unconventional secretion has not been resolved thoroughly. Translocation depending on the release of amphisomes, exosomes, microvesicles or pore formation in the lipid bilayer is currently debated. Adapted from Abrahamson and Stenmark (2010) and Curwin et al., (2016).

Among unconventional secretion pathways based on vesicular mechanisms, Acb1 from *S. cerevisiae* resembles a well-studied example. Unconventional secretion of Acb1 depends on the GRASP protein Grh1, autophagy-related proteins as well as the plasma membrane-specific t-SNARE Sso1 and components of the endosomal sorting complex required for transport (ESCRT)-machinery (Duran et al., 2010; Manjithaya et al., 2010). In addition, secretion of Acb1 requires the formation of compartments of unconventional secretion (CUPS) near the ER triggered by nitrogen starvation (Malhotra, 2013; Manjithaya et al., 2010). Phagophores seem to present the initial membranous structure which further develop into immature CUPS. The ESCRT-III component Snf7 stabilizes the CUPS and is needed for their development into functional, Acb1 containing, compartments. Supported by Sso1, CUPS can directly fuse with the plasma membrane and release Acb1 into the extracellular space (Curwin et al., 2016). A similar mechanism seems to apply for the secretion of interleukin-1 β (IL-1 β). Also here, a phagophore resembles the initial membranous stage which further develops into an IL-1 β -containing autophagosome. Triggered by pathogen- and disease-associated stimuli, the autophagosome can either directly target the plasma membrane or fuse with a multi-vesicular-body (MVB), forming an amphisome (Andrei et al., 1999; Zhang et al., 2015). However, the mode of IL-1 β secretion is currently still a matter of debate. Other potential mechanisms suggest the release of IL-1 β via exosomes (Dupont et al., 2011; Jiang et al., 2013) or shedding of microvesicles from the plasma membrane (Bianco et al., 2005; MacKenzie et al., 2001). Direct translocation across the membrane with concomitant death of the secreting cell was described additionally (Brough and Rothwell, 2007; Shirasaki et al., 2014). Pore-formation either by gasdermin-D, one major effector of pyroptosis, or self-mediated, comparable to FGF-2, are discussed as possible release mechanisms for IL-1 β (Brough et al., 2017).

Moreover, a couple of viral effector proteins are secreted by unconventional mechanisms. Among those, the trans-activator of transcription protein (Tat) from the human immunodeficiency virus-1 (HIV-1) has been identified. Tat is a small protein of 15 kDa responsible for the elongation of viral mRNA during the transcription process of viral long-terminal repeats (LTR) (Li et al., 2012; Rana and Jeang, 1999; Spector et al., 2019). Three different options for unconventional secretion of Tat are currently investigated. The first is similar to the self-mediated secretion of FGF-2, where Tat is recruited to the plasma membrane by interaction with PtdIns(4,5)P₂, followed by

oligomerization and pore formation. The interplay of two domains, rich in arginine and glutamine near the C-terminus of the protein, was found to be essential during this mode of translocation (Ciobanasu et al., 2010; Durzyńska and Goździcka-Józefiak, 2015). Of note, pore formation by Tat could be confirmed *in vivo* and *in vitro*. The second possible mechanism suggests the spontaneous translocation of Tat, again involving interaction with PtdIns(4,5)P₂ at the plasma membrane (Mele et al., 2018). The conserved residue W11 seems to provide membrane anchorage of Tat (Pantano and Carloni, 2005). pH-dependent conformational changes of Tat may finally drive its translocation across the membrane (Boll et al., 2011). However, a clear proof for the distinct separation from the oligomerization-mediated pore formation has yet to come. The third described mechanism involves incorporation and release of Tat by exosomes (Figure 1.2). Again, interaction with PtdIns(4,5)P₂ might target Tat to the sites of exosome formation (Yezid et al., 2009). Alternatively, Tat could be incorporated during formation of intraluminal vesicles in the cytosol, already (Kosaka et al., 2010; Muralidharan-Chari et al., 2010; Skog et al., 2008).

In *U. maydis*, analysing the apoplastic fluid of infected maize plants, allowed to identify multiple proteins which seem to be secreted unconventionally during the biotrophic phase. Among a total number of 143 detected proteins, 65 did not carry a conventional SP (Schipper, Brefort, Macek, Mann and Kahmann, unpublished). One candidate was the peroxisomal sterol carrier protein 2 (Scp2). Deletion mutants of *scp2* were impaired in plant penetration and showed an uneven distribution of peroxisomes in their cytoplasm (Krombach et al., 2018). Importantly, a fusion of a SP from the conventionally secreted effector protein Stp1 resulted in high amounts of secreted SP- Scp2 but was not able to complement the deletion phenotype of *scp2* (Krombach et al., 2018; Schipper, 2009). Thus, secretion of Scp2 via an unconventional pathway seems to be crucial for its localization to peroxisomes and its function as virulence factor during early stages of plant infection. A second proteomics approach identified the chitinase Cts1 as a target for unconventional secretion (Koepke et al., 2011).

1.3 Cytokinesis-dependent unconventional secretion in yeast-like cells of *U. maydis*

Cts1 belongs to the family of bacterial-like chitinases, harbouring a highly conserved Glyco-18 domain (Koepke et al, 2011). Interestingly, Cts1 activity can be detected on the cell surface of yeast-like cells and filaments, though lacking a SP for conventional

protein secretion. Importantly, two other chitinases of *U. maydis*, Cts2 and Cts3, carry SP and are thus likely secreted via the conventional pathway. Cts2, like Cts1, is produced during the yeast-like growth stage of the fungus. Both chitinases seem to have a redundant function since deletion of either gene does not impair growth or cell division. In contrast, a double deletion mutant shows severe defects in cytokinesis with branched and tree-like cell clusters (Langner et al., 2015).

To verify a secretory process allowing export of Cts1 from the cell without entering the ER, a reporter assay has been established. In this assay, the bacterial enzyme β -glucuronidase (Gus) serves as reporter protein being sensitive to *N*-glycosylation. Targeting Gus to the conventional pathway does not yield active protein in the culture supernatant. By contrast, using Cts1 as carrier, active Gus was co-exported into the supernatant of the *U. maydis* expression strain (Stock et al., 2012).

Microscopically analysis of a Cts1-eGfp fusion protein revealed accumulation of the chitinase in the fragmentation zone formed between mother and daughter cell during late cytokinesis (Figure 1.3, A) (Langner et al., 2015). Here, the chitinase is surrounded by plasma membrane and cell wall (Figure 1.3, C). Additionally, the fragmentation zone is enriched in Yup1-positive endosomes (Figure 1.3, D-E). Release of enclosed Cts1 into the extracellular space might be supported by weakening the cell wall through hydrolysis of the chitin portion (Langner et al., 2015; Reindl et al., 2019).

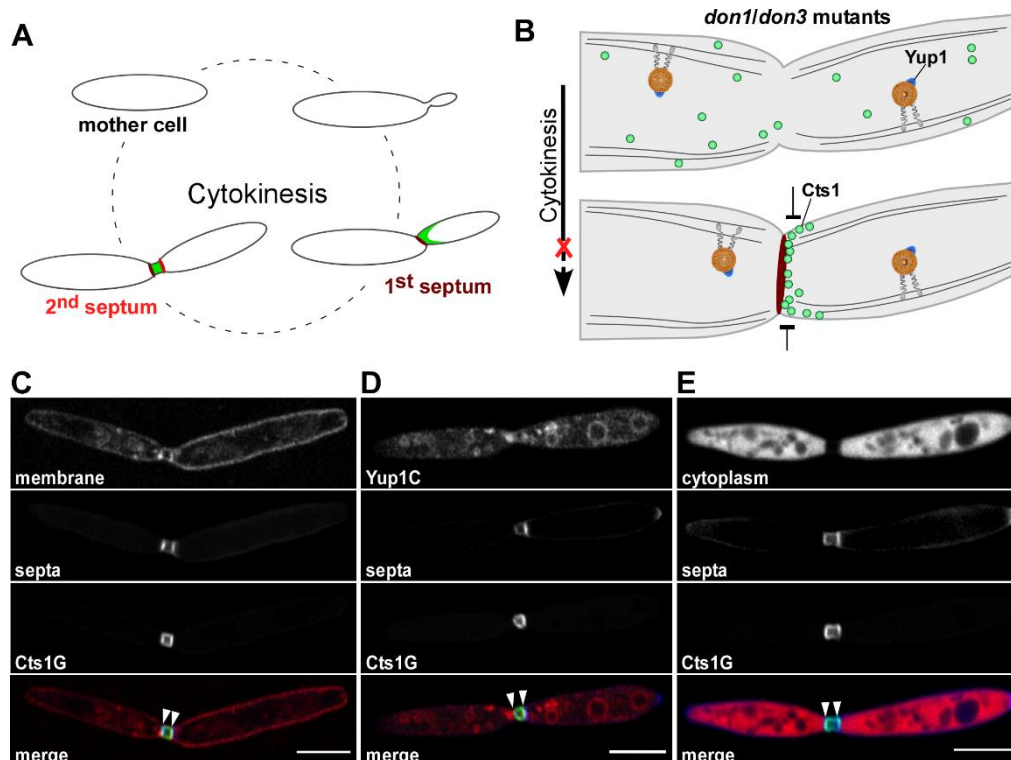


Figure 1.3: Cell cycle-dependent intracellular localization of chitinase Cts1. (A) During the late stage of cytokinesis, Cts1 (green) first localizes to the primary septum (violet) which is formed on the mother cell side. Upon formation of the secondary septum (red) by the daughter cell, Cts1 gets locked within the fragmentation zone. (B) In deletion mutants lacking the Ste20-like kinase Don3 or the Cdc42 GEF Don1, Cts1 (green circles) still localizes to the primary septum (violet). However, since deletion of either gene impairs formation of the secondary septum, secretion of Cts1 is abandoned. (C) Membrane staining using the lipophilic dye FM4-64. Cts1-eGfp localizes in the fragmentation zone which is surrounded by plasma membrane and cell wall. (D) The endosomal marker Yup1 was produced in fusion to mCherry. Cts1-eGfp co-localizes with Yup1-positive endosomes at the fragmentation zone. (E) A cytoplasmic version of mCherry served as cytoplasmic marker protein. No cytoplasmic mCherry signal can be observed in the fragmentation zone. Arrowheads mark the primary and secondary septum. Modified from Reindl et al., 2019.

In line with its localization, studies with the inhibitor hydroxyurea (HU) revealed a cell cycle dependant unconventional secretion of Cts1. HU inhibits DNA replication in the S-phase of the cell cycle, thus prevents the onset of mitosis and cell replication (Akerblom et al., 1981). After the addition of HU to the culture medium of the Gus-Cts1 reporter strain, Gus activity in the supernatant was compared to the activity of conventionally secreted arabinofuranosidase 2 (Afu2). Gus activity did not further increase after cell replication stopped, indicating a block of unconventional secretion. In contrast, the conventional secretion of Afu2 did not seem to be affected. Activity values were still slowly increasing over time (Aschenbroich et al., 2018).

Two factors influencing secretion of Cts1 indirectly are the germinal centre kinase Don3 and the guanine-exchange factor (GEF) Don1 (Aschenbroich et al., 2018; Langner, 2015; Weinzierl et al., 2002). Both proteins are essential for the formation of the secondary septum, a prerequisite for the physical separation of mother and daughter cell. Don3 belongs to the family of Ste20-like kinases and seems to be similar to the sporulation-specific protein Sps1 from *S. cerevisiae* (Friesen et al., 1994). Don1 specifically serves as GEF for the *U. maydis* GTPase homologue of yeast Cdc42. It harbours a FYVE domain for binding of PtdIns(3)P- containing early endosomes and a pleckstrin-homology (PH) domain to target the plasma membrane. Deletion of either gene does not only cause severe cell separation defects but also causes impaired secretion of Cts1 (Figure 1.3, B) (Aschenbroich et al., 2018; Weinzierl et al., 2002).

Albeit these first insights, the detailed mechanism of Cts1 translocation across the plasma membrane still needs to be resolved. To identify factors involved in this novel lock-type secretion process, a genetic screen based on UV-mutagenesis was designed (Reindl and Stock et al., 2020). A screening strain with special marker genes was generated to select mutants impaired in unconventional secretion after UV-mutagenesis. Three different marker genes were used to exclude false positive

candidates from the screen. Two marker genes consisting of *gus* and β -galactosidase (*lacZ*) fused to *cts1* were heterologously expressed by the strain. The resulting fusion Cts1-fusion proteins allowed export of Gus and LacZ by Cts1 via the unconventional pathway. Activity of both secreted enzymes could be analysed on selection plates containing the indicator substrates X-Gluc and X-Gal, respectively, resulting in colonies with a blue halo indicative for functional unconventional secretion (Figure 1.4, A). As a third marker, the extracellular activity of Cts1 served as read out for impaired or functional unconventional secretion. Only candidates without blue halos on both selection plates and with decreased extracellular Cts1 activity were considered for further analysis. Finally, whole genome sequencing of three selected mutant candidates revealed mutations within the open reading frame (ORF) of a single gene. Four independent single amino acid exchanges (Figure 1.4, B) leading to miss- and non-sense mutations (G335D; Q338STOP; W446STOP; W448STOP) led to impaired unconventional secretion of Cts1 (Reindl and Stock et al., 2020).

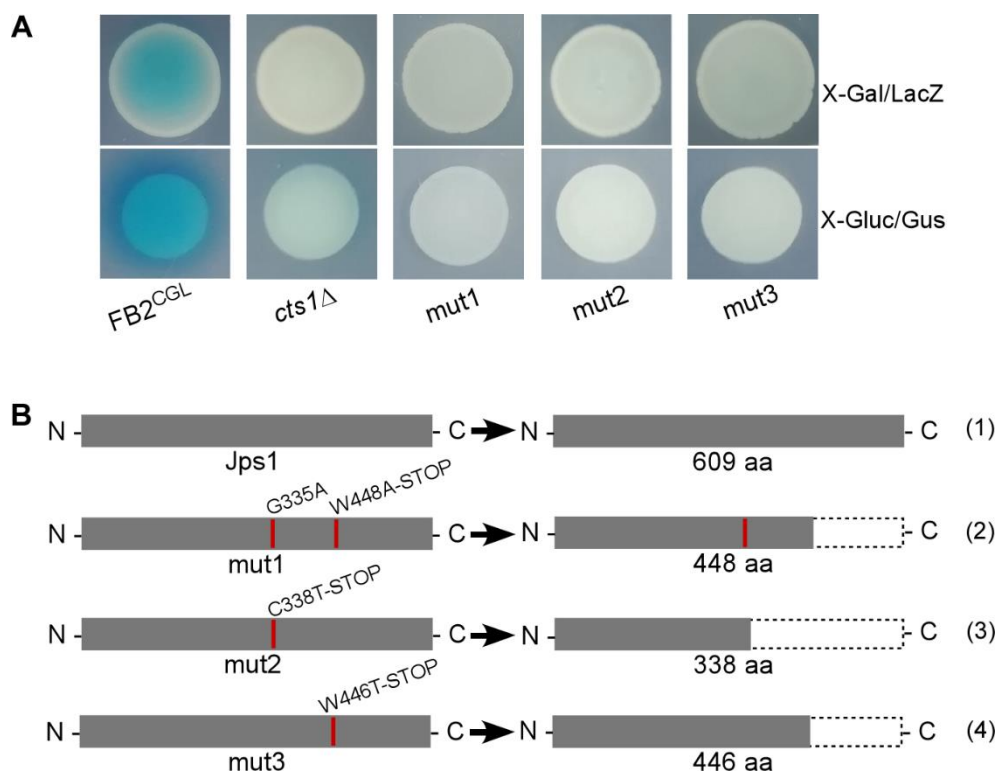


Figure 1.4: Identification of Jps1 as an essential factor for Cts1 secretion. (A) To identify mutant candidates of the marker strain impaired in unconventional secretion, X-Gluc and X-Gal containing indicator plates were used. Functional unconventional secretion of active Gus- and LacZ-Cts1 reporter constructs was indicated by colonies with blue halo. Candidates impaired in unconventional secretion showed no halo and were considered for further analysis. **(B)** Sequencing of mutants impaired in secretion of Cts1 revealed 4 independent mutations within the ORF of *umag_03776*. In contrast to the full-length protein product (1) (609 aa), the mutations lead to truncated protein versions with a length of 448 aa (mut1), 338 aa (mut2) and 446 aa (mut3), respectively. Modified from Reindl and Stock et al., 2020.

Since *umag_03776* encodes the first identified protein of the screen essential for Cts1 secretion, the corresponding protein was termed “Jammed in protein secretion screen1” (Jps1).

1.4 The machinery for cell polarization and cytokinesis in yeast cells of *U. maydis* and *S. cerevisiae*

In yeasts, the process of budding and cytokinesis is essential for reproduction. Determining the future zone of bud emerge goes in line with the establishment and maintenance of cell polarity (Pruyne and Bretscher, 2000). The processes involved are well studied in the yeast model organism *S. cerevisiae*. Several proteins were identified, sometimes belonging to multi-protein complexes. Interestingly, homologs to some of the yeast proteins are present in *U. maydis* (Banuett et al., 2008). However, only in some cases complete protein complexes seem to be conserved. On the one hand, this indicates a conservation of basic components for the establishment of polarity and the onset of budding between *S. cerevisiae* and *U. maydis* (Figure 1.5). On the other hand, it also demonstrates a divergent evolution and adaption of the processes to the different lifestyles of the fungi.

In *S. cerevisiae*, the spatial landmark is crucial for positioning and organization of the future division zone. Axial budding of haploid cells depends on a multi-protein complex consisting of septins, Axl1 and the proteins Bud3/4 and 10 (Casamayor and Snyder, 2002). This landmark is recognized by a GTPase module which finally determines the side of bud emerge. The module consists of the GTPase Bud1, its activating protein Bud2, and the GEF Bud5 and activates a second GTPase module. In this second module, the actin cytoskeleton is recruited by GTPase Cdc42, its GEF Cdc24 and the activating proteins Bem3 and Rga1/2 (Casamayor and Snyder, 2002; Chant, 1999). The actin cytoskeleton allows a polarized secretion, important for the delivery of cell-wall forming enzymes and other factors towards the growing daughter cell. Cdc42 resembles an essential protein in *S. cerevisiae*, deletion mutants are not viable (Pruyne and Bretscher, 2000). In *U. maydis*, the formation of a spatial landmark is one of the first steps during the establishment of cell polarity, too. Though the proteins Bud3 and Bud4 are missing, a homolog of Bud10 could be identified. Furthermore, a homolog of GTPase Cdc42 is present in *U. maydis*. In contrast to *S. cerevisiae*, absence of *UmCdc42* does not affect cell viability. Moreover, *UmCdc42* is not essential for polarized growth but involved in cell separation (Mahlert et al., 2006). In *U. maydis* and

several filamentous fungi a second GTPase, Rac1, seems to take over functions of Cdc42 including cell polarization. Rac1 resembles a homolog to mammalian Rho-type GTPases (Jaffe and Hall, 2005). A double deletion of *cdc42* and *rac1* is lethal. Of note, in contrast to Cdc42, Rac1 is mainly produced during filamentous growth of *U. maydis*. Since homologs of Rac1 are absent in *S. cerevisiae* and other yeasts, it resembles an additional component in the cell polarization machinery of dimorphic and filamentous fungi (Mahlert et al., 2006).

After the recruitment of major protein complexes to the future division site, the processes of septation and formation of the actomyosin ring (AMR) are initiated. Crucial for the assembly of the AMR are formins which continuously nucleate monomeric globular actin (G-actin) to filamentous actin (F-actin) (Evangelista et al., 2003). The AMR consists of antiparallel actin filaments and the motor protein myosin (Meitinger and Palani, 2016; Sellers, 2000). Constriction of the AMR at the end of cytokinesis supports the physical separation of mother and daughter cell (Chan et al., 2019). In *S. cerevisiae*, the formin Bni1 localizes near the tip and mainly contributes to the polymerization of actin filaments (Chang et al., 1997; Evangelista et al., 1997). *U. maydis* encodes two formins, of which Sfr1 is implicated in formation and constriction of the AMR. The second, Drf1, is an effector protein of Cdc42 and non-essential for cell division (Altamirano et al., 2017; Freitag et al., 2011). In addition to Sfr1, the F-BAR domain-containing protein Cdc15 supports constriction of the AMR in *U. maydis*. In absence of Cdc15, cells are not able to divide and form long cell chains (Böhmer et al., 2009).

Besides formins, the Arp2/3 complex is involved in the organization of the actin cytoskeleton during assembly of the AMR. The complex is conserved in most eukaryotic organisms, consisting of seven subunits (Welch et al., 1997). The subunits Arp2 and Arp3 are highly conserved and mainly involved in the nucleation of G-actin to form a cortical network of F-actin at the future division site. The other five subunits are poorly conserved and barely show homology to characterized proteins (Machesky and Gould, 1999). Interestingly, formins and the Arp2/3 complex compete for the pool of G-actin in the cell (Burke et al., 2014). This seems to allow a successful timing and coordination of AMR formation and constriction (Chan et al., 2019). In *S. cerevisiae*, members of the Arp2/3 complex localize to cortical actin patches, especially enriched in areas of polarized growth and septation (Welch et al., 1994). The proteins Las17

and Vpr1 are needed for the activation of the complex. Importantly, homologs of Arp2/3 and its activating proteins were identified in *U. maydis* (Winter et al., 1999). Thus, formation of the AMR seems to be organized similarly in *S. cerevisiae* and *U. maydis*.

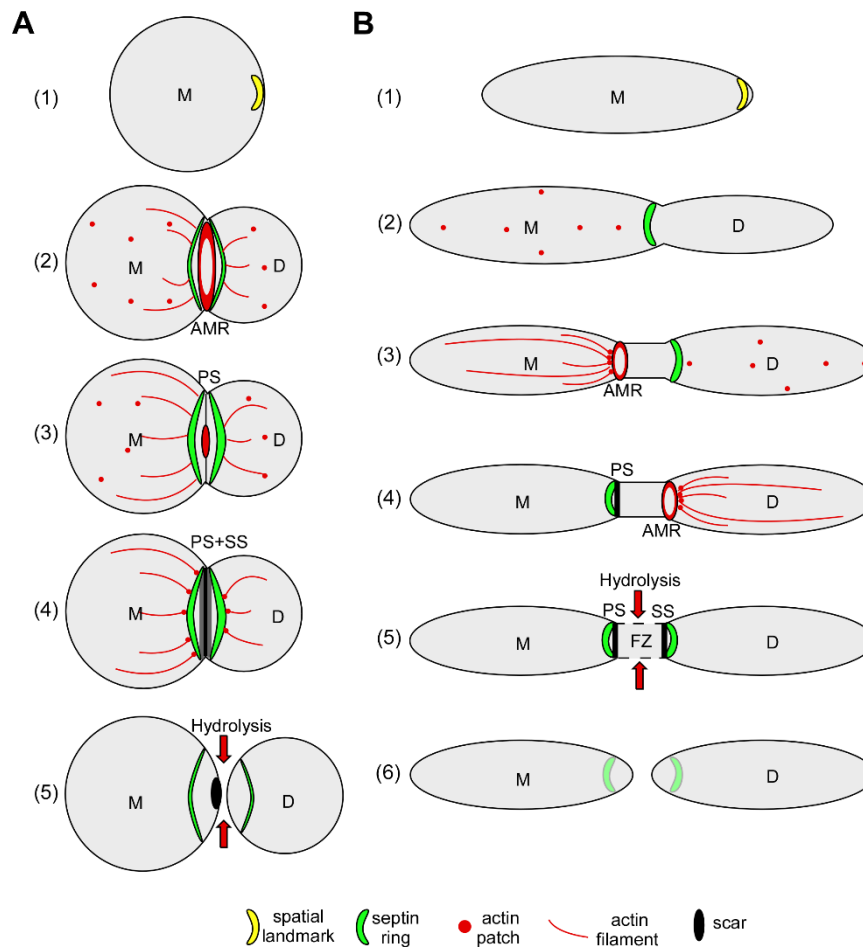


Figure 1.5: Comparative overview of major processes during polarized growth and cell separation in *S. cerevisiae* and *U. maydis*. (A) In *S. cerevisiae*, the establishment of cell polarity and bud emerge is directed towards a spatial landmark (1). Septins and proteins involved in the formation of the AMR are recruited to the landmark. Formation of septin rings and the AMR occurs in parallel. Monomeric actin patches are nucleated to form actin filaments; synthesis of the primary septum is initiated (2+3). After constriction of the AMR and synthesis of the primary septum, synthesis of a secondary septum starts adjacent to the mother and the daughter side of the primary septum (4). The primary septum is hydrolysed by cell wall degrading enzymes, leading to the physical separation of mother and daughter cell (5). (B) In *U. maydis* a spatial landmark is involved in the establishment of cell polarity, as well (1). It serves as a scaffold and recruits proteins needed for the formation of the future division zone. A septin ring assembles at the side of the mother cell (2). After disassembly of the septin ring, the AMR is formed. Before constriction, the septum ring reassembles (3). A primary septum is synthesised, delimiting the cytoplasm of the mother cell (4). Regulated by an independent signalling cascade, the same process of septin ring and AMR assembly is repeated on the side of the daughter cell (3+4). Finally, a secondary septum is formed, giving rise to a fragmentation zone (FZ) between mother and daughter cell (5). Remnant cell wall is hydrolysed by degrading enzymes completing cytokinesis (6). Modified from Juanes et al., 2016 and adapted for *U. maydis*.

The formation of septa is another important step towards the separation of mother and daughter cell. Septa function as scaffolds for the recruitment of cell division factors and serve as diffusion barriers between mother and daughter cell (Dobbelaere and Barral,

2004; Wloka et al., 2011). Seven septins were identified in *S. cerevisiae*, of which four are conserved in *U. maydis*: *UmCdc3*, *UmCdc10*, *UmCdc11* and *UmCdc12* (Altamirano et al., 2017; Alvarez-Tabarés and Pérez-Martín, 2010). During ongoing mitosis, the septins arrange from a patch into a higher complex ring-like structure at the bud neck. In *S. cerevisiae*, formation of the AMR and septation resemble parallel events (Fang et al., 2010; Schmidt et al., 2002; Vallen et al., 2000; VerPlank and Li, 2005). The invagination of a primary septum is directly followed by the formation of two additional secondary septa at each site of the primary septum (Kozubowski and Heitman, 2010). By contrast, in *U. maydis* the septin complex disassembles before AMR formation is initiated. It reassembles before AMR constriction takes place. In concert with the cell cycle, a primary septum is formed at the mother side of the bud neck (Böhmer et al., 2008). Regulated by a second independent pathway, a secondary septum assembles at the daughter side, leading to the generation of a fragmentation zone between mother and daughter cell (Weinzierl et al., 2002). Factors involved in the formation of the primary septum are unknown so far. The Ste20-like kinase Don3, Cdc42 and its GEF Don1 were identified as key players for the invagination process of the secondary septum (Böhmer et al., 2008). Hence, septation in *U. maydis* differs from *S. cerevisiae*, since an additional cascade of proteins is needed to coordinate the assembly of a second AMR followed by the invagination of a secondary septum on the side of the daughter cell.

The final steps of cytokinesis do not only depend on AMR constriction and invagination of septa. The action of cell wall degrading enzymes like chitinases is contributing to the physical separation of mother and daughter cell, as well. The genome of *S. cerevisiae* encodes two chitinases, *ScCts1* and *ScCts2* (Karlsson and Stenlid, 2008). *ScCts1* is specifically involved in the degradation of chitin during cell division, whereas the function of *ScCts2* is not fully understood to date. Deletion of *ScCts1* results in cell separation defects (Kuranda and Robbins, 1991). *ScCts1* is secreted conventionally. Interestingly, *ScCts2* lacks a predicted SP and might be secreted by an unconventional mechanism. In contrast, three chitinases have been identified in *U. maydis*, including unconventionally secreted *Cts1* and SP-containing *UmCts2* and *UmCts3*. *UmCts1* and *UmCst2* are active during the yeast-like growth stage of *U. maydis*, whereas *UmCts3* is not produced. The function of *UmCts1* and *UmCts2* during cell separation seems to be redundant. Only a deletion of both chitinase genes impairs cell division of mutant cells (Langner et al., 2015). Interestingly, the activity of

ScCts1 and *UmCts1/2* seems to be regulated differently. In *S. cerevisiae*, the transcription factor *Ace2* is transported to the nucleus of the daughter cell during late mitosis, initiating transcription of *cts1*. *ScCts1* localizes to the readily formed septum at the side of the daughter cell (Colman-Lerner et al., 2001). Such spatio-temporal regulation of gene expression has not been described for *UmCts1* and *UmCts2*.

1.5 Aim of this thesis

The overarching aim of this thesis was the initial characterization of Jps1, a novel factor for unconventional secretion of chitinase Cts1 identified by genetic screening. In the first part, bioinformatical analysis of Jps1 was conducted to determine its conservation and functional hints. Next, microscopy with fluorescently labelled proteins allowed to investigate the intracellular localization of Jps1 during the cell cycle. Since Jps1 is important for Cts1 release, it was analysed for putative unconventional secretion using the previously established Gus-reporter assay. In addition, a truncation analysis of Jps1 was used to identify essential regions of the protein. In the second part, a biochemical characterization of Jps1 was conducted. Here, expression and purification protocols for Jps1 were established in *Escherichia coli* to increase protein amounts for analysis. Then, structural studies were conducted to resolve the quaternary structure and membrane interaction was analysed with established biochemical methods.

2. Results

2.1 *In silico* analysis of Jps1

2.1.1 Jps1 is conserved among basidiomycetes and does not harbour known domains or motifs

The protein Jps1, with a molecular weight of 65 kDa, was identified in a genetic screen for factors involved in the unconventional secretion pathway of Cts1 (Reindl and Stock et al., 2020). Mutations, leading to the expression of truncated Jps1 protein versions, strongly impaired secretion of active Cts1 from cells. To deduce a putative function of Jps1, first orthologues were identified using the basic local alignment search tool (BLAST) from the National Centre for Biotechnology information (NCBI) (<https://blast.ncbi.nlm.nih.gov/Blast.cgi>). Interestingly, orthologs showing a high degree of sequence similarity (up to 80% identity) were found in close relatives of *U. maydis* like *Sporisorium relianum* and *Ustilago hordei* (Figure 2.1). By contrast, no orthologs are present in the division of ascomycetes like *S. cerevisiae* or *Candida albicans*, indicating that Jps1 represents a basidiomycete-specific protein. Next, amino acid (aa) alignments of the orthologs revealed, that the proteins contain both regions of high and more variable aa conservation. Of note, even Jps1 orthologs of more distantly related basidiomycete species showed similarity in a sequence region between aa 360 and 481 (red box in Figure 2.1). This indicates a high degree of conservation for this part of the protein. Interestingly, all mutations identified in the screen were located within this region. Three of the four mutations lead to the expression of non-functional truncated Jps1 variants (G335D; Q338STOP; W446STOP; W448STOP), supporting the importance of this conserved region.

To date none of the Jps1 orthologs has been further characterized. Since the presence of conserved domains might allow to deduce a putative function of the proteins, the Simple Modular Architecture Research Tool (SMART) from the EMBL (Heidelberg, Germany) was used (data not shown). However, this tool did not identify any yet characterized or conserved domains for Jps1 and its orthologs.

<i>U. maydis</i>	1	MPGISKKPSFNAQAQAGSPHVS	PHKKTVRLAENPHVSAFLSPKSRIF	TGGHGYPVPTRGNGPASSASTGTAGGF	GASASSEAF	84								
<i>S. reilianum</i>	1	MPGISKKPSFSSYQTGSPHS	PHKKTVRLAENPHVSAFLSPKSRIF	TGGHGYPVPTARGAGPASSSTAAGA	- - - F - SASASPEAF	80								
<i>U. hordei</i>	1	MPGISKKPSFSSNP - GSTPG	SPNNKTVRLAENPHVSAFLSPKSR	IYAGGHGYPGHPNPSKGN - - - -	HGPGAFSATSVTSDAF	77								
<i>P. aphidis</i>	1	MPGISKKPSFSHQ - - DSAPS	SPSKKTVRLAENPHVSAFLSPKSRIF	TGGHGYPGPPGPMAR - - - - -	QSYASASAVPDAF	72								
<i>P. antarctica</i>	1	MPGISKKPSFSHQ - - DSAPS	SPSKKTVRLAENPHVSAFLSPKSRIF	TGGHGYPGPPGPMAR - - - - -	QSYASASAVPDAF	72								
<i>U. maydis</i>	85	S IAGKQLTPEEVAQKI	ASMLKPGPPFFSRVSNADLIDY	ISDTSIMNCDKLRAQAA	AAVEAKKANRAAS	FAPSGTVVRRRAEEE	168							
<i>S. reilianum</i>	81	S ISGKQLTPEEVAQKI	ASMLKPGPPFFSRVSNADLIDF	ISDSSIMNCDKLRAQAE	ALEAKKHANRATTS	FVPSGTVVRRRAEEE	164							
<i>U. hordei</i>	78	A ISGKQLTPEEVAQKI	ASMLKPGPPFFSRVSNADLIDF	ISDGSIMNCDKLRAQAE	QLEAKKQASRANTAF	VPSGTVVRRRAEEE	161							
<i>P. aphidis</i>	73	SVNGKQLTPEEVAQKI	ASMLKPGPPFFSRVSNADLIDF	ISDGSIMNCDKLRAAAA	AAVEERKHANRALTA	FVPSGTVVRRRAEEE	156							
<i>P. antarctica</i>	73	SVNGKQLTPEEVAQKI	ASMLKPGPPFFSRVSNADLIDF	ISDGSIMNCDKLRAAAA	AAVEERKHANRALTA	FVPSGTVVRRRAEEE	156							
<i>U. maydis</i>	169	SWTGVGTWSSLDGLP	AGAGWSRIPGTPGSQTGS	TLSTKTSBS - - - -	TGALQDDGLWNAITL	SCDIDCTAVE	LAKSVVVP	248						
<i>S. reilianum</i>	165	RWTGVGTWSSLDGLP	AGAGWSRIPGTPASQNGS	TLSTKTSBS - - - -	TGALQDDGLWNAITL	SCDIDCTAVE	LAKSVVVP	248						
<i>U. hordei</i>	162	RWTGVGTWSSLDGLP	AGAGWSRIPGAPATVQGG	- - - - - SGFSTKSGSGG	MEDDGLWNAITL	SDIDCTVE	LAKSVVVP	240						
<i>P. aphidis</i>	157	RWTGVGTWSSLEGLP	AGAGWSRIPGTPGSL	- - - - - VRSQSG	VEDDGMWNAITL	SCDLDCCT	VELAKSVVVP	228						
<i>P. antarctica</i>	157	RWTGVGTWSSLEGLP	AGAGWSRIPGTPGSL	- - - - - VRSQSG	VEDDGMWNAITL	SCDLDCCT	VELAKSVVVP	228						
<i>U. maydis</i>	249	EKNHFFNGNTQC	LFDDIGAGVYKRF	DNLVGKASSG - GLRHK	QSSSALGN - - G -	ASKVAPNYLS	LSAYTDP	NSTAF	GATSFELK	327				
<i>S. reilianum</i>	249	QNNHFFNGNAQSL	LFDDIGAGVYKRF	DNLVGKASSG - GLRHK	ASSAALGS - - S	SAGSKIVPNYLS	LSAYTDP	NSTAF	STNSFELK	330				
<i>U. hordei</i>	241	QNNHFFYNGNAQSL	LFHDIGAGVYKRF	DNLVGKATG - - GLRHK	ASSSALGGAAGSS	GSKIAPNYLS	LSAYTDP	NNA - AFG	ANAFELK	321				
<i>P. aphidis</i>	229	HNNHFFNGNADSL	LFQDIGAGIKFK	FDSLTSKT - - - -	SLRHKPSSNLGG - - - -	GSKIMPSYLS	LSAYTDP	NN - AFT	SSAFELK	302				
<i>P. antarctica</i>	229	HNNHFFNGNADSL	LFQDIGAGIKFK	FDSLTSKT - - - -	SLRHKPSSNLGG - - - -	GSKIMPSYLS	LSAYTDP	NN - AFT	SSAFELK	302				
<i>U. maydis</i>	328	WPSWMPWVKKQ	TSTPANSDA - - - -	STPTMPADGGA	KRWVWPSSTKVS	IHASWGWYNYLYLP	QPVLD	SLDGDVDE	AEKIANL	INKCL	408			
<i>S. reilianum</i>	331	WPSWMPWVHK	KSSSTPAADGTP	ASGGDAAAGG	KRWVWPSSTKVS	IHASWGWYNYLYLP	QPVLD	AMGDVDE	AEKIANL	INKCL	414			
<i>U. hordei</i>	322	WPSWMPWVKKHT	PTATP - - - - -	TPEAGEHAGG	KRWVWPSSTKVS	IHASWGWYNYLYLP	QPVLD	SLDGDVDE	AEKIANL	INKCL	399			
<i>P. aphidis</i>	303	WPSWMPWVKKST	NPETA - - - - -	APE - TPVAGG	KRWVWPSSTKIS	IHASWGWYNYLYLP	QPVLD	SLDGDVDE	AEKVANL	INKCL	379			
<i>P. antarctica</i>	303	WPSWMPWVKKST	NPETA - - - - -	APE - TPVAGG	KRWVWPSSTKIS	IHASWGWYNYLYLP	QPVLD	SLDGDVDE	AEKVANL	INKCL	379			
<i>U. maydis</i>	409	NYILNNVPAGL	PAFAAVVTILKAI	APTGTG	ISTF IGWSWDTIK	FSNKGQGVVLS	ATWILP	VALIPRAWDAP	SSSAGGSTP	- -	490			
<i>S. reilianum</i>	415	TYILNNVPAGL	PAFAAVVTILKAI	APTGTG	ISTF IGWSWDTIK	FSNKGQGVVLS	ATWILP	VALIPRAWDAP	ATPSTGAPS	TP	498			
<i>U. hordei</i>	400	TFILNNVPAGL	PAFAAVVTILKAI	APTGTG	ISTF IGWSWDTIK	FSNKGQGVVLS	ATWILP	VALIPRAWDAP	ASFGS	IPT - TPV	482			
<i>P. aphidis</i>	380	TYILNNVPAGL	PAFGAVITILKAI	APTGTG	ISTF IGWSWDTIK	FSNKGQGVVLS	ATWILP	VALIPRAWDAP	TNPNSATP -	TP	462			
<i>P. antarctica</i>	380	TYILNNVPAGL	PAFGAVITILKAI	APTGTG	ISTF IGWSWDTIK	FSNKGQGVVLS	ATWILP	VALIPRAWDAP	TNPNSATP -	TP	462			
<i>U. maydis</i>	491	A - - - - -	PAAPTAT - - - - -	- - - - -	FSDDA - - - - -	S - - - - -	STPT - - - - -	- - - - -	PPTTGS - - - - -	S	517			
<i>S. reilianum</i>	499	TPTTGGTGS	VTTPSTDM	PATTSPSAGT	PSATTPS	SDTSP	ATAPSDT	PTSTPTT	PTATTP	VASPSG	TTTTTGAAAAS	IA	582	
<i>U. hordei</i>	483	TANPN - - - - -	- - - - -	PT - - - - -	PTTAP - - - - -	- - - - -	PSAP - - - - -	- - - - -	TDT - - - - -	APSTG	TSGSGMP	IT - - - - -	P	518
<i>P. aphidis</i>	463	DPTAT - - - - -	- - - - -	PT - - - - -	PTTAA - - - - -	- - - - -	PSAP - - - - -	- - - - -	AAPVS	ATPAGG	SGMP	VT - - - - -	A	500
<i>P. antarctica</i>	463	DPSAT - - - - -	- - - - -	PT - - - - -	PTTAA - - - - -	- - - - -	PSAP - - - - -	- - - - -	AAPVS	ATPAGG	SGMP	VT - - - - -	A	500
<i>U. maydis</i>	518	GTTMTAQD	TSTADPEDTLP	DPTKPAV	APGATLPP	TNPSTV	LDLFS	PPPSNETS	NAKYPGDQY	GRGGDQ	STSA	PMGDTP	PAPAN	601
<i>S. reilianum</i>	583	AARFYARDAT	INDPENTLP	SKNTPAV	APGATLPP	TDPSTV	LDLAPP	TNDTS	NAQYPGDAR	GRGGDQ	STSA	PMGDTP	PAPAN	666
<i>U. hordei</i>	519	QRYQRYRAYD	TDPENTP	IPILIT - NPV	APGATLPP	ANPSQIS	LDLTP	PPANDT	SNATYPGDAR	GRGGDPT	TSAS	MGNTP	PAPAN	601
<i>P. aphidis</i>	501	QD - - - - -	VTDPESVLP	DPNVPAP	APGATLPP	TNPSTV	NVLDL	SPPPANDT	ANATYPGDAR	GRGGDPT	TS	GMGNTP	PAPAN	576
<i>P. antarctica</i>	501	QD - - - - -	VTDPESVLP	DPNVPAP	APGATLPP	TNPSTV	NVLDL	SPPPANDT	ANATYPGDAR	GRGGDPT	TS	GMGNTP	PAPAN	576
<i>U. maydis</i>	602	QTP	IDAES											609
<i>S. reilianum</i>	667	RTP	IDAES											674
<i>U. hordei</i>	602	QVP	IDAES											609
<i>P. aphidis</i>	577	QTP	IDAES											584
<i>P. antarctica</i>	577	QTP	IDAES											584

Figure 2.1: Alignment of *Jps1* aa sequence from *U. maydis* and its basidiomycete orthologues. *Jps1* and orthologues of closely related Basidiomycetes were aligned using the multiple sequence alignment tool ClustalOmega (EMBL-EBI). Conserved aa residues are highlighted in different shades of blue (darker blue=high similarity; lighter blue=lower similarity). The red box shows an area of highest conservation in more distantly related species. Mutations identified during the UV-mutagenesis screen are marked (red asterisk): G335D; Q338STOP; W446STOP; W448STOP.

Taken together, none of the bioinformatic tools allowed to gather high confident information about the putative function of *Jps1*.

2.2 *In vivo* analysis of *Jps1*

2.2.1 Deletion of *jps1* does not alter growth or phenotype of yeast-like cells

To study the deletion phenotype of *jps1*, the genomic locus of *umag_03776* was replaced by a deletion cassette via homologous recombination. The cassette harboured a gene sequence coding for a hygromycin B phosphotransferase (*hph*) (Figure 2.2, A). Expression of *hph* mediates resistance to the antibiotic hygromycin, facilitating selection of deletion mutants. The cassette was flanked with sequences of approximately 1000 bp homologous to the 5' upstream and 3' downstream regions of *umag_03776* (Figure 2.2, B). Positive candidates were confirmed after transformation

of the deletion construct and subsequent Southern blot analysis of obtained mutants (Figure 2.2, C). Hence, *jps1* does not resemble an essential gene of *U. maydis*.

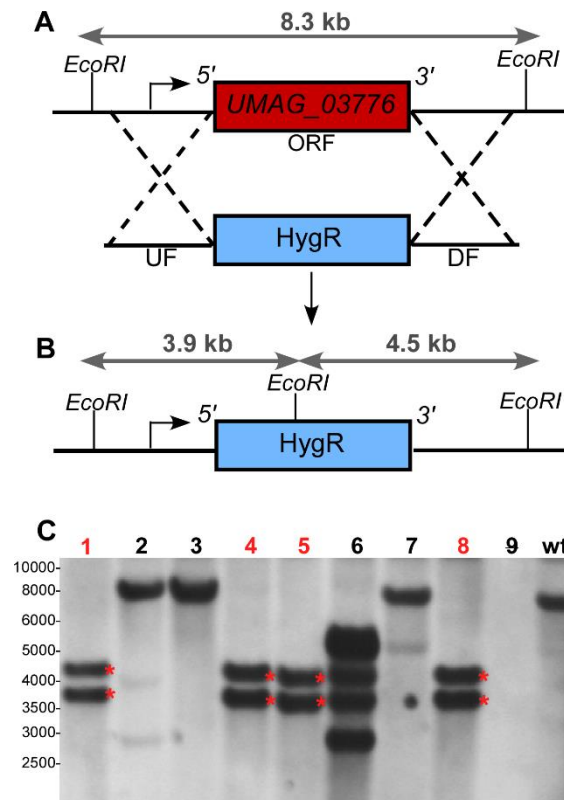


Figure 2.2: Gene deletion strategy for the genomic locus of *umag_03776*. (A) The genomic locus of *jps1* (*umag_03776*) was targeted for deletion by a replacement cassette (Terfrüchte et al., 2014) (B) Successful gene replacement was confirmed for hygromycin-resistant transformants by Southern blot analysis. Genomic DNA was hydrolysed by the endonuclease *EcoRI*. Flanks were used as probes. The sizes of the expected fragments are indicated. (C) Southern blot analysis of hygromycin resistant transformants. Confirmed transformants are shown in red. Red asterisks (*) indicate expected bands for positive deletion candidates. Southern blot analysis was conducted in collaboration with K. Hussnaetter.

The growth of *jps1*-deficient mutants was compared to the progenitor strain AB33. Both strains showed a similar growth rate: a doubling time of approximately 1.9 h for AB33, and 2.0 h for AB33_ *jps1*Δ (Figure 2.3, A). Next, to investigate if the morphology of *jps1*-deficient cells differs from those of AB33, cells were analysed by microscopy (Figure 2.3, B-C).

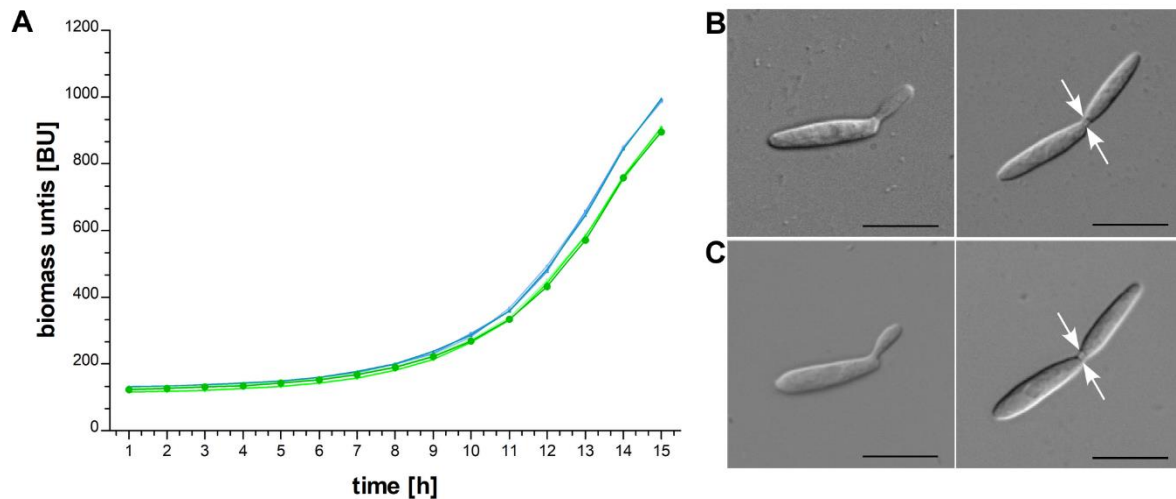


Figure 2.3: Growth and morphology of the *jps1*-deletion strain. (A) Real-time measurement of biomass forming units (BU) of AB33 (blue lines) and AB33_ *jps1*Δ (green lines) to follow cell growth over 15 h. Visual analysis of progenitor AB33 (B) and AB33_ *jps1*Δ (C) by light microscopy. Scale bar: 10 μm.

No difference in morphology was identified between *jps1*-deficient and AB33 yeast-like cells. Cells still had their characteristic cigar shape and buds formed at their distal cell pole developed into regularly shaped daughter cells. A fragmentation zone was formed between mother and daughter cell at the future site of cell division. These observations indicate unimpaired polarity and cytokinesis of AB33_ *jps1*Δ as already suggested by the data of the growth analysis.

In conclusion, deletion of *jps1* does not impair cytokinesis of yeast-like cells under conditions analysed.

2.2.2 Cts1 secretion and localization is impaired in absence of *jps1*

In order to confirm an effect on Cts1 secretion in the absence of *jps1*, extracellular chitinase activity was determined for AB33_ *jps1*Δ using the specific substrate 4- methylumbelliferyl-β-D-N, N', N''-triacetylchitotrioside (4-MUC) (Langner et al., 2015). AB33 and AB33_ *cts1*Δ served as positive and negative control, respectively. As expected, extracellular Cts1 activity values were high for AB33 (28000 RFU/OD₆₀₀), whereas barely any was observed for the *cts1*-deletion strain (4500 RFU/OD₆₀₀) (Figure 2.4, A).

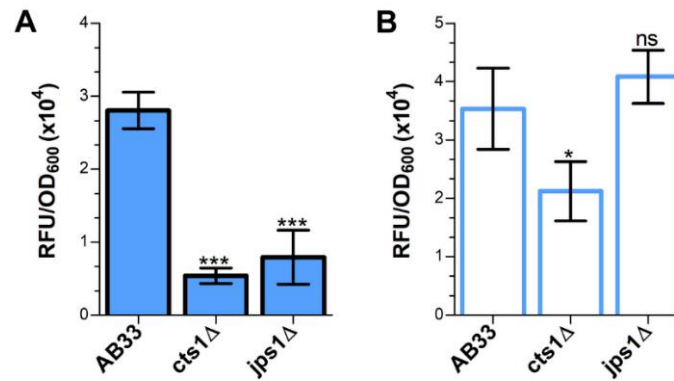


Figure 2.4: Cts1 activity assay of *jps1*-deficient cells. Extracellular (A) and intracellular (B) Cts1 activity (Koepeke et al., 2011; Langner et al., 2015) was determined for AB33_ *jps1*Δ. AB33 served as positive-, AB33_ *cts1*Δ as negative control. Assays were conducted in five biological replicates. Error bars indicate standard deviation. ***, p value < 0.0001; n.s., not significant, p value > 0,05 (two sample t-test, control: AB33).

The values obtained for the *jps1*Δ-strain indicated significantly reduced Cts1 activity (8000 RFU/OD₆₀₀) in line with the results obtained for the mutant candidates during the UV-mutagenesis screen (Reindl and Stock et al., 2020). In comparison to AB33, Cts1 activity values were up to 70 % reduced.

To analyse if deletion of *jps1* influences protein abundance of Cts1, chitinase activity was also determined in native cell extracts of AB33, AB33_ *cts1*Δ and AB33_ *jps1*Δ. However, Cts1 activity in the background of the *jps1*-deletion was similar to AB33. Values obtained for AB33 were around 35000 RFU/OD₆₀₀ and for AB33_ *jps1*Δ around 41000 RFU/OD₆₀₀, indicating no effect of the *jps1* deletion on the translation of *cts1*. In line with expectations, the lowest chitinolytic activity was observed in native cell extracts of the negative control AB33_ *cts1*Δ (2000 RFU/OD₆₀₀) (Figure 2.4, B).

To investigate the localization of Cts1 in absence of Jps1, a *jps1*-deficient strain in the background of AB33_ Cts1G was generated. In this strain, Cts1 is produced in a fusion to the enhanced green fluorescent protein (Gfp). Interestingly, according to microscopic analysis, Cts1G still localized to the primary and secondary septum of mother and daughter cell, respectively. However, in contrast to AB33, Cts1 was also present in the cytoplasm and did not localize within the fragmentation zone (Figure 2.5, A-C).

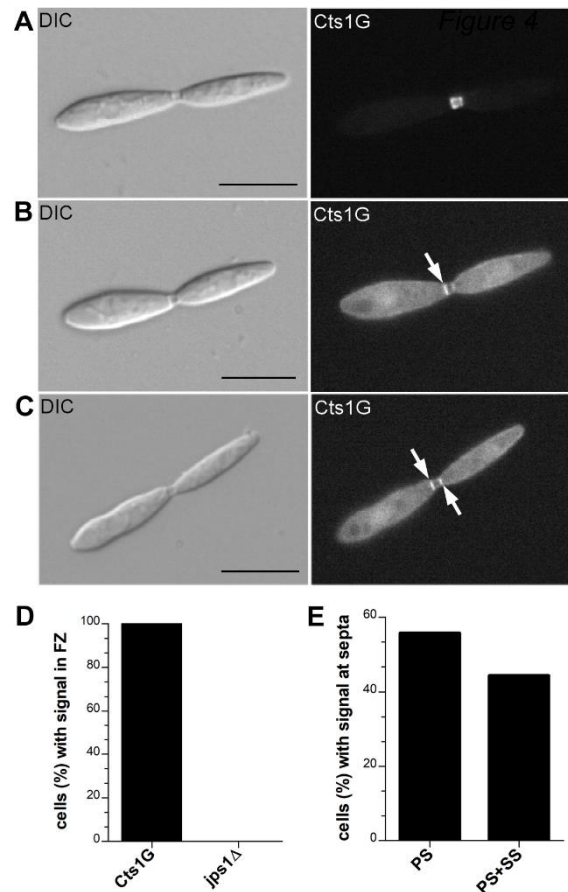


Figure 2.5: Localization of Cts1G in *jps1*-deficient cells. DIC images and fluorescence microscopy of positive control AB33 (A) and AB33_ *jps1*Δ (B)/(C). (D) Localization of Cts1G was quantified in AB33 and AB33_ *jps1*Δ. (E) Additionally, the ratio of Cts1G accumulation to the primary septum (PS) or both septa (PS+SS) was assessed. n= 1000 cells, counted in three biological replicates. Scale bar: 10 μm.

Quantification of Cts1G localization in the absence of *jps1* compared to AB33 confirmed the accumulation at the primary (57%) and secondary (43%) septum, depending on the stage of the cell cycle. In none of the *jps1*-deficient cells analysed, a localization inside the fragmentation zone was observed as for AB33 (Figure 2.5, D-E).

In summary, Jps1 influences localization of Cts1 into the fragmentation zone during late cytokinesis. In AB33_ *jps1*Δ, Cts1G accumulated at the primary and secondary septum. This result supports the observation of impaired secretion of Cts1 in absence of Jps1.

2.2.3 Jps1 and Cts1 co-localize during the late stage of cytokinesis

To analyse the localization of Jps1 *in vivo*, a co-localization study was conducted using fluorescence microscopy. Cts1 was expressed in fusion to Gfp and Jps1 in fusion to a derivative of the red fluorescent protein, mCherry. The respective gene fusions were

inserted in the native loci. As shown before, Cts1G localized to the fragmentation zone between mother and daughter cell (Aschenbroich et al., 2018; Langner et al., 2015; Reindl et al., 2019). Importantly, during late cytokinesis, Jps1C was detected in the fragmentation zone as well, resulting in a perfect overlay of the Gfp- and mCherry signal (Figure 2.6, A).

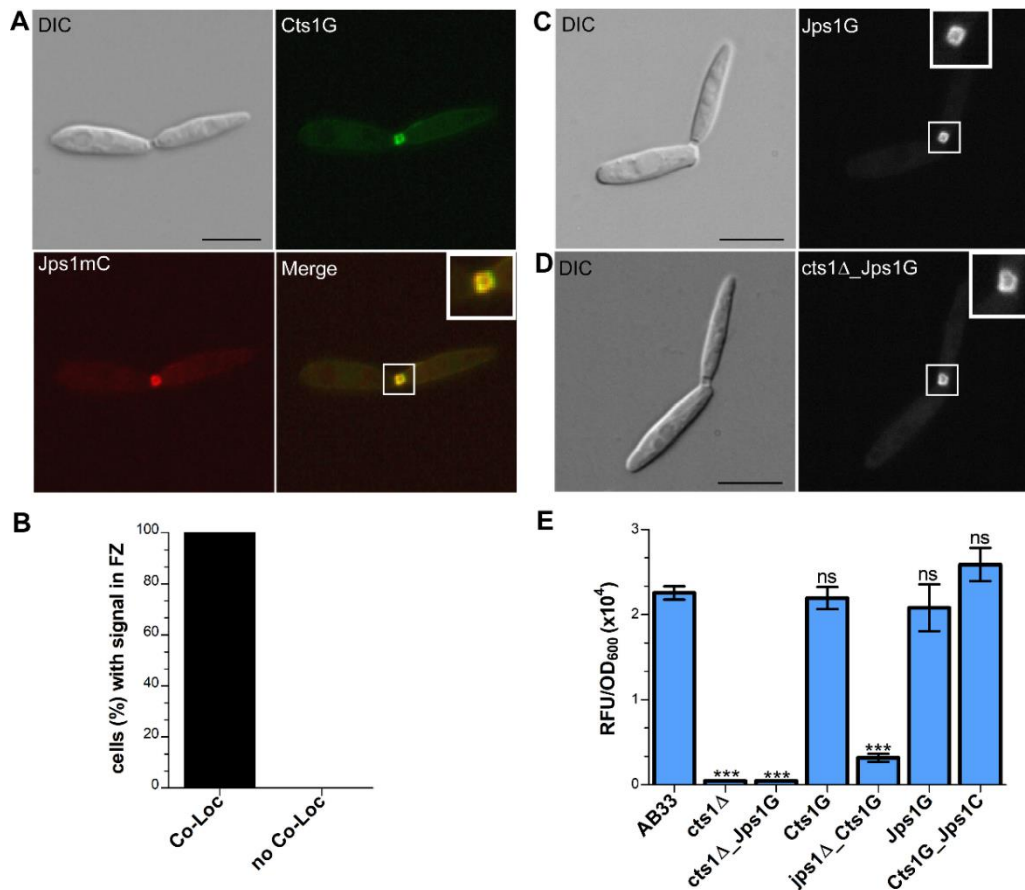


Figure 2.6: Localization of Jps1C and Cts1G during late cytokinesis (A) Fluorescence microscopy of Cts1G and Jps1C in AB33. Merge shows overlay of the Gfp and the mCherry channel. Scale bar: 10 μ m. **(B)** Quantification of intracellular Cts1G and Jps1C localization in yeast cells of AB33_Cts1G_Jps1C. n=1000 cells, counted in three biological replicates. **(C)** Fluorescence microscopy of AB33_Jps1G **(C)** and AB33_cts1 Δ _Jps1G **(D)** during late cytokinesis. Scale bar: 10 μ m. **(E)** Extracellular Chitinase activity (Koepeke et al., 2011; Langner et al., 2015) was determined for AB33_Jps1G and AB33_Cts1G_Jps1C. AB33 and AB33_Cts1G served as positive controls, AB33_cts1 Δ and AB33_cts1 Δ _Jps1G as negative controls. Error bars indicate standard deviation. ***, p value < 0.0001; n.s., not significant, p value > 0,05 (two sample t-test, control: AB33).

Quantifying co-localization of Cts1G and Jps1C (Figure 2.6, B) confirmed that indeed both proteins are found together in each analysed cell with a fragmentation zone.

To investigate if the absence of Cts1 affects localization of Jps1, a strain expressing Jps1G in background of a *cts1* deletion was generated. Microscopy results indicated unaffected localization of Jps1G to the fragmentation zone in absence of the chitinase

(Figure 2.6, D). Therefore, recruitment of Cts1 is dependent on functional Jps1 but not *vice versa*.

To validate functionality of fluorescently tagged Jps1, extracellular Cts1 activity was assayed for the different expression strains (Figure 2.6, E). Therefore, AB33 and AB33_Cts1G served as positive controls, AB33_cts1 Δ and AB33_cts1 Δ _Jps1G as negative controls. Extracellular Cts1 activity of AB33_Jps1G and AB33_Cts1G_Jps1C was similar to the positive controls AB33 and AB33_Cts1G, with around 20000 RFU/OD₆₀₀. In contrast, values observed for AB33_jps1 Δ _Cts1G were close to both negative controls, as expected (450 RFU/OD₆₀₀). Thus, the fusion of Gfp or mCherry to Jps1 did not affect unconventional secretion of Cts1.

Expression of all fusion proteins used for microscopy and determination of Cts1 activity was furthermore verified by Western Blot analysis (Figure 2.7). Signals for Cts1G and Jps1C were expected at approximately 100 and 110 kDa, respectively.

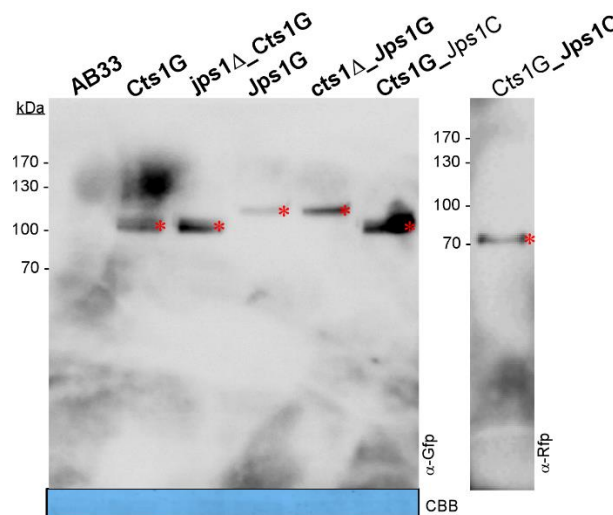


Figure 2.7: Production of Jps1G and Jps1C fusion protein. 10 μ g total protein from crude cell extracts was analysed by Western Blot. Anti-Gfp and -Rfp primary antibodies were used for detection. AB33 and AB33_Cts1G served as negative- and positive controls, respectively. Cts1G (100 kDa), Jps1G (110 kDa) and Jps1C (75 kDa) (red asterisks) were produced as full-length proteins. The CBB stained Western blot membrane indicates that similar amounts of total protein have been used for Western blot analysis.

All full-length fusion proteins were detected in the Western Blot analysis of cell extracts, indicating successful production of Cts1G, Jps1G and Jps1C by the different expression strains.

In conclusion, Jps1 localizes to the fragmentation zone in the late stage of cytokinesis. Thus, Jps1 and Cts1 co-localize and might interact. Interestingly, in contrast to Cts1, localization of Jps1 is independent from Cts1.

2.2.4 Jps1 is recruited to the zone of bud emerge during early cytokinesis

To dissect localization of Jps1 during cytokinesis more carefully, different growth stages of yeast-like cells were analysed by fluorescence microscopy in AB33_Jps1G. In this strain, expression of *jps1-gfp* was under control of the native *jps1*-promoter.

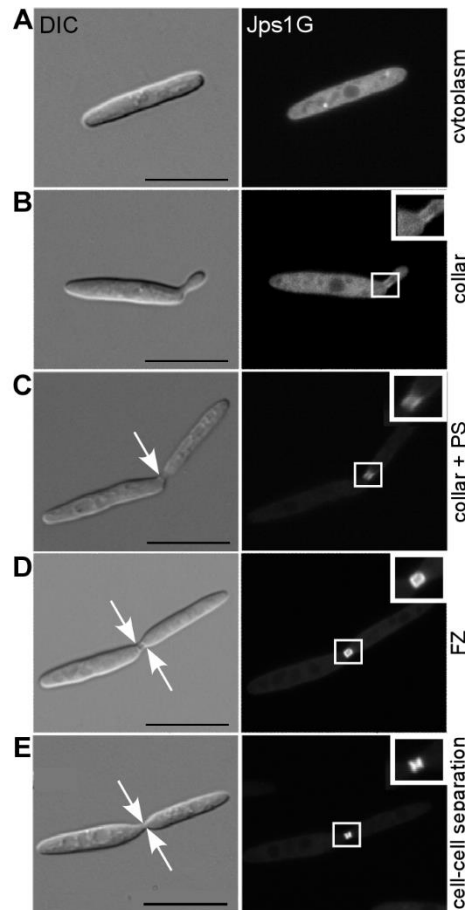


Figure 2.8: Localization stages of Jps1G. Fluorescence microscopy of AB33_Jps1G during different stages of the cell cycle (A-E). Typical localization patterns are indicated next to the respective images. Arrows indicate the presence of septa. Scale bars: 10 μ m.

Importantly, Gfp-signals related to expression of the Jps1G fusion protein were visible during early stages of the cell cycle, already (Figure 2.8, A-E). Before bud emerge, during interphase, Jps1G showed a cytoplasmic localization (A). When the process of budding was initiated, a Gfp signal was detected at the collar of the emerging bud (B). During ongoing expansion of the bud, Jps1G likely remained within the collar region between mother and daughter cell (C). After formation of the primary and secondary septum was completed, the Jps1G-signal enframed the fragmentation zone (D). The Gfp signal was still visible during the final steps of cell separation in late cytokinesis (E). Thus, in contrast to Cts1, Jps1G can be detected during bud emerge already.

2.2.5 Applying the Gus reporter assay to analyse potential secretion of Jps1

According to bioinformatical predictions Jps1, similar to Cts1, does not harbour an N-terminal signal peptide mediating secretion via the conventional secretion pathway (SignalP 5.1). However, due to its characteristic localisation in the fragmentation zone, it seemed reasonable to test a potential export of Jps1 by unconventional secretion. For this purpose, a strain expressing a fusion of *jps1* to the *gus* reporter gene under control of the strong constitutive *oma*-promoter was generated. To allow detection of the encoded fusion protein in Western blot analysis, a linker sequence encoding a Strep-, an HA- and a sextuple histidine-tag (SHH-tag) was incorporated between *gus* and *jps1*. If Jps1 is secreted unconventionally, it will serve as carrier protein and mediate the export of active bacterial Gus enzyme into the extracellular medium (Figure 2.9, A). Additionally, the *gus-jps1* construct was transformed into AB33_cts1Δ to evaluate impact of Cts1.

To verify successful expression of the Gus-Jps1 fusion protein in the different strain backgrounds, a Western blot assay was conducted with crude cell extracts of the expression strains (Figure 2.9, B). AB33 and AB33_Gus_{cyt} were included as negative controls. AB33_Gus_{cyt} produces a cytoplasmic version of the Gus enzyme without carrier protein. Hence, the enzyme should not be exported into the culture supernatant. AB33_Gus-Cts1 served as positive control since active extracellular Gus can be detected in this strain (Stock et al., 2012). For Gus-Jps1 and Gus-Cts1 a detection signal at a size of about 150 kDa was expected and for Gus without fusion partner at about 75 kDa.

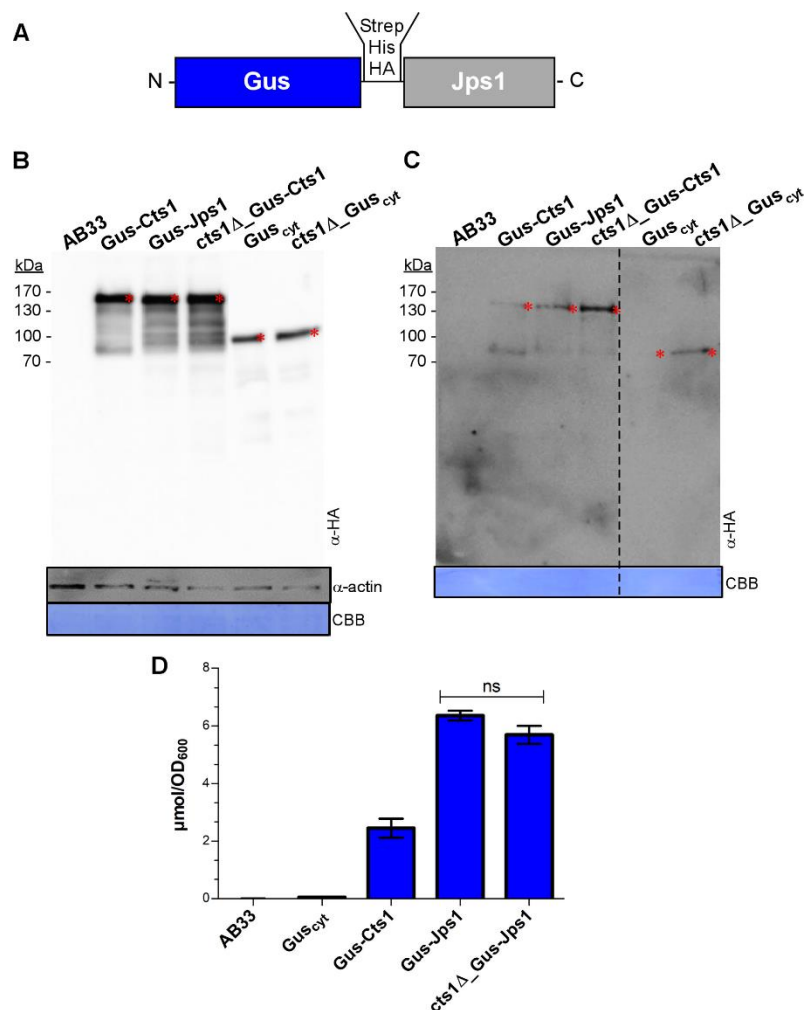


Figure 2.9: Gus reporter assay to analyse secretion of Jps1. (A) Scheme of the Gus-Jps1 reporter protein. (B) Production of Gus-Jps1 (150 kDa) and Gus_{cyt} (75 kDa) full-length fusion proteins (red asterisk) was analysed in 10 μg total protein from crude cell extracts by Western blot. Anti-HA primary antibody was used for detection. AB33 served as a negative control, AB33_Gus-Cts1 (100 kDa) as positive control. The anti-actin Western Blot confirms analysis of intracellular proteins. The CBB stained Western Blot membrane indicates that similar amounts of total protein have been used. (C) Secretion of Gus-Jps1 (150 kDa) (red asterisk) was investigated in TCA-precipitated supernatants of AB33_Gus-Jps1 by Western Blot. Anti-HA primary antibody was used for detection. AB33 and AB33_Gus_{cyt} (75 kDa) served as negative control, AB33_Gus-Cts1 (150 kDa) as positive control. The CBB stained Western Blot membrane indicates that similar amounts of total protein have been used. (D) Gus reporter assay (Stock et al., 2012) with culture supernatants of AB33_Gus-Jps1 and AB33_cts1Δ_Gus-Jps1. AB33_Gus-Cts1 served as positive control, AB33 and AB33_Gus_{cyt} as negative controls. The assay was conducted in three biological replicates. Error bars indicate standard deviation. n.s., not significant, p value > 0,05 (two sample t-test). All strains analysed are derivatives of AB33.

The Gus-Jps1 full-length fusion protein was successfully produced by AB33_Gus-Jps1 and AB33_cts1Δ_Gus-Jps1. As expected, bands were detected at 150 kDa. Signals for the Gus-Cts1 (150 kDa) and cytoplasmic Gus (75 kDa) were detected at full-length, as well. In line with expectations, no signal showed up in the sample of negative control AB33.

To investigate secretion of Gus-Jps1 into the culture supernatant of AB33_Gus-Jps1 and AB33_cts1 Δ _Gus-Jps1, TCA precipitated supernatants were analysed by Western Blot (Figure 2.9, C). The same positive (AB33_Gus-Cts1) and negative controls (AB33 and AB33_Gus_{cyt}) as used for analysis of crude cell extracts before, were included. No signal was detected for AB33, as expected. For the Gus-Cts1 and both Gus-Jps1 expression strains, signals were observed at 150 kDa, suggesting secretion of the reporter proteins. However, unexpectedly, a signal was obtained for cytoplasmic Gus, indicating its presence in the culture supernatant. This phenomenon was observed in TCA-precipitated supernatants of *U. maydis* strains harbouring the *oma*-promoter before (Aschenbroich, 2019). One potential explanation is the export of misfolded proteins by a route similar to the misfolding-associated-protein-secretion (MAPS) pathway. MAPS seems to be present in most eukaryotic cells and targets overexpressed proteins impaired in folding to the ER membrane. The proteins are packed into vesicles by the ER-resident deubiquitinase USP19 and delivered to the plasma membrane for secretion (Volkmar et al., 2016). Therefore, proteins secreted by the MAPS pathway are likely incorrectly folded and inactive.

Next, Gus activity was determined in culture supernatants of AB33_Gus-Jps1 and AB33_cts1 Δ _Gus-Jps1 (Figure 2.9, D). Conversion of the substrate 4-methylumbelliferyl- β -D-glucuronide (MUG) into the fluorescent product 4-methylumbelliferon (4-MU) served as a read-out for actively secreted Gus enzyme. AB33 and AB33_Gus_{cyt} served as negative controls. AB33_Gus-Cts1 was again included as positive control. Active Gus reporter enzyme was secreted into the supernatant of both Gus-Jps1 expression strains. Of note, Gus activity values were about 6.0 μ mol/OD₆₀₀ and thus up to three-fold elevated in comparison to Gus-Cts1 (2.3 μ mol/OD₆₀₀). Furthermore, this result supports independence of Jps1 from Cts1 in terms of unconventional secretion. As expected, barely any Gus activity was determined in culture supernatants of both negative controls. This result implies, that detection of Gus in supernatants of AB33_Gus_{cyt} during Western Blot analysis, was not related to cell lysis but rather to release of defective protein, eventually by a route similar to the MAPS pathway.

Overall, results of the Gus reporter assay showed that Jps1 is secreted using an unconventional mechanism, similar to Cts1. Moreover, the export of active Gus by Jps1

into the supernatant of AB33_cts1 Δ confirmed independence of Jps1 localization and secretion from Cts1.

2.2.6 N-terminal truncation of Jps1 impairs localization and unconventional secretion of Cts1

Since none of the bioinformatic prediction tools allowed to identify domains or motifs within Jps1, different truncated versions of the protein were generated and expressed in fusion to the Gus reporter enzyme. This should allow to identify regions within the aa sequence that are crucial for function using Gus activity as read out. Furthermore, detection of extracellular Cts1 activity was determined to identify essential parts of Jps1 important for activity and secretion of the chitinase. All reporter gene constructs were inserted ectopically in a specific locus of AB33_jps1 Δ _Cts1G by homologous recombination. In this strain, the endogenous copy of *jps1* is deleted and thus, the different Gus-Jps1 truncation variants (Gus-Jps1_{trunc}) can be assayed for functional complementation. Moreover, the intracellular localization of Cts1 can be assessed by microscopy.

Positions of the different truncations within the 609 aa long sequence of Jps1 were chosen in respect to variable and highly conserved regions indicated by the alignment of Jps1 and its orthologs (see Figure 2.1). Already identified truncations of Jps1 from the UV-mutagenesis screen were considered as well (Figure 2.10, B) (Reindl and Stock et al., 2020). N-terminal truncations were generated by removal of aa 1-21 and 1-87 (Figure 2.10, A). The truncation of aa 1-21 excludes a variable, non-conserved sequence part of Jps1, whereas removal of aa 1-87 eliminates a highly conserved part of the sequence in addition. Furthermore, a larger part of the C-terminal protein region was removed (aa 480-609). This truncation includes a variable and a conserved sequence part of Jps1. To analyse functionality of Jps1 in absence of both variable domains, the truncations of aa 480-609 and aa 1-21 were combined in a single protein variant (aa 21-480). Moreover, Gus in fusion to full-length Jps1 (aa 1-609) expressed in the same strain background served as control, to evaluate complementation of the endogenous *jps1* deletion.

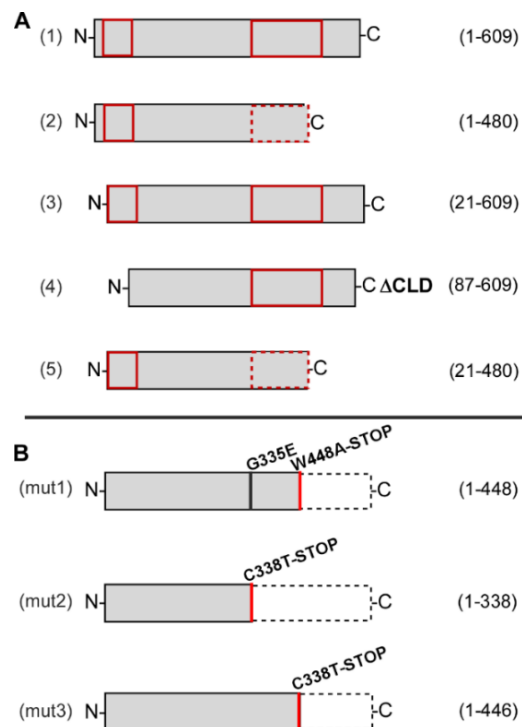


Figure 2.10: Schematic overview of analysed Jps1 truncations. (A) Four different truncations were expressed in fusion to the reporter enzyme Gus (2-5). Lengths (aa) of the different Jps1-truncation versions are indicated next to the schematic truncation variants. Orange regions indicate variable, grey portions conserved regions in comparison to orthologs of Jps1. **(B)** Schematic representation of the Jps1 truncations identified in the UV mutagenesis screen. Extracellular Cts1 activity was diminished comparable to the *jps1* deletion for all three mutant versions.

First, production of the Gus-Jps1_{trunc} reporter proteins was verified by Western Blot analysis. All generated truncated versions of Jps1 were successfully produced (Figure 2.11, A). Signals were detected at the expected sizes for all Gus-Jps1_{trunc} reporter proteins. As expected, no signal was obtained in the sample of progenitor AB33_*jps1* Δ _Cts1G. Bands detected below the main signal likely indicate protein degradation.

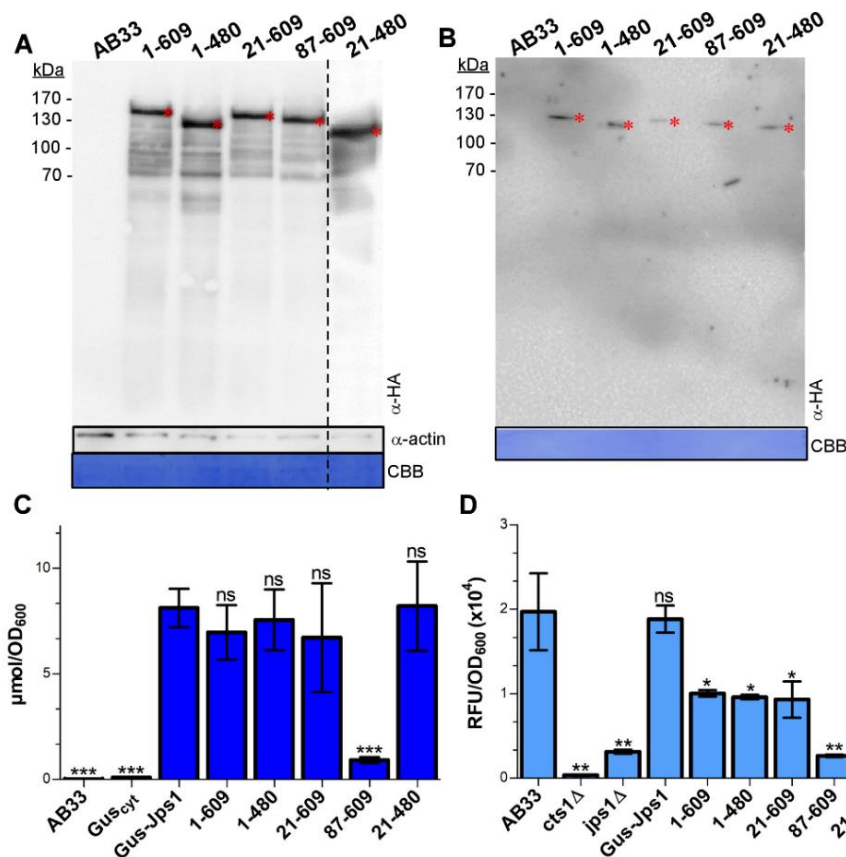


Figure 2.11: Production and secretion of truncated Jps1 variants. Production and secretion of the Gus-Jps1_{trunc} variants: (1-609):150 kDa, (1-480):135 kDa, (21-609):145 kDa, (87-609):140 kDa and (21-480):130 kDa (red asterisks) was analysed by Western Blot in 10 µg total protein from crude cell extracts (**A**) and TCA precipitated supernatants (**B**). AB33_jps1Δ_Cts1G served as a negative control. Anti-HA primary antibody was used for detection. The anti-actin Western Blot confirms analysis of intracellular proteins. The CBB stained Western Blot membrane indicates that similar amounts of total protein have been used. (**C**) Gus activity assay (Stock et al., 2012) in supernatants of the different Gus-Jps1_{trunc} expression strains. AB33 and AB33_Gus_{cyt} served as negative control, AB33_Gus-Jps1 (CbxR) and Gus-Jps1_{trunc} (1-609) as positive controls. The assay was conducted in three biological replicates. Error bars indicate standard deviation. ***, p value < 0.0001; n.s., not significant, p value > 0,05 (two sample t-test, control: Gus-Jps1). (**D**) Extracellular Cts1 activity assay (Koepke et al., 2011; Langner et al., 2015) was analysed for the Gus-Jps1_{trunc} expression strains. AB33, AB33_Gus-Jps1 (CbxR) and AB33_Gus-Jps1 (1-609) served as positive controls, AB33_cts1Δ and AB33_jps1Δ as negative controls: The assay was conducted in three biological replicates. Error bars indicate standard deviation. ***, p value < 0.0001; n.s., not significant, p value > 0,05 (two sample t-test, control: AB33). All strains analysed are derivatives of AB33.

To analyse secretion of the truncated Jps1 proteins, TCA precipitated supernatants of the expression strains were analysed by Western Blot (Figure 2.11, B). All signals detected again corresponded to the expected sizes of the Gus-Jps1_{trunc} full-length proteins. Thus, none of the Jps1 truncations seems to abandon unconventional secretion of the Gus-Jps1_{trunc} reporter protein in general.

To quantify unconventional secretion of the Gus-Jps1_{trunc} reporter proteins, Gus activity was analysed in supernatants of the different expression strains (Figure 2.11, C). The progenitor strain AB33 and a strain producing cytoplasmic Gus (AB33_Gus_{cyt}) served

as negative controls. AB33_Gus-Jps1 (CbxR) and AB33_Gus-Jps1 (1-609), expressing the full-length fusion proteins in different strain backgrounds from the *jp*-locus, were included as positive controls. As expected, both negative controls showed barely any Gus activity in the supernatants. Interestingly, Gus activity values obtained for the Gus-Jps1_{trunc} versions (1-480), (21-609) and (21-480) were similar to those of the positive controls, with around 8 $\mu\text{mol}/\text{OD}_{600}$. Hence, removal of the more variable regions from the N- and C-terminus of Jps1 did not impair its function as carrier protein for Gus. In contrast, Gus activity values for truncation variant (87-609) were significantly lower (1.5 $\mu\text{mol}/\text{OD}_{600}$) and around 89 % reduced compared to the other truncation versions. This result indicates impaired unconventional secretion of Jps1 in the absence of aa 22-87.

To also investigate the impact on secretion of Cts1, extracellular Cts1 activity was determined for the respective Jps1_{trunc} expression strains (Figure 2.11, D). AB33, AB33_Gus-Jps1 (CbxR) and AB33_Gus-Jps1 (1-609) were used as positive controls. Negative controls were represented by AB33_cts1 Δ and AB33_jps1 Δ . Both strains are expected to show no or strongly reduced extracellular chitinase activity (Aschenbroich et al., 2018; Langner et al., 2015; Reindl and Stock et al., 2020). In line with expectations, both positive controls showed high extracellular Cts1 activity with up to 20000 RFU/ OD_{600} . For both negative controls, extracellular Cts1 activities of 300 (cts1 Δ) and 3000 (jps1 Δ) RFU/ OD_{600} were detected and thus, were significantly reduced as expected. Chitinase activity values for strains producing the Gus-Jps1_{trunc} reporter proteins (1-480), (21-609) and (21-480) were comparable to those of AB33_Gus-Jps1 (1-609) with about 9000 RFU/ OD_{600} . Similar to results of the Gus activity assays, the strongest decrease of Cts1 activity was determined for the Jps1 truncation (87-609) with about 2500 RFU/ OD_{600} . Thus, chitinase activity was about 28 % reduced in comparison to strains producing the other Jps1 truncation proteins and comparable to AB33_jps1 Δ . Of note, Cts1 activity in the strain background of AB33_Gus-Jps1 (1-609) complemented with full-length Gus-Jps1 was reduced in general, suggesting either positional effects or slight interference of Gus with Jps1 function. Comparing activity values of AB33 to AB33_Gus-Jps1 (1-609) revealed a 50% reduction of extracellular chitinase activity.

In summary, combined results of the Gus reporter- and Cts1 activity assays implied importance of the N-terminally located aa-stretch (22-87) of Jps1 for functional

secretion of Jps1 and Cts1. Absence of this protein region resembled the *jps1* deletion phenotype in terms of extracellular Cts1 activity.

Next, microscopic analysis of Cts1G in background of the different Jps1-truncations was conducted to additionally investigate potential effects on the intracellular localization of the chitinase. Interestingly, localization of Cts1 was only changed in the strain synthesizing Gus-Jps1_{trunc} (87-609) (others not shown). Instead of localizing within the fragmentation zone, Cts1G accumulated at the primary or secondary septum (Figure 2.12, A-B). Hence, Cts1 localization resembled the *jps1*Δ phenotype.

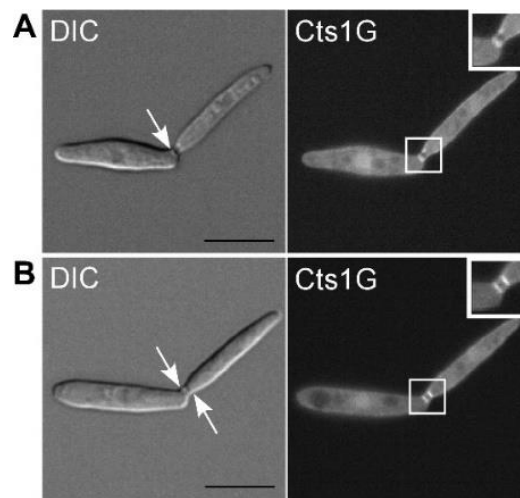


Figure 2.12: Localization of Cts1G in an AB33 derivative producing Gus-Jps1_{trunc} (87-609). Fluorescence microscopy of Cts1G in AB33_Gus-Jps1_{trunc} (87-609). Arrows indicate the presence of septa. A primary septum is visible in (A), primary and secondary septum in (B). Scale bars: 10 μm.

Taken together, this microscopic study supports the finding of strongly reduced extracellular chitinase activity obtained for AB33_Gus-Jps1_{trunc} (87-609). Absence of the domain resembled the *jps1*Δ phenotype, in terms of Cts1 activity and localization. Hence, this missing aa sequence of Jps1 might resemble a domain crucial for correct targeting of Cts1 into the fragmentation zone. In the following, this first putative domain of Jps1 will be referred to as Cts1 localization domain (CLD).

2.2.7 Jps1^{ΔCLD} does not localize to the fragmentation zone during late cytokinesis

In the next step intracellular localization of Jps1 was analysed in absence of the CLD. Therefore, *jps1*^{ΔCLD}-*gfp* was expressed under control of its putative native promoter sequence from the ectopic *ip*^s-locus in two different strain backgrounds: AB33, still harbouring the endogenous copy of *jps1* and AB33_*jps1*Δ. Additionally, full-length *jps1*

in fusion to *gfp* was expressed from the *ip^s*-locus in the same strain backgrounds to verify complementation of the endogenous *jps1* deletion in terms of localization.

First, production of the full-length fusion proteins Jps1G and Jps1^{ΔCLDG} by AB33 and AB33_ *jps1*Δ was investigated by Western Blot analysis (Figure 2.13, A). Cell extracts from AB33_ *Cts1*G were included as positive control (T. Langner, Diss. 2015) and from AB33 as negative control.

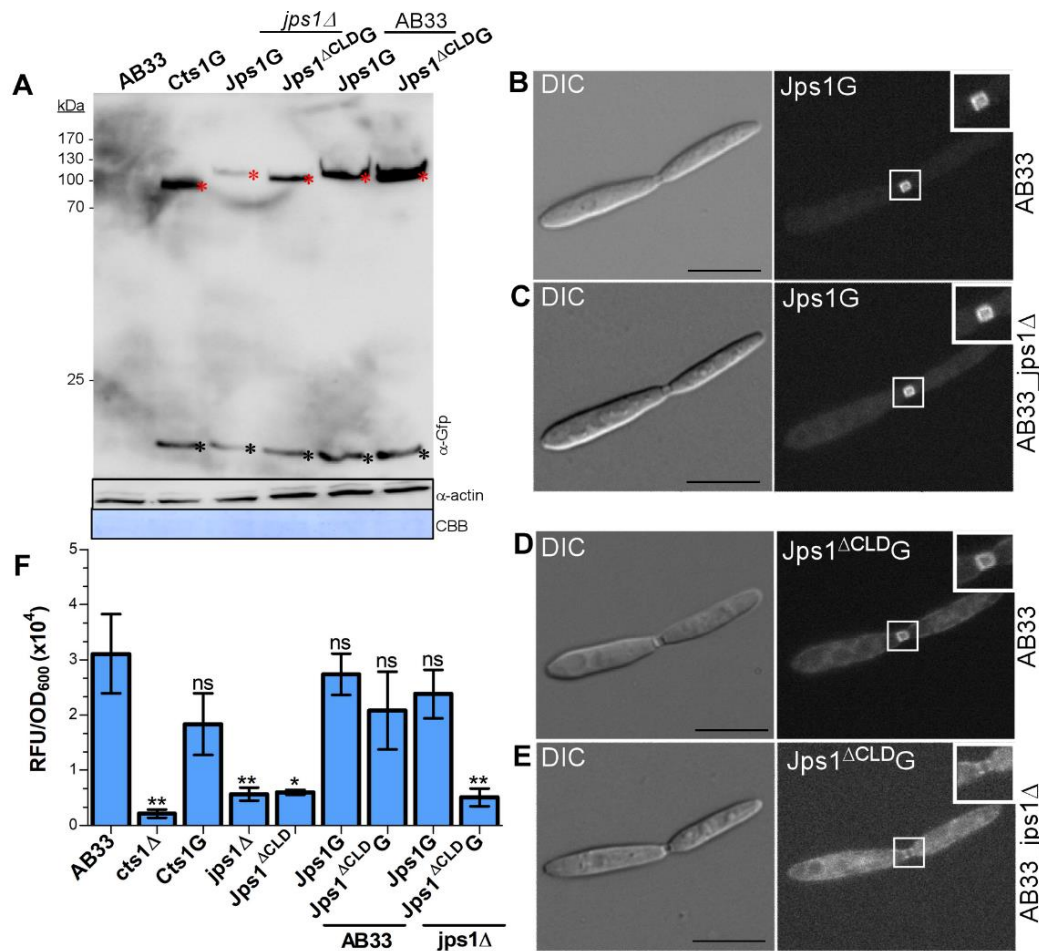


Figure 2.13: Intracellular localization of Jps1^{ΔCLD}. (A) Western Blot to verify production of Jps1G (110 kDa) and Jps1^{ΔCLDG} (105 kDa) full-length proteins (red asterisk). 10 μg total protein from crude cell extracts was used for analysis. AB33 served as negative and AB33_ *Cts1*G (100 kDa) as positive control. An anti-Gfp primary antibody was used for detection. The anti-actin Western Blot confirms analysis of intracellular proteins. The CBB stained Western Blot membrane indicates that similar amounts of total protein have been used for analysis. Fluorescence microscopy of Jps1G in AB33_ *Jps1*G (B) and AB33_ *jps1*Δ_ *Jps1*G (C). Fluorescence microscopy of AB33_ *Jps1*^{ΔCLDG} (D) and AB33_ *jps1*Δ_ *Jps1*^{ΔCLDG} (E). (F) Extracellular Cts1 activity (Koepeke et al., 2011; Langner et al., 2015) was analysed for AB33_ *Jps1*^{ΔCLDG}, AB33_ *jps1*Δ_ *Jps1*^{ΔCLDG} and AB33_ *jps1*Δ_ *Jps1*G. AB33 and AB33_ *Cts1*G served as positive controls, and AB33_ *cts1*Δ, AB33_ *jps1*Δ and AB33_ *Gus*-*Jps1*_{trunc} (87-609) as negative controls. The assay was conducted in three biological replicates. Error bars indicate standard deviation. ***, p value < 0.0001; n.s., not significant, p value > 0,05 (two sample t-test, control: AB33). All strains analysed are derivatives of AB33.

In line with expectations, no signal was observed for AB33 but for *Cts1*G at the corresponding size. Jps1G and Jps1^{ΔCLDG} were produced as full-length fusion proteins

by AB33 and AB33_jps1Δ. Additional bands observed in every sample, except for AB33, at approximately 15 kDa likely indicate presence of free Gfp.

Next, the intracellular localization of Jps1G and Jps1^{ΔCLD} was analysed by fluorescence microscopy (Figure 2.13, B-E). A signal inside the fragmentation zone, related to presence of Jps1G, was detected in AB33 (B) and AB33_jps1Δ (C) backgrounds. This result confirmed functionality of the chosen *jps1* promoter region and functional complementation of the endogenous *jps1* deletion by expressing *jps1* from the *ip^s*-locus. By contrast, Jps1^{ΔCLD}G (E) did not localize within the fragmentation zone of AB33_jps1Δ. In striking contrast, in AB33 with presence of the endogenous full-length copy of Jps1, Jps1^{ΔCLD}G was detectable inside the fragmentation zone (D). This indicated a recruitment of Jps1^{ΔCLD}G to the fragmentation zone, likely by full-length Jps1. Of note, the fluorescence signal within the fragmentation zone seemed to be reduced in comparison to Jps1G in AB33 or AB33_jps1Δ. Moreover, an elevated cytoplasmic background signal indicated mis-localization of some Jps1^{ΔCLD}G molecules. Thus, Jps1 can possibly recruit other Jps1 proteins *in vivo*.

Extracellular Cts1 activity of the expression strains was determined to verify complementation of the endogenous *jps1* deletion by Jps1G and Jps1^{ΔCLD}G in terms of Cts1 secretion (Figure 2.13, F). AB33 and AB33_Cts1G served as positive controls. AB33_cts1Δ, AB33_jps1Δ and AB33_Gus-Jps1_{trunc} (87-609) were included as negative controls. As expected, the Cts1 activity values of AB33_Jps1G and AB33_jps1Δ_Jps1G (23800 RFU/OD₆₀₀) were comparable to the positive control AB33_Cts1G (18300 RFU/OD₆₀₀). As suggested by the restored localization of Jps1^{ΔCLD}G to the fragmentation zone during microscopy, Cts1 activity values in AB33_Jps1^{ΔCLD}G were about 20300 RFU/OD₆₀₀, thus similar to the positive controls. In contrast, activity values obtained for AB33_jps1Δ_Jps1^{ΔCLD}G were strongly reduced (5100 RFU/OD₆₀₀) and on the level of both negative controls (5500 RFU/OD₆₀₀). Hence, secretion of active Cts1 was only detectable in the presence of functional full-length Jps1.

In summary, absence of functional Jps1 impairs localization of Jps1^{ΔCLD}G to the fragmentation zone and restricts unconventional secretion of Cts1. Thus, Jps1 might show self-interaction.

2.2.8 Bioinformatic predictions suggest the formation of amphipathic helices by the CLD

Having a first potential sequence for a functional Jps1 domain in hands, bioinformatic analyses were conducted. According to PSI-BLAST analysis, the CLD shows weak similarity to an ANTH-domain containing protein from *Schizopora paradoxa* (Figure 2.14, A). ANTH-domains likely interact with PtdIns(4,5)P₂ containing membranes like the plasma membrane (Lemmon, 2008). Moreover, the prediction tool HeliQuest indicated potential formation of amphipathic helices within the CLD (Figure 2.14, B). The aa composition of such domains allows to form an α -helix with hydrophobic and hydrophilic faces for membrane association (Lai et al., 2012).

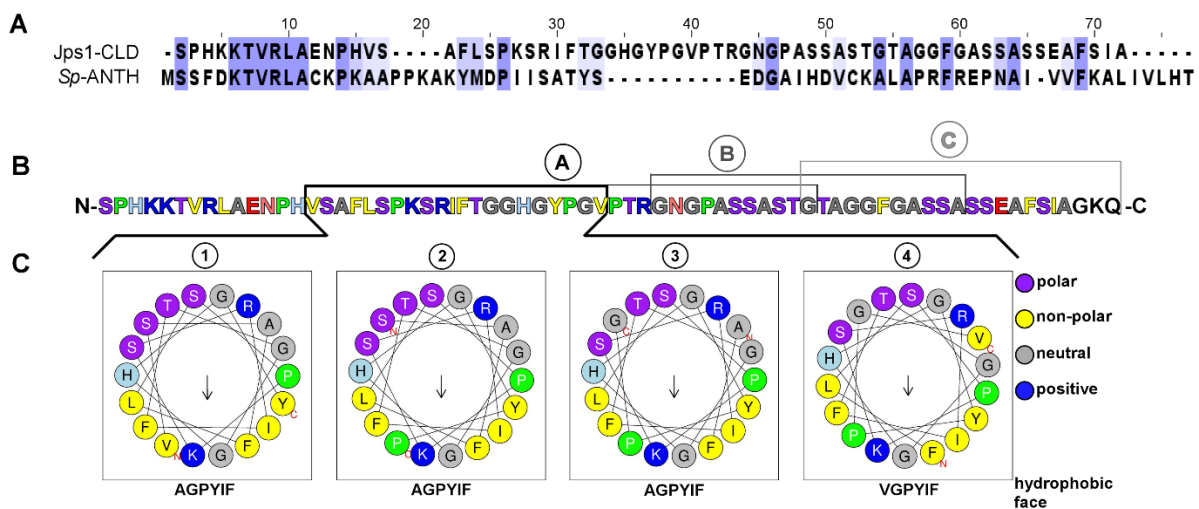


Figure 2.14: ANTH-domain similarity and putative formation of amphipathic helices within the CLD of Jps1. (A) Global pairwise alignment of the CLD and the N-terminal region (aa 1-66) of an ANTH-domain containing protein from *Schizopora paradoxa*. Conserved aa residues are highlighted in shades of darker blue, less conserved in lighter blue (BLOSUM62 Score, JalView). (B) aa sequence of the CLD. Colours represent aa groups: purple=polar; yellow=non-polar; grey=neutral; blue=positive; green=proline (poorly hydrophobic); blue-grey=histidine (poorly hydrophobic). The CLD can be divided into three parts: A, B and C. Each part contains a stretch of polar and non-polar aa, potentially able to form amphipathic helices for membrane association. Part C involves aa directly adjacent to the CLD, depicted in black. (C) Helical wheels exemplarily displaying the potential aa arrangement to form amphipathic helices within a stretch of CLD part A. Each wheel depicts 18 aa. The hydrophobic face of each wheel is indicated underneath. The highlighted section of CLD part A, allows the formation of four potential amphipathic helices. Prediction by HeliQuest (see Mat/Met pp. 96).

Figure 2.14, C exemplarily depicts helical wheels for one sequence part of the CLD. Each wheel contains a stretch of 18 aa analysed by the algorithm for amphipathic helix formation. The hydrophobic face of the helix must at least contain an uninterrupted sequence of five to six non-polar aa. Glycine residues are considered as neutral aa. If they are present within or adjacent to a stretch of polar or hydrophobic aa, they are included into the respective group by the algorithm of the program. The CLD contains

three parts (A, B and C; Figure 2.14, B), each harbouring a composition of polar and non-polar aa capable to form amphipathic helices. In part A, aa would allow to assemble into amphipathic helices with four possible hydrophobic faces (1-4).

In conclusion, an essential Jps1 domain (CLD) was identified, crucial for sufficient secretion and intracellular localization of Cts1. It shows properties pointing towards a membrane interaction.

2.3 *In vitro* analysis of Jps1

2.3.1 Biochemical analysis of Jps1

In order to analyse Jps1 in terms of structure and to verify the *in silico* and *in vivo* results indicating self-interaction and membrane association, high amounts of Jps1 protein were needed. Therefore, heterologous expression of Jps1 in *E. coli* was established. BL21 (DE3) was used as expression strain since it is engineered to be compatible with the strong pET vector system. BL21 is a lysogen of bacteriophage DE3, thus harbouring a genomic copy of the T7 polymerase gene. Expression of the T7 polymerase is under control of the lacUV5 promoter and therefore inducible upon addition of IPTG. The genomic sequence of *jps1* was inserted into pET22b), harbouring the T7-specific promoter sequence and coding for a sextuple histidine-tag. Once transcription of the T7 polymerase has been initiated in the presence of IPTG, Jps1^{His} should be produced in high amounts. Of note, the *peIB*-leader sequence in pET22b, allowing for a periplasmic expression of heterologous proteins, was removed.

2.3.2 Recombinant Jps1 forms a homo dimer

To investigate heterologous expression of Jps1^{His} using the strong pET system, Jps1^{His} was produced in BL21(DE3) and purified from cell extracts of the expression strain using immobilized metal chelate affinity chromatography (IMAC) via a nickel-nitrilotriacetic acid (Ni-NTA) matrix. The chromatogram obtained during the purification (Figure 2.15) using the ÄKTA prime system (GE Healthcare) depicts UV absorbance (mAU) and allows to follow the different steps of the purification. Aromatic aa within the protein backbone absorb UV light at 280 nm. The first plateau in the chromatogram (40-130 mL/ 1480 mAU) is related to loading of the protein-rich cell extract onto the column, a binding phase and a flow-through of unbound protein from the column. The next small peak at 150 mL represents the washing step and is related to more

unspecifically bound protein which is eluted. The next longer plateau (180-260 mL/ 1100 mAU) is caused by an additional washing step with ATP, also absorbing at 280 nm. This washing step should eliminate DnaK, an *E. coli* contaminant, from the column. The final peak in the chromatogram (305 mL/ 980 mAU) represents the elution of putative Jps1^{His}.

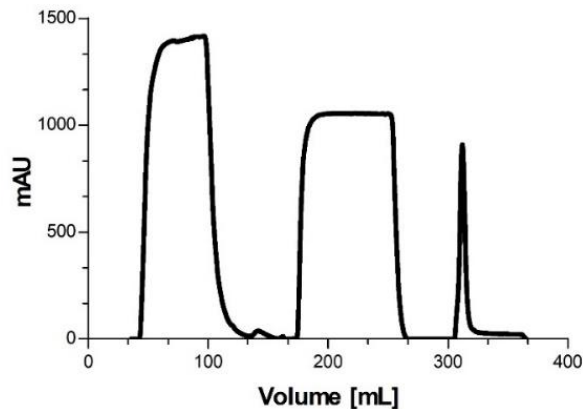


Figure 2.15: Purification of recombinant Jps1^{His}. The protein was expressed and purified from *E. coli* cell extracts by IMAC. The chromatogram depicts UV absorbance values at 280 nm (mAU) obtained during the purification. HisTrap HP column (GE Healthcare).

To assess homogeneity and determine the molecular weight of purified Jps1^{His} size exclusion chromatography (SEC) was conducted in comparison to a previously determined size standard (see Mat/Met p.119, Table 13). Larger molecules, like oligomeric protein complexes, have a shorter retention time on the SEC column than smaller ones, since they do not interact with pores of the column matrix. Jps1 in its monomeric state has a size of around 65 kDa. Thus, elution from the column would be expected after approximately 14 mL.

The first fraction of Jps1^{His} eluted directly after the void volume of the column at approximately 8 mL, indicated by a small peak in the UV spectrum at 58 mAU (Figure 2.16, A).

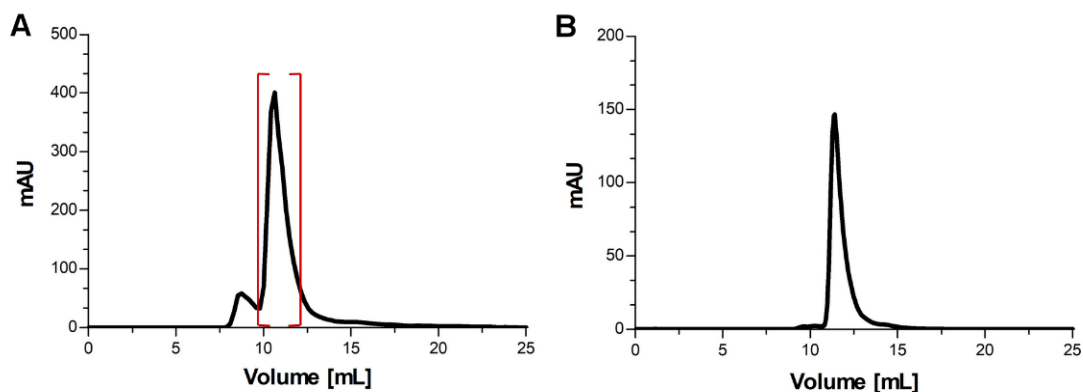


Figure 2.16: SEC of recombinant Jps1^{His}. (A) 6 mg/mL of IMAC purified and concentrated (Amicon Ultra, 50K) Jps1^{His} were used for analysis. (B) Second SEC of peak fraction [] from SEC1. 2 mg/mL purified protein were used for analysis. Dead volume of the column :8 mL, Superdex 200 10/30 GL column.

Interestingly, this might either correspond to an oligomer of Jps1 or to a protein aggregate. The small peak was directly followed by another one at 11.8 mL and 405 mAU, presenting the main peak of the SEC. Compared to the size standard, elution at this volume would resemble a protein of approximately 400 kDa, equalling a hexameric complex of Jps1.

To eliminate the putative aggregate eluting directly before the main fraction of Jps1, only the latter fraction was reloaded onto the SEC column. Apparently, this time only the main peak was obtained after 11.8 mL (Figure 2.16, B). Therefore, sequential SEC of the main fraction from SEC1 allowed to diminish the putative aggregate peak at the void volume of the column.

To verify if observed peaks in the chromatograms indeed correspond to purified Jps1^{His} full-length protein, collected fractions were analysed by SDS-PAGE followed by Coomassie Brilliant Blue (CBB) staining and Western Blot analysis. A signal corresponding to the presence of Jps1^{His} was expected at 70 kDa.

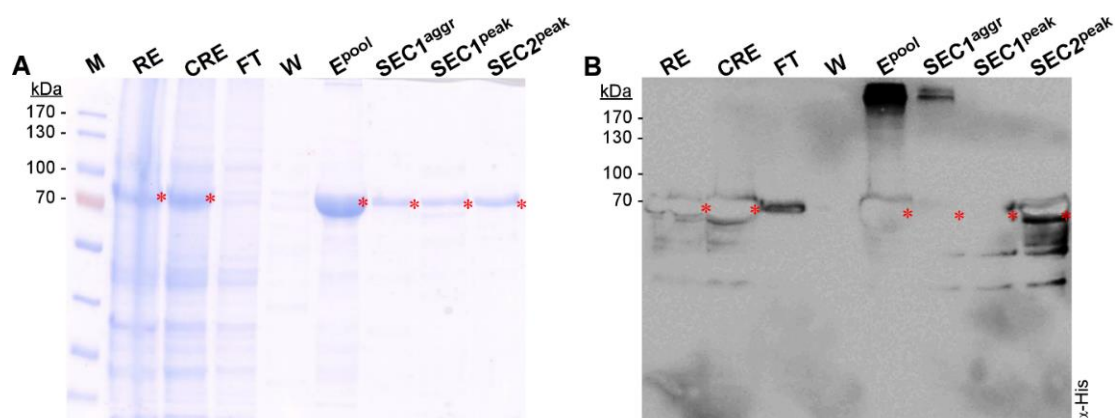


Figure 2.17: Purification of Jps1^{His}. Production and purification of recombinant Jps1^{His} after IMAC and SEC was analysed by SDS PAGE with subsequent CBB staining (A) and Western Blot. (B). Jps1^{His} has a theoretical molecular mass of 70 kDa (red asterisk). Anti-His antibody was used for detection. M=Marker, RE=Raw Extract, CRE=Cleared Raw Extract, FT=Flow Through, W=Wash, Epool= pooled Elution fraction, SEC1_Agg: Aggregate Peak fraction of SEC 1, SEC1_Peak: Main Peak fraction of SEC 1, SEC2_Peak: Main Peak fraction of SEC 2.

A band at 70 kDa was present in the raw extract (RE) and the cleared raw extract (CRE) fractions, indicating successful expression of Jps1^{His} (Figure 2.17, A). In line with expectations, no bands were visible in the flow through (FT) and the wash fractions (W), suggesting efficient binding of Jps1^{His} to the Ni-NTA matrix. Elution of Jps1^{His} from the IMAC column was confirmed by the band detected in the pooled elution fractions (Epool), again at 70 kDa. Bands obtained for full-length Jps1 in the size-exclusion runs SEC1 and SEC2 indicate elimination of contaminant proteins still present in the Epool fraction after IMAC.

To confirm identity of Jps1^{His} and to exclude that signals obtained in the CBB staining are related to host-encoded histidine-rich proteins, Western Blot analysis was performed (Figure 2.17, B). Signals were detected at 70 kDa in the RE, CRE, Epool and SEC1/2 fractions, confirming successful purification of Jps1^{His}. However, results of the Western Blot analysis indicate partial degradation of Jps1^{His} in the different fractions, due to the presence of weaker bands below the full-length band at 70 kDa.

In the next step, the oligomerization of Jps1, as suggested by the SEC experiments, was analysed by multi angle light scattering (MALS) (performed in cooperation with Olivia Spitz (Institute for Biochemistry I, HHU)) (Figure 2.18).

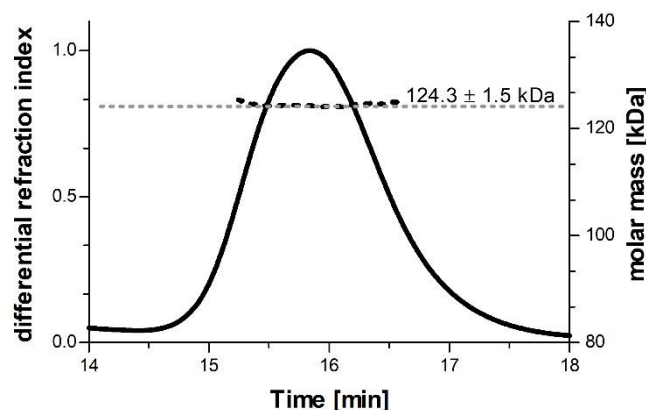


Figure 2.18: MALS of recombinant Jps1^{His}. 2 mg/mL of homogeneously purified Jps1^{His} were used for analysis. The chromatogram shows the differential refraction index obtained during analysis. Performed in cooperation with Olivia Spitz (Institute for Biochemistry I, HHU, Univ. Prof. Lutz Schmitt). SEC: Superdex 200 10/30 GL column, miniDAWN,TREOS.

With a differential refraction index of 1.0 after 16 minutes' retention time on the analytic column, results of the MALS analysis pointed towards a molecular weight of around 125 kDa, indicating that recombinant Jps1 resembles a homo dimer rather than a hexamer.

2.3.3 Recombinant Jps1^{ΔCLD} forms a homo dimer

To also investigate the biochemical properties of Jps1^{ΔCLD}, heterologous expression in *E. coli* was established as well. Again BL21 (DE) was used as expression host and the genomic sequence of *jps1*^{ΔCLD} was integrated into the pET22b_6xHis expression vector, without *pelB* leader sequence.

Similar to Jps1^{His}, successful expression and purification was again achieved by IMAC using a Ni-NTA matrix and the ÄKTA prime system (GE Healthcare).

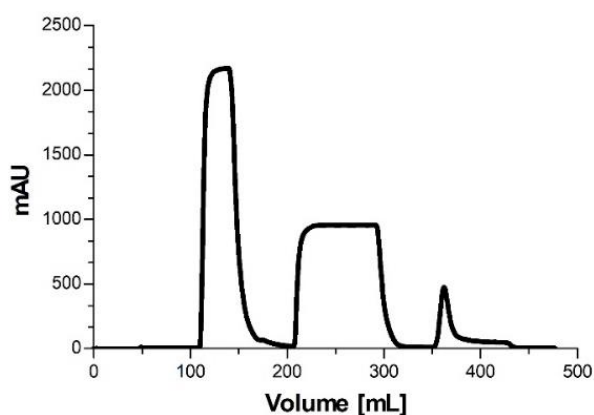


Figure 2.19: Purification of recombinant Jps1^{ΔCLDHis}. The protein was expressed and purified from *E. coli* cell extracts by IMAC. The chromatogram depicts UV absorbance values at 280 nm (mAU) obtained during the purification. HisTrap HP column (GE Healthcare).

Jps1^{ΔCLDHis} was successfully purified, indicated by the final peak in the chromatogram after 355 mL at 480 mAU (Figure 2.19).

Homogeneity and molecular weight of Jps1^{ΔCLDHis} were further determined by SEC (Figure 2.20). Jps1^{ΔCLDHis} has a size of around 60 kDa. Hence, elution from the column would be expected after 14 mL (see Mat/Met p. 119, Table 13). As observed for Jps1^{His} before, the first fraction of Jps1^{ΔCLDHis} eluted directly after the void volume of the column at approximately 8 mL, indicated by a small peak in the UV spectrum at 58 mAU. It was directly followed by the main peak after 11.8 mL and 900 mAU. Again, elution after this volume would correspond to hexameric complex of Jps1^{ΔCLD}. In contrast to

Jps1^{His}, SEC was only performed once for Jps1^{ΔCLDH_{is}}, since the protein partly precipitated on the column.

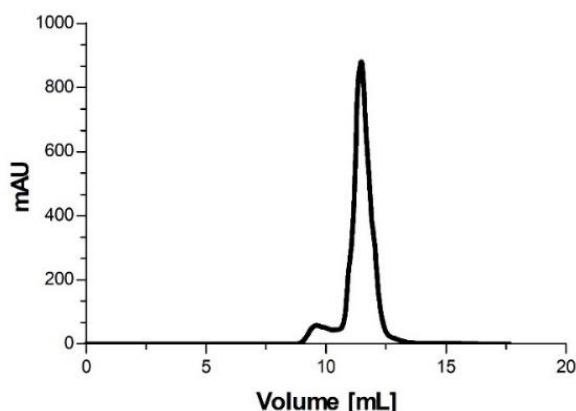


Figure 2.20: SEC of recombinant Jps1^{ΔCLDH_{is}}. 6mg/mL IMAC-purified and concentrated (Amicon Ultra, 50K) Jps1^{ΔCLDH_{is}} were used for analysis. Dead volume of the column: 8 mL; Superdex 200 10/30 GL column.

To verify purification of Jps1^{ΔCLDH_{is}} full-length protein, fractions collected during IMAC and SEC were analysed with SDS-PAGE followed by CBB staining and Western Blot. A signal corresponding to Jps1^{ΔCLDH_{is}} was expected at 65 kDa.

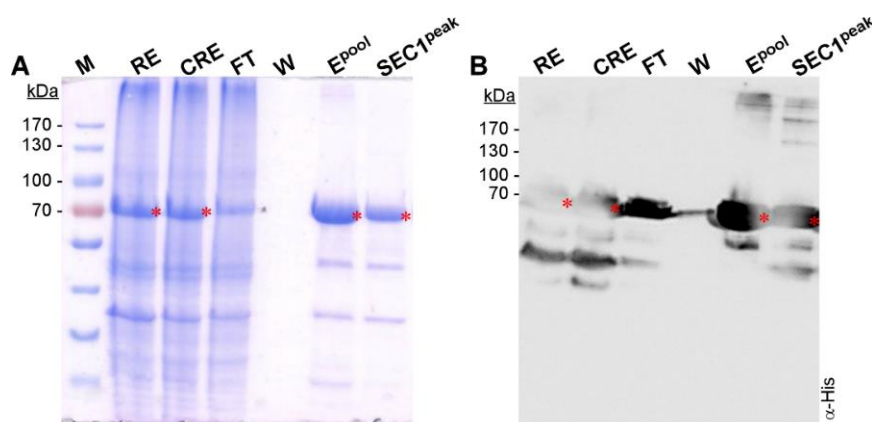


Figure 2.21: Purification of Jps1^{ΔCLDH_{is}}. Production and purification of recombinant Jps1^{ΔCLDH_{is}} after IMAC and SEC was analysed by SDS PAGE with subsequent CBB staining (A) and Western Blot (B). Jps1^{ΔCLDH_{is}} has a theoretical molecular mass of 65 kDa (red asterisk). Anti-His antibody was used for detection. M=Marker, RE=Raw Extract, CRE=Cleared Raw Extract, FT=Flow Through, W=Wash, Epool= pooled Elution fraction, SEC1_Agg: Aggregate Peak fraction of SEC 1, SEC1_Peak: Main Peak fraction of SEC 1.

Indeed, bands obtained after CBB-staining at 65 kDa in the raw extract (RE), the cleared raw extract (CRE) and the pooled elution fractions (Epool), indicated successful expression and purification of Jps1^{ΔCLDH_{is}} (Figure 2.21, A). Bands visible below 65 kDa likely indicate degradation of Jps1^{ΔCLDH_{is}} or the presence of histidine-rich contaminants from the *E. coli* cell extract.

The presence of Jps1^{ΔCLDHis} in the elution and SEC fractions was further confirmed by Western Blot analysis (Figure 2.21, B). Signals detected at 65 kDa confirmed successful purification of Jps1^{ΔCLDHis}. Additional bands detected below the main band at 65 kDa in the Epool and SEC fraction, indicate degradation of full-length Jps1^{ΔCLDHis}. MALS analysis was again used to further determine the molecular weight of Jps1^{ΔCLDHis} (performed in cooperation with Olivia Spitz (Institute for Biochemistry I, HHU)). Results interestingly pointed towards a molecular weight of around 121 kDa. Thus, recombinant Jps1^{ΔCLD}, similar to full-length Jps1, resembles a homo dimer (Figure 2.22).

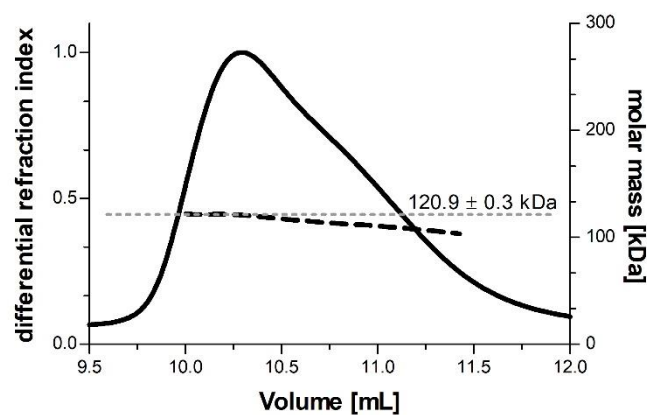


Figure 2.22: MALS of recombinant Jps1^{ΔCLDHis}. 2 mg/mL of homogeneously purified Jps1^{ΔCLDHis} were used for analysis. The chromatogram shows the differential refraction index obtained during analysis. Performed in cooperation with Olivia Spitz (Institute for Biochemistry I, HHU, Univ. Prof. Lutz Schmitt). SEC: Superdex 200 10/30 GL column; miniDAWN, TREOS.

2.3.4 Blue Native PAGE confirms homo-dimerization of Jps1 and Jps1^{ΔCLD}

To further verify the dimerization of Jps1^{His} and Jps1^{ΔCLDHis} as calculated from MALS, a Blue Native PAGE (BNP) was conducted. Here, proteins are separated according to their molecular weight and native structure. Hence, protein dimerization and oligomerization should be indicated by this method. The BNP revealed homo-dimerization of both, Jps1^{His} and Jps1^{ΔCLDHis} (Figure 2.23). In comparison to the size marker, the main portion of Jps1^{His} and Jps1^{ΔCLDHis} was observed at around 140 and 150 kDa, respectively.

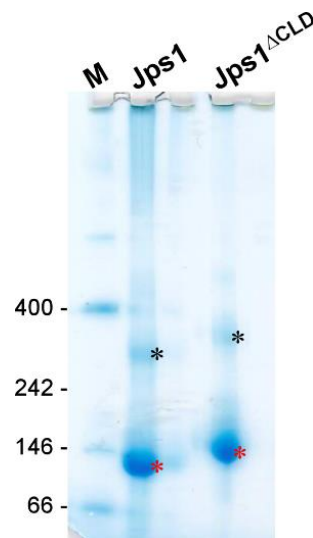


Figure 2.23: Blue native PAGE of Jps1^{His} and Jps1^{ΔCLDHis}. 2 μg of recombinant, IMAC-purified protein was used for analysis. Proteins were separated on TRIS acetate gels. Jps1^{His} has a theoretical molecular mass of 70 kDa, Jps1^{ΔCLDHis} of 65 kDa. Red asterisks indicate dimeric species of both protein variants, black asterisks tetrameric species. M= molecular size standard (see Mat/Met pp.119).

Interestingly, additional protein bands running at a size of approximately 300 kDa indicated formation of even higher oligomeric complexes, e.g. homo-tetramers, for both proteins. Of note, bands obtained for Jps1^{ΔCLDHis} ran slightly higher compared to Jps1^{His}, though Jps1^{ΔCLDHis} has a lower molecular weight. BNP is a method optimized to separate globular proteins according to their size. Hence, an altered running behaviour of Jps1^{ΔCLDHis}, likely caused by changes in the conformation of this mutant protein variant, might be responsible for this observation.

In conclusion, biochemical analysis of recombinant Jps1^{His} and Jps1^{ΔCLDHis} reveal a homo-dimeric conformation for both protein variants. Moreover, MALS and BNP indicate the additional assembly to higher-order complexes like tetramers.

2.3.5 Jps1 binds to phosphatidyl-inositol-phosphates on lipid strips via the CLD domain

The intracellular localization near the plasma membrane, its unconventional secretion and the presence of the amphipathic CLD domain in Jps1 suggest that the protein interacts with lipids. Thus, lipid interaction of the recombinant protein was analysed with lipid strips and giant unilamellar vesicle (GUV) binding assays. To investigate an impact of the CLD in membrane association of Jps1, lipid affinity of Jps1^{ΔCLD} was investigated, as well.

To get a first impression on the lipid binding profile of Jps1, lipid affinity was tested with commercial phosphoinositol-phosphate-containing PIP strips (Echelon). Lipids commonly found in mammalian and fungal cells are present on these strips. Incubation with the purified protein of interest should allow to detect protein-lipid affinities. Therefore, recombinant Jps1^{His} was purified from *E. coli* cell extracts. As a positive control, another lipid strip was incubated with a PiP₂-binding protein (Echelon). Interestingly, Jps1^{His} associated with all kinds of PtdInsPs and phosphatidic acid (PA), but not with phosphatidylserine (PS) or phosphatidylcholine (PC), also abundant in the plasma membrane (Figure 2.24, A).

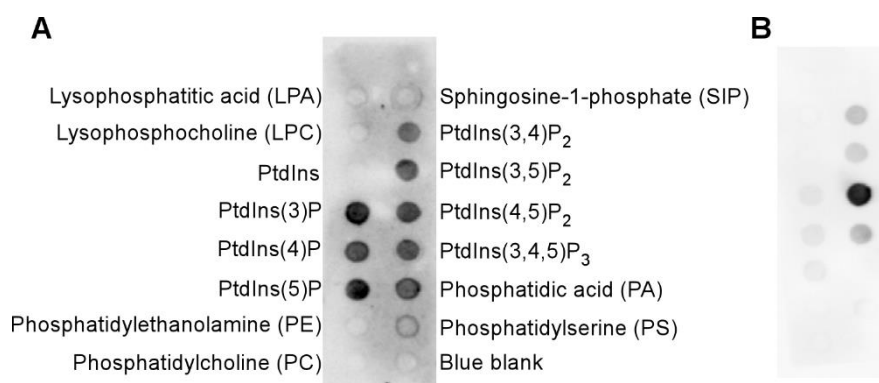


Figure 2.24: Lipid binding analysis of recombinant Jps1^{His}. (A) PIP strip was incubated with 5 µg/mL of IMAC-purified Jps1^{His}. Protein-lipid interactions were detected using an anti-His antibody. (B) A PiP₂-binding protein was used as a positive control and incubated with another PIP strip. Binding signals were detected with an anti-GST antibody.

Functionality of the assay procedure was confirmed by the expected detection signal for the PiP₂-binding protein at the PtdIns(4,5)P₂ lipid spot (Figure 2.24, B).

Next, the assay was repeated using recombinant Jps1^{ΔCLDHis}. This should allow to identify impact of the CLD on the lipid binding behaviour of Jps1 *in vitro*. The PiP₂-binding protein was again included as positive control. Importantly, in contrast to Jps1^{His}, no signals related to lipid association of Jps1^{ΔCLDHis} were detected (Figure 2.25, A).

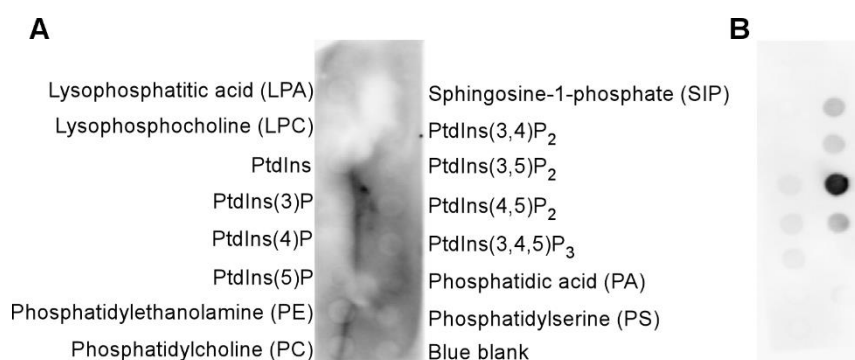


Figure 2.25: Lipid binding analysis of recombinant Jps1^{ΔCLDHis}. (A) PIP strip was incubated with 5 μg/mL of recombinant, IMAC-purified Jps1^{ΔCLDHis}. Protein-lipid interactions were detected using an anti-His antibody. (B) A PiP₂-binding protein was used as a positive control and incubated with another PIP strip. Binding signals were detected with an anti-GST antibody.

A signal obtained for the PiP₂-binding protein at the PtdIns(4,5)P₂ lipid spot confirmed functionality of the assay (Figure 2.25, B).

In summary, results indicate lipid affinity of Jps1 to PtdInsPs and PA. Interestingly, lipid binding of Jps1 seems to be abolished in absence of the CLD.

2.3.6 Jps1 binds PtdIns(4,5)P₂ but not PtdIns(3,4,5)P₃ containing GUVs

To verify PtdIns lipid affinity of Jps1 as indicated by the result of the lipid strip binding assay, PtdIns(4,5)P₂- and PtdIns(3,4,5)P₃ containing GUVs were generated. For this assay, *jps1* was expressed in fusion to *gfp* allowing visualization of the corresponding fusion protein by confocal fluorescence microscopy (in cooperation with S. Hänsch, Centre of advanced imaging, HHU).

Successful expression and purification of recombinant Jps1G^{His} was analysed by SDS PAGE followed by CBB staining and Western Blot analysis (Figure 2.26, A-B). A signal corresponding to Jps1G^{His} was expected at 100 kDa.

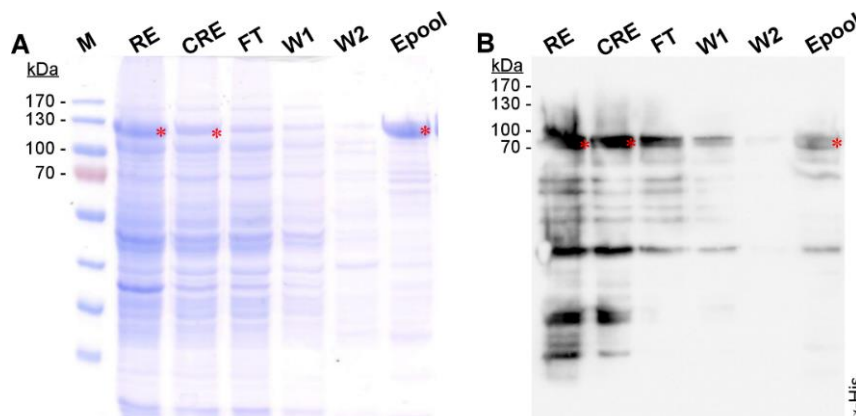


Figure 2.26: Purification of recombinant Jps1G^{His}. Purification of Jps1G by IMAC was analysed by SDS-PAGE with subsequent CBB staining (A) and Western Blot (B). Jps1G has a theoretical molecular mass of 100 kDa, anti-His primary antibody was used for detection. M=Marker, RE=Raw Extract, CRE=Cleared Raw Extract, FT=Flow Through, W=Wash, Epool= pooled elution fraction.

Indeed, a band at approximately 100 kDa was observed in the CBB-stained fractions of Jps1G^{His} (Figure 2.26, A). Unfortunately, bands at 100 kDa were present in the flow through (FT) and wash fraction 1 (W1), as well. This likely indicates overloading of the purification column with protein. Nevertheless, a band at 100 kDa was obtained for the pooled elution fraction (Epool), indicating successful purification of Jps1G^{His} (Figure 2.26, B). The fractions were analysed by Western Blot to exclude enrichment of

histidine-rich contaminants from the *E. coli*. As expected, signals detected at 100 kDa. in the pooled elution fraction (Epool) confirmed the presence of Jps1G^{His}.

GUVs produced by osmotic swelling (see Mat/Met, pp. 122) were labelled with the red-fluorescent dye Texas Red coupled to the lipid 1,2-dihexadecanoyl-sn-glycero-3-phosphoethanolamine (DHPE). Gfp^{His} served as negative control to exclude unspecific binding of Gfp to both PtdInsPs. Importantly, no binding of Gfp^{His} to either PtdIns(4,5)P₂ nor PtdIns(3,4,5)P₃ was observed (Figure 2.27, B/D).

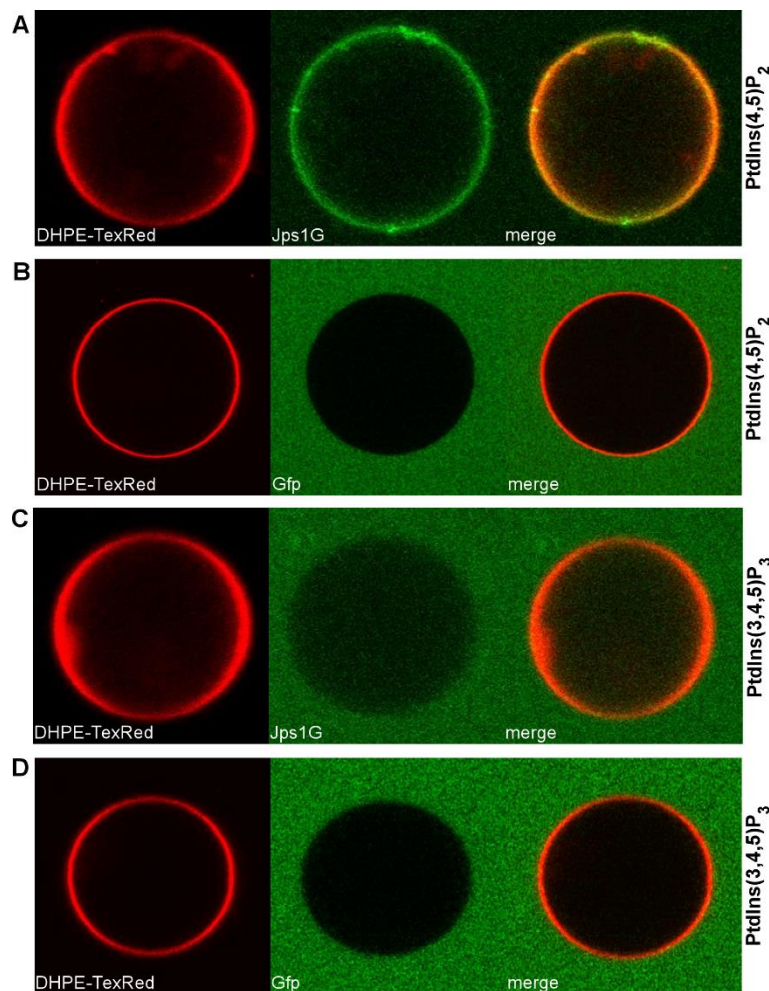


Figure 2.27: GUV binding studies of recombinant Jps1G^{His}. 60 μ g of IMAC-purified Jps1G^{His} was used for analysis. Lipid binding of Jps1G^{His} was analysed for PtdIns(4,5)P₂ (**A**) and PtdIns(3,4,5)P₃- (**C**) containing GUVs. 60 μ g of recombinant, IMAC-purified Gfp^{His} served as negative control (**B/D**). DHPE-TexRed: Signal for GUVs, Gfp: Signal for binding of Jps1G^{His}, merge: overlay of red and green channel. Microscopy was performed in cooperation with S. Hänsch (CAI, HHU).

For Jps1G^{His}, overlay of signals detected in the mCherry (GUV) and Gfp channel confirmed binding of Jps1G^{His} to PtdIns(4,5)P₂ containing GUVs (Figure 2.27, A). Of note, Jps1G^{His} seemed to form punctate accumulations on the GUV surface, resembled by small dot-like signals in the Gfp-channel (Figure 2.28). In contrast, no binding was observed for Jps1G^{His} to PtdIns(3,4,5)P₃ (Figure 2.27, C). Hence, affinity

to PtdIns(3,4,5)P₃, as observed during the lipid strip assay before, was not confirmed in this experiment.

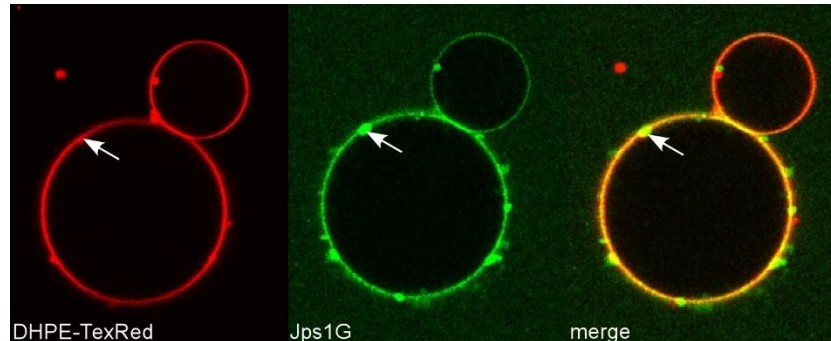


Figure 2.28: Binding studies of recombinant Jps1G^{His} to PtdIns(4,5)P₂-containing GUVs. (A) 60 µg of IMAC-purified Jps1G^{His} was used for analysis. GUVs were analysed after 1 h of incubation with Jps1G^{His} by Airy Scan confocal microscopy (Zeiss, LSM 880). Merge shows overlay signal of the red (lipid) and green (Jps1) channel. DHPE-TeXRed: Signal for GUVs, Gfp: Signal for binding of Jps1G^{His}. Microscopy was performed in cooperation with S. Hänsch (CAi, HHU).

Interestingly, incubation of Jps1G^{His} with the PtdIns(4,5)P₂ containing GUVs for more than one hour likely induced membrane blebbing (Figure 2.29). This was not true for longer incubation of Jps1G^{His} with PtdIns(3,4,5)P₃ containing GUVs. For the negative control, Gfp^{His}, no membrane blebbing or other membrane deformations were visible after longer incubation with both GUV variants (not shown).

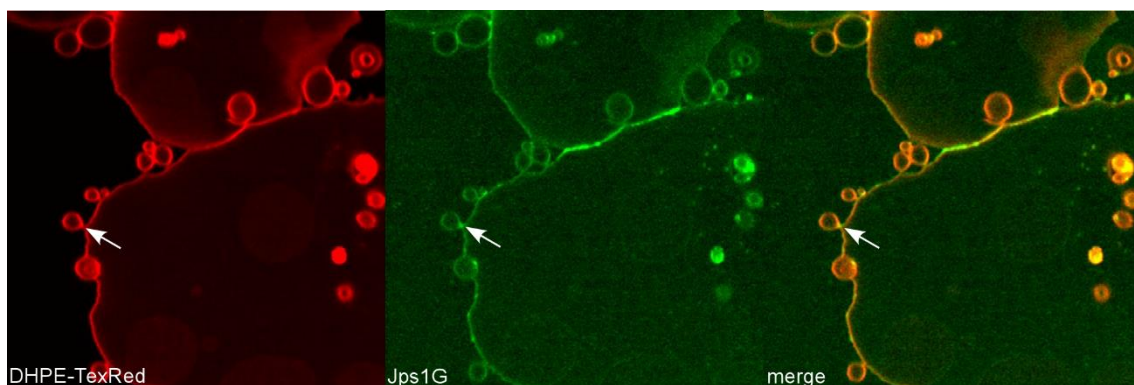


Figure 2.29: Membrane deformation analysis of PtdIns(4,5)P₂-containing GUVs by Jps1G^{His}. 60 µg of IMAC-purified Jps1G^{His} was used for analysis. GUVs were analysed after 1 h of incubation with Jps1G^{His} by Airy Scan confocal microscopy (Zeiss, LSM 880). Merge shows overlay signal of the red (lipid) and green (Jps1) channel. DHPE-TeXRed: Signal for GUVs, Gfp: Signal for binding of Jps1G^{His}. Microscopy was performed in cooperation with S. Hänsch (CAi, HHU).

In summary, the lipid binding activity of Jps1 observed in the lipid strip experiments was partly confirmed in the GUV assays. Jps1 shows affinity to PtdIns(4,5)P₂ but not to PtdIns(3,4,5)P₃.

2.4 Interaction studies

2.4.1 Pull-down analysis of Jps1G from cell extracts identifies putative interaction partners

To shed light on the function or the cellular mechanism Jps1 might be involved in, a pull-down analysis of Jps1G from cell extracts of AB33_Jps1G was conducted, followed by mass spectrometry. Gfp-coupled beads were used to isolate Jps1G and associated proteins. A strain expressing cytoplasmic Gfp (AB33_G) was included as negative control to exclude affinity of potential interactions partners to Gfp. The volcano plot in figure 2.30 summarizes the results of the statistical analysis comparing the enrichment of proteins identified in the pull-down analysis. The fold change between both samples was plotted against the negative log p-value for each protein identified. A protein with a high fold change and a low p-value will appear in the upper right corner of the plot. Proteins were considered enriched significantly (high fold change, high negative log p-value) in samples of AB33_Jps1G, if the fold change between both samples was above 2.0 with a negative log p-value of at least -1.5. Such proteins are represented by red dots in the plot.

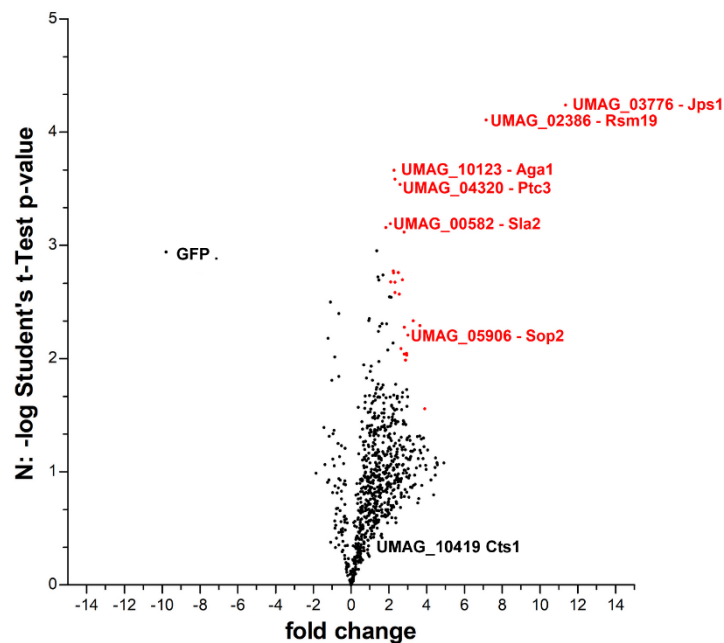


Figure 2.30: Volcano plot of enriched protein candidates identified in the pull-down analysis of Jps1G. Each dot in the volcano plot represents a protein enriched in the pull-down experiments of AB33_Jps1G and the negative control AB33_G. The more abundant a protein was in one of both samples, the higher it appeared on the upper right side of the plot. Red dots mark significantly enriched proteins in the samples of AB33_Jps1G. The assay was conducted in three biological replicates.

According to the volcano plot, protein candidates like Aga1 (UMAG_10123), Ptc3 (UMAG_04320), Sla2 (UMAG_00582) and Sop2 (UMAG_05906) were enriched significantly in the pull-down fraction of Jps1G. Therefore, they resemble putative interaction partners of Jps1. Interestingly, these candidates are orthologues of yeast proteins involved in the regulation of the cell cycle (Aga1/Ptc3) and assembly of the cytoskeleton (Sla2/Sop1), respectively (<https://yeastgenome.org>, last accession: 05/2020). Ribosomal proteins like Rsm19 (UMAG_02386) were quite abundant, as well. However, this might be related to the exponential growth stage of the cells, where protein synthesis is increased. Thus, these proteins might represent contaminants rather than true interaction partners. Unexpectedly, Cts1 (UMAG_10419) was not detected upon the best-hit candidates in the interactome of Jps1.

In essence, putative interaction partners of Jps1 were identified. Interestingly, they belong to cellular complexes crucial for determining cell polarity. Similar to Jps1, these proteins act early in the cell cycle and show a bud-near localization in *S. cerevisiae*. Hence, results of the interactome study suggest a function for Jps1 during establishment of cell polarity.

3. Discussion

3.1 Jps1 resembles a novel protein crucial for unconventional secretion of Cts1

Jps1 was identified during a UV-mutagenesis screen and resembles a novel protein in the lock-type secretion mechanism of Cts1 (Reindl and Stock, 2020). It is conserved in basidiomycetes closely related to *U. maydis*. However, for none of the Jps1 orthologs a putative function has been assessed to date. Importantly, Jps1 is not conserved in ascomycetes like the yeast *S. cerevisiae* and the filamentous fungus *Aspergillus niger*.

Jps1 is not essential for cytokinesis. Deletion of the open reading frame in the genome did not cause changed doubling times or aberrant phenotypes in yeast-like cells. The only protein identified being affected by the absence of Jps1, so far, is Cts1. In line with results of the screen, Cts1 activity was significantly reduced in the extracellular medium of *jps1*-deficient cells in comparison to AB33. Furthermore, microscopic analysis of Cts1G in AB33_ *jps1*Δ showed a mis-localization of Cts1 in the late stage of cytokinesis. Instead of localizing inside the fragmentation zone (Aschenbroich et al., 2018; Langner et al., 2015), Cts1 accumulated at the primary or both septa (Reindl and Stock et al., 2020). Microscopic localization studies also demonstrated that both proteins were present within the fragmentation zone at the same time. Importantly, only localization and secretion of Cts1 depends on Jps1 and not *vice versa*. The perfect co-localization suggests that the two proteins might interact. These observations nicely fit to results obtained during yeast-two-hybrid (Y2H)- and co-purification assays (K. Hussnaetter, Master thesis 2016; S. Wolf, Master thesis 2019). In the Y2H analysis, weak interaction of Jps1 and Cts1 was detected but only when Jps1 was fused to the activating domain of the Gal4 transcription regulator. Successful co-purification was achieved with Jps1 as bait protein, covalently attached to the column matrix. By contrast, in the Jps1 interactome obtained by pull-down analysis, Cts1 was not detected upon the best-hit candidates. This result suggests that the interaction of both proteins might be rather weak or transient than stable and permanent.

Similar to the strategy used by Stock and colleagues (2012) to determine the secretion mode of Cts1, results of the Gus-reporter assay revealed unconventional secretion of Jps1. Gus was transported into the culture supernatant in its active state when fused

to Jps1, confirming evasion of the ER. Interestingly, comparing activity values obtained for Gus-Jps1 to those of Gus-Cts1, extracellular Gus activity was up to three-fold elevated when Jps1 served as carrier protein. This result indicates either a higher protein abundance or a higher secretion rate of Jps1.

3.2 Jps1 might resemble an accessory factor for cell polarization

Apart from the localization of Jps1 in the assembled fragmentation zone, Jps1G was detected early on at the side of bud emerge. It remained in a collar region formed between mother and growing daughter cell until both septa had been formed completely. This observation suggests that Jps1 might be involved in early processes during establishment of the future division zone.

Interestingly, the *U. maydis* septins Cdc3/10/11/12, the septin-specific protein kinase Gin4 and myosin Cdc4 localize to the collar of the division zone during early cytokinesis, too (Böhmer, 2009; Böhmer et al., 2009; Alvarez-Tabarés and Pérez-Martín, 2010). Gin4 is crucial for correct assembly and disassembly of the septins, deletion of the corresponding gene results in impaired cell separation. In contrast to Jps1, Gin4G can be detected in the collar region only until synthesis of the primary septum is initiated. Subsequently, it is not present at the septum but resides in the cytoplasm. Moreover, the localization of the septins and Cdc4 undergoes a transition from the collar into a ring-like structure during septum formation (Böhmer, 2009; Böhmer et al., 2009, Alvarez-Tabarés and Pérez-Martín, 2010). Thus, none of the proteins mentioned above is present in the collar or the septum permanently throughout the cell cycle. Therefore, the constant presence of Jps1 in the collar and finally at both septa indicates that Jps1 might have an accessory function in organizing and maintaining the future division zone. This is supported by the fact, that absence of the septins *cdc10*, *cdc3* and other factors like the Ste20-like kinase *don3* and the GEF *don1* did not affect the localization of Jps1G (data not shown). Importantly, deletion of the single septin genes has drastic impact on cytokinesis and morphology of yeast-like cells. Although deletion of *cdc3* leads to a lemon-like shape, often only with a single septum inserted in the centre of the cell (Alvarez-Tabarés and Pérez-Martín, 2010; Boyce et al., 2005), Jps1 still assembled at the septum. Thus, Cdc3 does not seem to influence Jps1 localization. Cells deficient in *don3* and *don1* can no longer form a secondary septum, crucial for separation of mother and daughter cell (Weinzierl et al., 2002). Tree-like cell clusters result from the missing factors which regulate the

disassembly of the septin collars and the formation of the AMR (Böhmer et al., 2009). However, Jps1G still was detectable in the collar and at the primary septum of the interconnected cells of the respective mutants. Hence, Don1 and Don3 also do not have impact on the intracellular targeting of Jps1.

In *S. cerevisiae*, proteins localizing early to the side of bud formation are usually important for determining cell polarity and organization of the cytoskeleton. The proteins Bni and Bud, for instance, are involved in septum formation and polarization of the actin cytoskeleton. The proteins Bni4 and Bni5 both resemble septin interacting proteins important for correct assembly of the septum ring (Lee et al., 2002; Sanz et al., 2004). Moreover, Bni4 was shown to interact with chitin synthase Chs4, thus it is involved in coordinating the proper assembly of the chitin ring for separation, additionally (DeMarini et al., 1997; Kozubowski et al., 2003). The Ras-like GTPase Bud1, its GEF Bud5 and its GTPase-activating protein Bud2 function as a module to determine the site of budding. Their action is initiated in response to a landmark protein complex which consists of Bud proteins and septins (Casamayor and Snyder, 2002; Chant, 1999). Since some Bni- and Bud orthologs could not be identified in *U. maydis* (Banuett et al., 2008), Jps1 might present one missing factor of this protein family. However, the function of Jps1 also could be different to described proteins from *S. cerevisiae*. Asco- and basidiomycete fungi have evolved differentially and adapted cellular processes to their special needs, including clade-specific protein factors (Carbó and Pérez-Martín, 2010). One major difference between yeast cells from *U. maydis* and *S. cerevisiae* during cytokinesis is the fragmentation zone formed between dividing mother and daughter cell (Langner et al., 2015; Reindl et al., 2019). In *S. cerevisiae*, non-such isolated zone is present between the juxtaposing primary and secondary septa (Bhavsar-Jog and Bi, 2017). Hence, *U. maydis* might require additional proteins involved in the establishment and maintenance of this unusual compartment. Jps1 could resemble one of those, beside factors like Don1 and Don3, which are also not conserved in *S. cerevisiae*.

Importantly, mass spectrometric analysis of the Jps1 interactome obtained by pull-down assays suggested a putative interaction between Jps1 and proteins involved in the early organization of the cytoskeleton and endocytosis. Homologs of the yeast proteins Sla2 (UMAG_00582) and Sop2 (UMAG_05906) were identified during mass spectroscopy. In *S. cerevisiae*, Sla2 serves as an adaptor protein linking actin to

endocytosis. It is present at the cortical actin patch during bud emerge (Wesp et al., 1997). Sop2 is involved in the regulation of cell proliferation and exocytosis. Interacting with the SNARE protein Sec9, it functions in connecting post-Golgi vesicles to the plasma membrane (Lehman et al., 1999).

Hence, results of the pull-down analysis in combination with the microscopic study of Jps1G, hint towards an accessory function of Jps1 in the early establishment of cell polarity.

3.3 The CLD is crucial for unconventional secretion but not for dimerization of Jps1

The analysis of different truncated Jps1 versions allowed to identify a first essential region near its N-terminus, which was termed CLD. Secretion of Cts1 and the Gus-Jps1 reporter protein was unaffected as long as weakly conserved regions of Jps1 were missing. Absence of the CLD, however, resulted in strongly reduced extracellular activity and intracellular mis-localization of Cts1, similar to a *jps1*-deletion background.

Analysing the localization of Jps1 Δ CLD-G in AB33_*jps1* Δ helped to understand mis-targeting of the chitinase: Without CLD Jps1 itself was no longer detectable in the fragmentation zone. Instead, it seemed to localize to the endomembrane system. Importantly, the additional presence of endogenous full-length Jps1 allowed to restore the localization of Jps1 Δ CLD-G and extracellular activity of Cts1. Thus, results hint towards a self-interaction of Jps1. Indeed, comparative size exclusion chromatography (SEC), multi angle light scattering (MALS) and blue native PAGE of both, recombinant Jps1 and Jps1 Δ CLD, confirmed a pre-dominant homo-dimeric conformation. Furthermore, even the formation of tetrameric complexes for a small fraction was indicated.

The exact region mediating the dimerization of Jps1 has not yet been resolved. A region in the very C-terminus, enriched in prolines (aa 490-609), could contribute to the self-association of Jps1. Poly-proline-rich motifs are present in pro- and eukaryotic organisms and known to mediate a range of interactions. However, often the binding ability of such motifs is weak and not very specific (Williamson, 1994). Thus, poly-proline motifs rather allow the spontaneous and reversable association of proteins, as observed for the pre-initiation complex of RNA-polymerase-II (Williamson, 1994), than long-lasting and stable interactions.

Interestingly, the association of FGF-2 monomers is accomplished via cysteine disulphide bridges after recruitment to the plasma membrane by PtdIns(4,5)P₂. There, a slightly less-reducing redox environment compared to the cytoplasm seems to favour the formation of intermolecular disulphide bridges (Müller et al., 2015). The C-terminally located C95 was identified to be crucial for dimerization and displays a unique surface cysteine. Loss or replacement resulted in impaired unconventional secretion of FGF-2 (Müller et al., 2015). A comparable mechanism might apply for association of Jps1. The protein harbours a total number of five cysteine residues (C131, C228, C232, C260, C407) which could form intra- or intermolecular disulphide bridges. Nevertheless, to verify a potential role of the cysteine residues in dimerization and unconventional secretion of Jps1, structural data need to be generated. Analysis of cysteine-replacement mutants can be conducted concomitantly.

3.4 The CLD is involved in lipid binding of Jps1

The apparent proximity to the plasma membrane of Jps1 throughout the cell cycle suggested that the protein might bind to membranes. Hence, lipid affinity was tested. On commercial lipid strips, Jps1 bound to different PtdInsPs and PA. In absence of the CLD, lipid affinity was abolished. This is in line with the mis-localization observed for Jps1 Δ CLD-G during microscopy and highlights the importance of the CLD for the membrane-standing localization of Jps1.

The high abundance of basic and hydrophobic aa residues in the CLD could favour association with lipid membranes through hydrophobic interactions or the formation of amphipathic helices (Martin, 2012; McLaughlin et al., 2002). Interestingly, according to predictions by HeliQuest (<http://heliquet.ipmc.cnrs.fr/>) the CLD might indeed have intrinsic properties to form amphipathic helices. Such helices can insert into the inner leaflet of the plasma membrane (Parton et al., 2006). Moreover, amphipathic helices were shown to function in the sensing or induction of membrane curvature, as observed for α -synuclein and annexin B12 by Jensen and colleagues (2011). A role in sensing of membrane curvature would fit to the early localization of Jps1 to the zone of bud emerge.

Moreover, based on predictions by the NCBI server PSI-BLAST, the CLD seems to display similarity (25%) to the N-terminal portion (aa 1-66) of an ANTH-domain containing protein from the basidiomycete mushroom *Schizopora paradoxa* (see

results, pp. 50). ANTH-domains preferably interact with PtdIns(4,5)P₂ and are usually located in the N-terminus of proteins (Ford et al., 2002; Hom et al., 2007). Importantly, in GUV binding assays with PtdIns(4,5)P₂ and PtdIns(3,4,5)P₃, Jps1 only bound to PtdIns(4,5)P₂. Of note, both PtdInsPs are enriched in the plasma membrane (Di Paolo and De Camilli, 2006). Interestingly, PtdIns(4,5)P₂ is a common molecule involved in membrane recruitment of unconventionally secreted proteins. For instance, assembly of FGF-2 and HIV Tat monomers at the plasma membrane depends on interaction with PtdIns(4,5)P₂ and is a prerequisite for pore formation and translocation into the extracellular space (Zeitler et al., 2015).

Of note, the plasma membrane-binding ability of the putative interaction partner of Jps1 obtained by a pull-down analysis, Sla2, is mediated by an N-terminal ANTH-domain (Wesp et al., 1997). Hence, it is conceivable that the ANTH-like CLD of Jps1 promotes its recruitment to the future division zone.

3.5 The characteristics discovered for Jps1 reveal similarity to the annexin family

Results obtained in interaction-, lipid-binding and bioinformatical studies provide first insights into possible roles of Jps1 in cellular processes. Jps1 is secreted unconventionally and crucial for cytokinesis-dependent unconventional secretion of Cts1, though not essential for cytokinesis *per se*. It forms homodimers and potentially interacts with proteins involved in organization of the actin cytoskeleton and endocytosis. Furthermore, Jps1 might be a direct target of serine/threonine kinase Aga1. As observed during the GUV-binding assays, Jps1 does not only bind membranes enriched in PtdIns(4,5)P₂ but might even induce changes in the membrane integrity (e.g. curvature and blebbing).

Structural predictions suggested similarities to DNA- and RNA polymerases (PredictProtein, RaptorX), thus indicating DNA- and RNA binding abilities, respectively. RNA-binding of Jps1 was indeed observed in a preliminary individual-nucleotide resolution UV crosslinking and immunoprecipitation (iCLIP) experiment (personal communication: N. Stoffel, Institute for Microbiology, HHU Düsseldorf). Moreover, similarity to Z-DNA binding proteins was predicted (FUGUE server).

Proteins fulfilling various intracellular functions including membrane-deformation phenomena as observed for Jps1 are represented by the family of annexins. They

interact with the plasma membrane marker lipid PtdIns(4,5)P₂ and are involved in organizing the cytoskeleton during cytokinesis (Yin and Janmey, 2003). Furthermore, annexins present direct targets of serine/threonine kinases and are capable of binding to Z-DNA and RNA (Burgoyne and Geisow, 1989; Krishna et al., 1990). However, the majority of annexins seems to have accessory functions, since deletion of single genes rarely results in impaired viability or phenotypic abnormalities (Moss and Morgan, 2004). Importantly, similar to Jps1, annexins were initially described for higher eukaryotes but are present in basidiomycetes while not conserved in the clade of ascomycetes (Maryam et al., 2019).

Another similarity between Jps1 and annexins is their release into the extracellular space. Most likely, the underlying mechanism does not depend on conventional secretion, since annexins do not harbour signal peptides. For the annexins A2 and A5 Stewart and colleagues (2018) proposed secretion by unconventional means in mammalian cells. The precise export mechanism of both proteins has not been studied thoroughly to date, but is thought to be similar to the self-mediated secretion of FGF-2 (Popa et al., 2018; Steringer et al., 2014). Recent work of Stewart and colleagues (2018) described the crucial function of scramblase TMEM16F in phospholipid flipping to facilitate the translocation across membranes for annexin A2 and A5.

Another parallel to Jps1 is the ability for self-association in several annexins. This feature might be implicated in their membrane aggregation activity, especially for the linkage of membrane surfaces during endo- or exocytosis (Creutz, 1992; Futter and White, 2007). In annexins, self-association usually depends on calcium-binding. It allows to initiate conformational changes in the protein structure crucial for the exposure of amino acid residues, helices or domains that interact or insert into the membrane (Rosengarth and Luecke, 2003). Non-such ion-binding sites were predicted or identified for Jps1, so far. Common sequence motifs (e.g. (L,M)-K-G-X-G-T-(38 residues)-(D,E)) or domains for calcium-binding, like EF-hands, are absent (Raynal and Pollard, 1994). However, calcium-independent membrane-binding of annexins was observed, e.g. under acidic pH, too. Slightly acidic pH seems to favour structural changes and the exposure of membrane-interacting structures of the proteins. Moreover, annexins have been identified which are able to bind curved membranes independent from calcium at neutral pH (Fischer et al., 2007; Gerke and Moss, 2002). Among those are the mammalian annexins B12, A2 and A6. Annexin A2 and A6 bind

to endosomal membranes in the absence of calcium (Jost et al., 1997) and annexin B12 senses membrane curvature via amphipathic helices. Highly curved membranes seem to trigger huge conformational changes in B12 since they contain a high value of free energy due to improper lipid composition (Fischer et al., 2007). A similar mechanism of curvature-sensing could apply for membrane recognition and association of Jps1. Amphipathic helices are predicted to be formed in the CLD. They could mediate sensing of the apical membrane curvature during bud emerge.

Of note, fungal and oomycete annexins have only been poorly characterized to date and seem to differ from the well-characterized vertebrate annexins. Interestingly, for an annexin homologue in the oomycete *Saprolegnia* an interaction with a cell-wall-resident enzyme, a β -D-glucan synthase, was discovered (Bouzenzana et al., 2006). Bouzenzana and colleagues (2006) suggested a role for the *Saprolegnia* annexin in modulating the activity of this cell-wall enzyme and were able to confirm a positive effect on its synthase activity. In addition, they could show the modulation being dependent on an optimal annexin / β -D-glucan synthase ratio. Jps1 might have a similar function in modulating the activity of Cts1, e.g. by the cell-cycle dependent recruitment of Cts1 to the fragmentation zone. Unregulated spatio-temporal activity of the chitinase might be detrimental for the cytokinesis process. Cts1 hydrolysing the connecting portion of cell wall between mother and daughter cell, before both septa have been formed, could result in cell death. Of note, Jps1 does not seem to be involved in regulating the enzymatic activity of *cts1* in general. Intracellular chitinase activity can be detected in *jps1*-deletion strains with values comparable to the wild type strain. If Jps1 indeed represents an RNA-binding protein, it might be involved in recruiting *cts1* RNA for local translation of Cts1 at the future fragmentation zone. In the absence of *jps1*, the *cts1* mRNA might still be translated but probably by cytoplasmic or early-endosome mediated moving ribosomes (Koepke et al., 2011; Zander et al., 2016). This would explain the localization of Cts1G next to both septa in *jps1* deletion strains.

Recently a novel annexin-like protein in *C. neoformans* termed *AnxC1* was described by Maryam and colleagues (2019). Though it strongly differs from the sequence of the already identified and annotated cryptococcal AnnexinXIV (Brown et al., 2014), it showed similar characteristics as observed and described for annexin-like proteins (Maryam et al., 2019). Unfortunately, due to the absence of homologs and missing phenotypes of deletion strains, the researchers were not able to proof their hypothesis.

The same might apply for Jps1. *U. maydis* has one annotated annexin, Anx1 (*umag_03580*). However, Jps1 and Anx1 do not share sequence homology (see supplementary material, p. 132). Nevertheless, both proteins seem to present non-essential accessory proteins. Similar to *jps1*, preliminary studies in this work indicated that deletion of *anx1* does not render growth, cell division or morphology of yeast-like cells (data not shown).

As research on fungal annexins has not made much progress since first discovered in *Neurospora crassa* by Braun and colleagues (1998), it's conceivable that new sequence motifs and species-specific features will be discovered. To clade Jps1 and its orthologs into a protein family of basidiomycete-specific, annexin-like proteins, further proof needs to come by additional experimental and bioinformatical approaches.

3.6 Conclusion and current model for unconventional secretion of Cts1

The characteristics of Jps1 identified in the course of this work contribute to the currently described model for the novel “lock-type” secretion mechanism of Cts1 (Reindl et al., 2019). Results hint towards a core regulatory function of Jps1 in the cell-cycle dependent localization of Cts1 into the fragmentation zone, which is disturbed in *jps1* deletion mutants. Jps1 assembles to the zone of bud emerge early in the cell cycle likely by interaction with PtdIns(4,5)P₂ in the plasma membrane, which is also involved in the self-mediated unconventional secretion of FGF-2 and Tat (Zeitler et al., 2015) (Figure 3.1, 1). Jps1 remains in the expanding collar formed between mother and growing daughter cell (2,3). Cts1 seems to be recruited after the primary septum has been formed at the side of the mother cell (4). After insertion of the secondary septum, Jps1 and Cts1 localize together inside the fragmentation zone, surrounded by plasma membrane and cell wall (5).

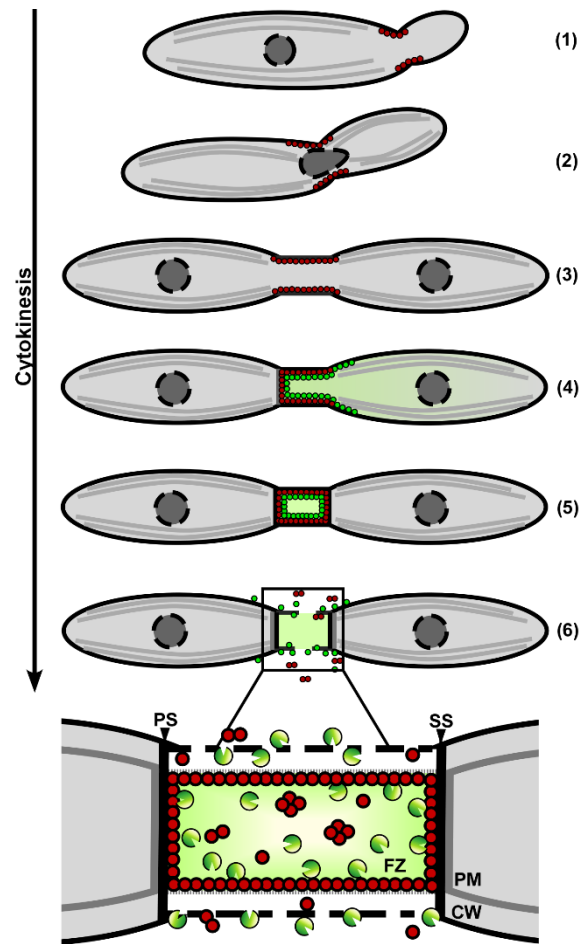


Figure 3.1: Scheme of the current model for lock-type secretion of Cts1. Red dots present Jps1, green dots/pacmen Cts1. PS: primary septum; SS: secondary septum; PM: plasma membrane; CW: cell wall; FZ: fragmentation zone.

Jps1 might facilitate passage of the plasma membrane for Cts1 which could finally hydrolyse the cell wall for release (6).

In conclusion, Jps1 could represent a novel annexin-like protein in basidiomycetes. The initial interaction profile obtained, in combination with results from localization studies and bioinformatics, hint towards diverse intracellular functions during the cell cycle. Moreover, the presence of orthologues in for example *S. reilianum* and *U. hordei* indicate a conservation of the lock-type secretion mechanism in other basidiomycete fungi. At least for *S. reilianum* the growth and division of yeast-like cells in axenic culture has been investigated and seems to be comparable to *U. maydis* (Martinez et al., 2002). However, structural details like the formation of a fragmentation zone, have not been published to date and need to be addressed in the future.

3.7 Future perspectives

To get further insights into the cellular role of Jps1, more structural and biochemical characterization of the protein needs to be done. A crystal structure might help to identify or confirm functions predicted or identified so far. For instance, the ability to bind DNA and RNA might be confirmed by the presence of specific binding pockets in the protein structure. Moreover, structural homologs of Jps1 might be identified which cannot be deduced from protein sequence comparisons. However, initial crystallization approaches failed so far (results not shown). Thus, methods like circular dichroism-spectroscopy (CD) or small angle X-ray light scattering (SAXS) might help to get a hint towards the secondary structure of Jps1 (Beychok, 1966; Kikhney and Svergun, 2015). CD-spectroscopy allows to identify the ratio of secondary structure elements (α -helices, β -sheets and amphipathic helices) within a protein by measuring its absorbance in far UV-light (Beychok, 1966). SAXS analysis can be used additionally. This method provides low resolution information on the overall structural conformation and assembly state of a protein. Moreover, it's even suitable for intrinsically disordered proteins (Kikhney and Svergun, 2015). This method could also allow to further verify the oligomerization state of Jps1 and to roughly resolve the architecture of the dimer/oligomer.

To assess the complete lipid binding profile of Jps1, GUVs with different membrane identities need to be analysed. Beside other PtdInsPs, sphingolipids should be tested, which serve as marker lipids for the side of polarized growth in *U. maydis* (Cánovas and Pérez-Martín, 2009). E.g. the early localization of several proteins including septins and the motor protein Myo5 are dependent on proper biosynthesis and positioning of sphingolipids during the cell cycle (Cánovas and Pérez-Martín, 2009). Additionally, the GUV assays should be performed with recombinant Jps1 Δ CLD to validate the impaired lipid-binding ability of this protein version. Moreover, replacements of basic aa within the CLD could help to localize the exact region involved in membrane association.

To further address the putative ability of Jps1 to induce membrane curvature and blebbing, dextran molecules of different molecular weight labelled with the fluorescent protein fluorescein (FITC) can be added to the GUV assays. FITC-dextran is not able to penetrate the GUV membrane (Drücker et al., 2013). Presence of FITC-dextran

inside of membrane blebs or vesicles would hint towards vesicle formation and budding triggered by Jps1.

Additionally, apart from GUVs, more natural systems like nanodiscs can be applied. Here, a discoidal membrane lipid bilayer is stabilized between an encircling belt of amphipathic membrane scaffold proteins (MSP) (Nath et al., 2007). The membrane-binding protein of interest can be reconstituted into this lipid bilayer for further analysis. Similar to GUVs and liposomes, the lipid composition of the nanodiscs is variable and can be adopted for the individual protein (Rouck et al., 2017). Here, PtdInsPs mixed with other plasma membrane lipids can be used to study the binding and assembly of Jps1 with the membrane. Especially in the potential case that Jps1 integrates into the lipid bilayer, similar to FGF-2, nanodiscs would allow to best mimic a natural membrane environment.

Interaction of Jps1 with Cts1, as indicated by the co-localization studies and Y2H experiments, should be studied further using for example isothermal titration calorimetry (ITC). ITC measures the thermodynamic properties of a protein-protein interaction by determining the heat evolved upon binding of a protein to its ligand (Pierce et al., 1999). Therefore, it would also allow to estimate the strength of the Jps1 and Cts1 association which might be, according to results of the interactome pull-down study, only weak or transient. In addition to revealing quantitative values for the binding affinity of two proteins (K_a value) ITC allows to determine the stoichiometry of the interaction (n) (Pierce et al., 1999). Hence, ITC could also help to further resolve the putative homo-tetramerization of Jps1.

The putative interaction partners of Jps1 identified during pull-down analysis need to be verified, additionally. Y2H assays could help to identify direct interactions of the proteins (Fields and Song, 1989). In addition, deletion of corresponding genes in a Jps1G producing strain would allow to investigate an effect on the localization of Jps1.

To further investigate the mechanism of unconventional protein secretion in *U. maydis*, the dihydrofolate reductase (DHFR) assay could help to determine the folding conformation of Jps1 and Cts1 during membrane translocation. Proteins secreted across the plasma membrane usually need to get unfolded before being translocated into the extracellular space (Schatz and Dobberstein, 1996). The DHFR assay was used for studies on FGF-2 before and revealed secretion of the protein in its readily folded conformation (Backhaus et al., 2004). The system is based on the enzyme

DHFR which is fused to the protein of interest. Addition of the folate derivate aminopterin stabilizes the three-dimensional structure of DHFR. Thus, proteins which need to be unfolded for membrane translocation will get stuck in the bilayer (Eilers and Schatz, 1986). If Jps1 is secreted by a similar mechanism as FGF-2 or Tat, the DHFR-Jps1 fusion protein would be detectable in the culture supernatant of *U. maydis*.

Until now, work on Jps1 focussed on the yeast stage. In the future, the importance of Jps1 during filamentous growth of *U. maydis* should be analysed. Its impact on the biogenesis of filaments can be investigated in AB33_ *jps1*Δ. Additionally, the localization of Jps1G during hyphal growth should be determined. If Jps1 indeed resembles an RNA-binding protein, as suggested by initial experiments, Jps1G might be visible on moving mRNPs, similar to the RNA-binding protein Rrm4 (Koenig et al., 2009; Koepke et al., 2011).

4. Material and Methods

4.1 Material

4.1.1 Chemicals

Chemicals used in this work were purchased from the following companies unless otherwise specified: Sigma-Aldrich, Merck, New England Biolabs, Thermo Scientific, Fluka, Roche, Difco, Serva, Supelco, Avanti Lipids, Echelon, Promega, BioRad, GE Healthcare, Pharmacia, Invitrogen and Carl Roth.

4.1.2 Media and solutions

4.1.2.1 Standard media used for cultivation of *E. coli*

For the cultivation of *E. coli*, following media were used and prepared according to protocols of (Ausubel et al., 1991) and (Sambrook et al., 1989). Before use, media were autoclaved for 5 min at 121°C.

<u>dYT liquid medium</u>	1.6% (w/v)	tryptone peptone
<u>(Sambrook et al., 1989):</u>	1.0% (w/v)	yeast extract
	0.5% (w/v)	NaCl
<u>YT solid medium</u>	0.8% (w/v)	tryptone peptone
	1.0% (w/v)	yeast extract
	0.5% (w/v)	NaCl
	1.3% (w/v)	bacto agar

prepared in ddH₂O and autoclaved

4.1.2.2 Antibiotics used for selection in *E. coli*

Antibiotics used for selection in *E. coli* are listed below (Table 1).

Table 1: Antibiotics used for selection in *E. coli*.

Antibiotic	Stock [mg/mL]	Concentration liquid medium [µg/mL]	Concentration solid medium [µg/mL]
Ampicillin	10 (in ddH ₂ O)	100	100

Chloramphenicol	50 (in 100% EtOH)	34	34
Kanamycin	10 (in ddH ₂ O)	50	50
Gentamycin	10 (in ddH ₂ O)	50	50

4.1.2.3 *E. coli* strains used for cloning purposes

The *E. coli* K-12 derivative Top10 (*F-mcrAΔ(mrr-hsdRMS-mcrBC)φ-80lacZ-ΔM15 ΔlacX74-recA1-araD139Δ(araleu)7697gal-Ugal-Krps-Lend-A1nupGP3*: Kan R; Amp R; (am) Tet; R (am)) (Grant et al., 1990), (Invitrogen/Life Technologies) was used for cloning purposes.

The *E. coli* strain BL21 (DE3) (*E. coli* str. *B F-ompTgaldcmlonhsdSB(rB-mB-)λ(DE3 [lacI-lacUV5-T7p07-ind1-sam7-nin5])[malB+]K-12(λS)*) (Studier and Moffatt, 1986), (Invitrogen/Life Technologies) was used for heterologous protein expression and purification.

4.1.2.4 Standard media used for cultivation of *U. maydis*

For the cultivation of *U. maydis*, media listed below were used. All media were autoclaved for 5 min at 121°C, unless otherwise stated. For agar-containing plates, 2.0 % (w/v) agar (Difco) was added to the medium before autoclaving. To pour plates, 1% glucose and selective antibiotics (if needed) were added when medium was cooled down to 60°C.

<u>Complete medium</u>	0.25% (w/v) casamino acids
<u>(Holliday, 1974):</u>	0.1% (w/v) yeast extract
	1.0% (v/v) vitamin solution (Holliday, 1974)
	6.25% (v/v) trace elements (Holliday, 1974)
	0.05% (w/v) herring sperm DNA
	0.15 % (w/v) NH ₄ NO ₃ after autoclaving
	as needed:
	1% (w/v) glucose

<u>Vitamin solution</u>	0.1% (w/v) thiamine
<u>(Holliday, 1974):</u>	0.05% (w/v) riboflavin
	0.05% (w/v) pyridoxine
	0.2% (w/v) calcium pantothenate
	0.05% (w/v) para amino-benzoic acid
	0.2% (w/v) nicotinic acid
	0.2% (w/v) choline chloride
	1.0% (w/v) myo-inositol
	filtered sterile, stored at -20°C
<u>NSY glycerin:</u>	0.8% (w/v) nutrient broth
	0.1% (w/v) yeast extract
	0.5% (w/v) sucrose
	69.6% (v/v) glycerine
<u>Salt solution (Holliday, 1974):</u>	1.6% (w/v) KH_2PO_4
	0.4% (w/v) Na_2SO_4
	0.8% (w/v) KCl
	0.4% (w/v) $\text{MgSO}_4 \times 7 \text{H}_2\text{O}$
	0.132% (w/v) $\text{CaCl}_2 \times 2 \text{H}_2\text{O}$
	0.8% (v/v) trace element solution in ddH ₂ O, filtered sterile
<u>Trace element solution:</u>	6.0% (w/v) H_3BO_3
	14.0% (w/v) $\text{MnCl}_2 \times 4 \text{H}_2\text{O}$
	40.0% (w/v) ZnCl_2
	4.0% (w/v) $\text{NaMoO}_4 \times 2 \text{H}_2\text{O}$
	10.0% (w/v) $\text{FeCl}_3 \times 6 \text{H}_2\text{O}$ 4.0% (w/v) $\text{CuSO}_4 \times 5 \text{H}_2\text{O}$
	in ddH ₂ O, filtered sterile

<u>Ammonium minimal medium:</u>	0.3% (w/v) (NH ₄) ₂ SO ₄ 6.25% (v/v) salt solution (Holliday, 1974) in ddH ₂ O, autoclaved after autoclaving: 1% (w/v) glucose
<u>YEPSlight:</u>	1% (w/v) yeast extract 0.4% (w/v) bacto peptone 0.4% (w/v) sucrose in ddH ₂ O autoclaved

4.1.2.5 Antibiotics used for selection in *U. maydis*

Antibiotics used for selection in *U. maydis* are listed below (Table 2).

Table 2: Antibiotics used for selection in *U. maydis*.

Antibiotics	Stock [mg/mL]	Concentration liquid medium [µg/mL]	Concentration solid medium [µg/mL]	Concentration solid medium RegLight Bottom layer [µg/mL]
Carboxin (Cbx)	5 (in MeOH)	2	2	4
Hygromycin (Hyg)	50 (in PBS)	200	200	400
Nourseothricin (cloNat)	200 (in ddH ₂ O)	150	150	300
Genticin (G418)	50 (in ddH ₂ O)	500	500	1000

4.1.2.6 Oligonucleotides used in polymerase chain reaction (PCR)

Oligonucleotides used for PCR are listed below (Table 3).

Table 3: Oligonucleotides used for PCR.

Designation	Primer sequence	Purpose
MF502	5'-ACGACGTTGTAAAACGACGGCCAG-3'	Generation of <i>cbx</i> -probe for Southern blot analysis

4. Material and Methods

MF503	5'-TTCACACAGGAAACAGCTATGACC-3'	Generation of <i>cbx</i> -probe for Southern blot analysis
MB372	5'-TTAGGCGCGCCATGCCAGGCATCTCC -3'	Amplification of <i>Jps1</i>
MB373	5'-TTAGGGCCCTTAGGATTCCGCATCGATTGGGG -3'	Amplification of <i>Jps1</i>
MB449	5'-ATTGCTCTTCGTCGATGGTGAGCAAGGGCGAGG-3'	mCherry-Sapl storage vector
MB450	5'-ATTGGCGCGCCGGCCGCTTTACTTGTACAGC-3'	mCherry-Sapl storage vector
MB455	5'-GGCGCGCCATGGTACGTCCTGTAGAAACC-3'	Amplification of <i>Gus</i>
MB456	5'-GGGCCCTTGTTTGCCTCCCTGCTGCGG-3'	Amplification of <i>Gus</i>
MB457	5'-CGGGATCCATGCCAGGCATCTCCAAGAAGCC-3'	Amplification of <i>Jps1</i>
MB458	5'-GACTAGTGGATTCCGCATCGATTGGGG-3'	Amplification of <i>Jps1</i>
MB459	5'-ATTGGCGCGCCATGCCAGGCATCTCCAAGAAGCC-3'	Truncation of <i>Jps1</i>
MB460	5'-ATTGGGCCCCGGAGCATCCAAGCTCGCGG-3'	Truncation of <i>Jps1</i>
MB461	5'-ATTGGCGCGCCTCGCCTCACAAAAGACGGTGC-3'	Truncation of <i>Jps1</i>
MB462	5'-ATTGGGCCCTTAGGATTCCGCATCGATTGG-3'	Truncation of <i>Jps1</i>
MB463	5'-ATTGGCGCGCCGGAAAGCAGCTCACTCCGG-3'	Truncation of <i>Jps1</i>
MB464	5'-GCTCTTACGGAGCATCCAAGCTCGCGG-3'	Truncation of <i>Jps1</i>
MB465	5'-GCTCTTACCGCCCACCAAACCTGCGGTTCC-3'	Truncation of <i>Jps1</i>
MB557	5'-ATTGGCGCGCCGGTCCGGAGCGGCATGG-3'	Sequencing of SHH-tag

4. Material and Methods

MB572	5'-CCTCTAGCACTAGTGCGGCCAACGCGGCC-3'	Amplification of SHH-tag
MB573	5'-GGCATGGCGCGCCGGTCCGGAGCGGCATGGTGG-3'	Amplification of SHH-tag
MB582	5'-ATTGCTCTTCTGCTGCTGCTGCTGCTGCTGCTCG ACTGGCGGAGAACC-3'	polyA-replacement in CLD
MB583	5'-ATTGCTCTTCTAGCGACGTGAGGACTGCCCGCC-3'	polyA-replacement in CLD
MB584	5'-ATTGCTCTTCTGCTGCTGCTGCTGCTGCTCATGTCT CGGCTTTCC-3'	polyA-replacement in CLD
MB585	5'-ATTGCTCTTCTAGCCACCGTCTTTTTGTGAGG-3'	polyA-replacement in CLD
MB586	5'-ATTGCTCTTCTGCTGCTGCTGCTGCTGCTCTCTCTC CTAAATCGCG-3'	polyA-replacement in CLD
MB587	5'-ATTGCTCTTCTAGCGTTCTCCGCCAGTCGCACC-3'	polyA-replacement in CLD
MB588	5'-ATTGCTCTTCTGCTGCTGCTGCTGCTGCTATCTT TACCGGTGG-3'	polyA-replacement in CLD
MB589	5'-ATTGCTCTTCTAGCGAAAGCCGAGACATGAGG-3'	polyA-replacement in CLD
MB590	5'-ATTGCTCTTCTGCTGCTGCTGCTGCTGCTGCTTACCCCGG TGTTCTACACG-3'	polyA-replacement in CLD
MB591	5'-ATTGCTCTTCTAGCACGCGATTTAGGAGAGAGG-3'	polyA-replacement in CLD
MB592	5'-ATTGCTCTTCTGCTGCTGCTGCTGCTGCTGCTCGAGGCAAT GGTCCTGCC-3'	polyA-replacement in CLD
MB593	5'-ATTGCTCTTCTAGCATGACCACCGTAAAGATACG-3'	polyA-replacement in CLD
MB594	5'-ATCAGGATCCCCGCCATGGTACGTCC-3'	polyA-replacement in CLD
MB599	5'-CTCTATCAGGATCCATGCCAGGCATCTCCAAG-3'	Cloning of Jps1-Gus-fusion
MB600	5'-CTTGGAGATGCCTGGCATGGATCCTGATAGAG-3'	Cloning of Jps1-Gus-fusion

4. Material and Methods

MB601	5'-CCAATCGATGCGGAATCCACTAGTGCGGCCAACGCGG-3'	Cloning of Jps1-Gus-fusion
MB602	5'-CCGCGTTGGCCGCACTAGTGGATTCCGCATCGATTGG-3'	Cloning of Jps1-Gus-fusion
MB603	5'-CCATGCCGCTCCGGACCGGCGGCCATGGTACGTCC-3'	Cloning of Jps1-Gus-fusion
MB604	5'-GGACGTACCATGGCGCGCCGGTCCGGAGCGGCATGG-3'	Cloning of Jps1-Gus-fusion
MB605	5'-CCGCAGCAGGGAGGCAAACAAGGGCCCTAGCCG CGGTGCGGC-3'	Cloning of Jps1-Gus-fusion
MB606	5'-GCGCGACCGCGGCTAGGGCCCTTGTTGCCTC CCTGCTGCGG-3'	Cloning of Jps1-Gus-fusion
MB631	5'-AATGGCGCGCCAGTCCTCACGTCTCGCC-3'	Amplification of CLD
MB632	5'-AATCCCGGGAGCGATTGAAAAGGCCTCGG-3'	Amplification of CLD
MB945	5'-GGAATTCCATATGCCAGGCATCTCCAAGAAGCC-3'	Cloning of Jps1 into pET22b
MB946	5'-CCGCTCGAGGGATTCCGCATCGATTGGGGTTTGG-3'	Cloning of Jps1 into pET22b
MB966	5'-GGAATTCATGCCAGGCATCTCCAAGAAGC-3'	Cloning of Jps1 into ptac/lac
MB967	5'-GGGTACCTCATCATCAGTGGTGGTGGTGG TGCTCGAGGGATTCCGCATCGATTGGGGTTTGG-3'	Cloning of Jps1 into ptac/lac
UP65	5'-GGAATTCCATATGGCGAGCCTTGAGGCTGCGTTCC-3'	Amplification of putative Pjps1
UP66	5'-CGGGATCCGATTTGCAAGTCGTGGGCCTTCG-3'	Amplification of putative Pjps1
UP67	5'-CGGGATCCATGGCCGAAAGCAGCTCACTCCGG-3'	Amplification of CLD from Jps1
UP68	5'-CCGCGGCCGTA CTGGTCTCCTGG-3'	Amplification of CLD from Jps1
UP176	5'-CCGCTCGAGATGCCAGGCATCTCCAAGAAGC-3'	Cloning of Jps1 into pBAD expression vector (<i>E. coli</i>)

4. Material and Methods

UP177	5'-GGAATTCAGGATTCCGCATCGATTGG-3'	Cloning of Jps1 into pBAD expression vector (<i>E. coli</i>)
UP211	5'-GGTCCCTACACAGGAGTTGGAGAAGAACC-3'	Cloning of Jps1 into pTAC expression vector (<i>E. coli</i>)
UP212	5'-GTGTCGCCCATGGGGGCGGAGGTGGATTGG-3'	Cloning of Jps1 into pTAC expression vector (<i>E. coli</i>)
UP348	5'-TCCCCGCGGCCGTACTGGTCTCCTGGGTATT-3'	Amplification of Jps1ΔCLD
UP489	5'- GGAATTCATATGATGTCGATTACATCTCAGATACGAGC -3'	Amplification of Jps1ΔCLD
UP490	5'- CCGCTCGAGGGATTCCGCATCGATTGGGGTTTGG -3'	Amplification of Jps1ΔCLD
UP510	5'- GGAATTCATATGCCAGGCATCTCCAAGAAGCC -3'	Amplification of Jps1 for insertion into pET15b
UP511	5'- CGCGGATCCGGATTCCGCATCGATTGGGGTTTGG -3'	Amplification of Jps1 for insertion into pET15b
UP751	5'- GGAATTCATATGGCCGAAAGCAGCTCACTCCGG -3'	Amplification of Jps1ΔCLD
UP752	5'- CCGCTCGAGGGATTCCGCATCGATTGGGGTTTGG -3'	Amplification of Jps1ΔCLD
UP832	5'-GAATTCGAGCTCGCTCTTCGTCGATGGTGTCCGAGCTC ATCAAGG -3'	Amplification of mKate2
UP833	5'-TTGGCGGCCATGGCGGTGACCGAGTTTCGAGG -3'	Amplification of mKate2
UP927	5'- GGAGGATCCATGAGTCCTCACGTCTCGCC -3'	Amplification of CLD for dimerization
UP928	5'- GGAAGATCTTGAGGCGGCAGCAGCGATTGAAAAGGCCTCGG -3'	Amplification of CLD for dimerization
UP929	5'- CGCGGATCCATGGGCGGCAGCAGTCCTCACGTCTCGCC -3'	Amplification of CLD for dimerization
UP938	5'- TCCAGATCTGCTGCCGCCAGCGATTGAAAAGGCCTCGG -3'	Amplification of CLD for dimerization
UP939	5'- GGAAATTCATATGAGTCCTCACGTCTCGCC -3'	Amplification of CLD for dimerization

UP940	5'- CGGCTCGAGTCAGCTGCCGCCAGCGATTGAAAAGG -3'	Amplification of CLD for dimerization
UM94	5'- TTGGCGCGCCATGAGTCCTCACGTCTCGCC -3'	Amplification of CLD
UM95	5'- AATGGGCCCTTAAGCGATTGAAAAGGCCTCGGACG -3'	Amplification of CLD
UM379	5'- CGCGGATCCATGGTGAGCAAGGGCGAGGAGC -3'	Amplification of CLD for eGfp fusion
UM380	5'- CTAGACTAGTCTTGACAGCTCGTCCATGCCG -3'	Amplification of CLD for eGfp fusion
UM987	5'-GGAATTCCATATGCCAGGCATCTCCAAGAAGCC -3'	Amplification of Jps1 for eGfp fusion
UM988	5'-CGCGGATCCTTACTTGTACAGCTCGTCC -3'	Amplification of Jps1 for eGfp fusion
UM989	5'-GGGAATTCCATATGGCCGAAAGCAGCTCACTCCGG -3'	Amplification of Jps1ΔCLD for eGfp fusion
UM990	5'-CGCGGATCCTTACTTGTACAGCTCGTCCATGCC -3'	Amplification of Jps1ΔCLD for eGfp fusion
UM991	5'-GGGAATTCCATATGTCGGGCCAAACGCTCACGGATCG -3'	Amplification of ANTH domain for eGfp fusion
UM992	5'- GGCCACGTCGGCCTTTCTTTCTTCTAATGTATTTAGATGC-3'	Amplification of ANTH domain for eGfp fusion

4.1.3 Plasmids

Plasmid vectors were generated following standard molecular cloning techniques published by Sambrook et al., (1989). Oligonucleotides used in this thesis are listed in the Table above. Generated constructs were confirmed by sequencing at the Institute for Genetics at Ludwig-Maximilians-Universität (München) or Eurofins overnight sequencing service.

4.1.3.1 Expression plasmids for *U. maydis*

For gene expression in *U. maydis*, integrative vectors were used (Table 4). All integrative vectors display derivatives of p123 (Aichinger et al., 2003) and were inserted via homologous recombination into the endogenous *ip* locus of *U. maydis* or into the

respective locus of the endogenous gene for the generation of deletion mutants or fusions to the open reading frame.

pRabX1_Poma:Gus-SHH-Jps1 (pUMa3012): A 1.8 kb fragment was amplified from pUMa2913 using MB372 and MB373. It was ligated to the backbone fragment of pUMa2113 (8.6 kb) having Ascl/Apal restriction sites.

pRabX1_Poma:Gus-SHH-Jps1(1-1441) (pUMa3057): A 1.5 kb fragment was amplified from pUMa3012 using MB459 and MB460. It was ligated to the backbone fragment of pUMa3012 (8.6 kb) having Ascl/Apal restriction sites.

pRabX1_Poma:Gus-SHH-Jps1 (61-1830) (pUMa3058): A 1.79 kb fragment was amplified from pUMa3012 using MB461 and MB462. It was ligated to the backbone fragment of pUMa3012 (8.6 kb) having Ascl/Apal restriction sites.

pRabX1_Poma:Gus-SHH-Jps1 (261-1830) (pUMa3059): A 1.59 kb fragment was amplified from pUMa3012 using MB463 and MB462. It was ligated to the backbone fragment of pUMa3012 (8.6 kb) having Ascl/Apal restriction sites.

pRabX1_Poma:Gus-SHH-Jps1 (61-1441) (pUMa3113): A 1.4 kb fragment was amplified from pUMa3012 using MB461 and MB460. It was ligated to the backbone fragment of pUMa3012 (8.6 kb) having Ascl/Apal restriction sites.

pJps1eGfp_NatR (pUMa3147): Exchange of resistance cassette in storage vector. A 2.5 kb fragment was isolated from pStor1694 using SacII/Sfil. It was ligated to the backbone (4.6 kb) of pStor2779.

pPjps1-Jps1-eGfp (pUMa3293): A 1.65 kb fragment (Pjps1) was amplified from pUMa3112 using UP65 and UP66. It was ligated to the backbone fragment of pUMa3095 (7.1 kb) having BamHI/NdeI restriction sites.

pPjps1-Jps1 Δ CLD-eGfp (pUMa3294): A 1.5 kb fragment (Pjps1) was amplified from pUMa3112 using UP67 and UP68. It was ligated to the backbone fragment of pUMa3095 (7.1 kb) having compatible restriction sites.

Golden Gate generated vectors:

pDest_UMAG_03776-mCherry (pUMa3034): Upstream and downstream were amplified on gDNA of Uma521 using the primer combinations DD824 x DD825 (1.0 kb)

and DD819 x DD820 (0.92 kb), respectively. In a OnePot reaction with Sapl, pStor3035 and pDest2074 the final plasmid was generated.

pDest_mKate2-Jps1_HygR (pUMa3634): Upstream and downstream were amplified on gDNA of Uma521 using the primer combinations DD824 x DD825 (1.0 kb) and DD819 x DD820 (0.92 kb), respectively. In a OnePot reaction with Sapl, pStor3632 and pDest2074 the final plasmid was generated.

Table 4: Overview of used and generated plasmids for transformation of *U. maydis*.

pUMa number	Genotype	Insert amplification and backbone insertion	Linearization	Insertion locus	Reference
3012	pRabX1_Poma:Gus-SHH-Jps1	MB372 x MB373 on pUMa2913 (1.8 kb); inserted into pUMa2113 with Ascl/Apal	Sspl	<i>ip^S</i>	This work
3034	pDest_UMAG_03776-mCherry (Golden Gate with Sapl)	UF: DD824 x DD825 on gDNA of UMa521 (1.0 kb). DF: DD819 x DD820 on gDNA of UMa521 (0.92 kb) One Pot reaction with pStor3035 and pDest2074	Sspl	<i>um03776</i>	This work
3057	pRabX1_Poma:Gus-SHH-Jps1(1-1441)_CbxR -truncation	MB459 x MB460 on pUMa3012 (1.5 kb) inserted into pUMa3012 with Ascl/Apal	Sspl	<i>ip^S</i>	This work
3058	pRabX1_Poma:Gus-SHH-Jps1 (61-1830)_CbxR truncation	MB461 x MB462 on pUMa3012 (1.79 kb) inserted into pUMa3012 with Ascl/Apal	Sspl	<i>ip^S</i>	This work
3059	pRabX1_Poma:Gus-SHH-Jps1 (261-1830)_CbxR truncation	MB463 x MB462 on pUMa3012 (1.59 kb) inserted into pUMa3012 with Ascl/Apal	Sspl	<i>ip^S</i>	This work
3113	pRabX1_Poma:Gus-SHH-Jps1 (61-1441)_CbxR- truncation	MB461 x MB460 on pUMa3012 (1.4 kb) inserted into pUMa3012 with Ascl/Apal	Sspl	<i>ip^S</i>	This work

3147	Jps1eGfp_NatR	Resistance cassette exchange (Hyg→Nat): Cut pStor1694 SacII/SfiI (2.5 kb). Insert in pStor2779.	Sspl	um03776	This work
3293	pPjps1-Jps1-eGfp_cbxR	UP65 x UP66 on pUMa3112 (1.65 kb → Pjps1) inserted into pUMa3095 with BamHI/NdeI	Sspl	ip ^S	This work
3294	pPjps1-Jps1ΔCLD-eGfp_CbxR	UP67 x UP68 on pUMa3059 (1.5 kb) inserted into pUMa3293 with BamHI/SacII	Sspl	ip ^S	This work
3634	pDest_mKate2-Jps1_HygR (Golden Gate with SapI)	UF: DD824 x DD825 on gDNA of UMa521 (1.0 kb). DF: DD819 x DD820 on gDNA of UMa521 (0.92 kb) One Pot reaction with pStor3632 and pDest2074	Sspl	um03776	This work

4.1.3.2 Expression plasmids for *E. coli*

For gene expression in *E. coli*, ectopic vectors were used. All vectors display derivatives of pET15b), pET22b) or pGex) (Novagen, Sigma-Aldrich) (Table 5) and were transformed via heat shock into derivatives of strain BL21 (DE3).

Table 5: Overview of plasmids used and generated for transformation of *E. coli*.

pUMa number	Genotype	Insert amplification and backbone insertion	Reference
1951	pET15b_6xHis-Cts1	/	Terfrüchte et al., 2017
2154	pET15b_6xHis-Cts1-Gfp	/	Terfrüchte et al., 2017
2156	pET15b_6xHis- Gfp	/	Terfrüchte et al., 2017

2913	pGex_Gst-Jps1	/	Kai Hussnaetter, master thesis 2017
3257	pET22b_Jps1-6xHis (w/o <i>peIB</i> leader)	MB945 x MB946 on pUMa2913 (1.84 kb) inserted into pUMa3262 with NdeI/XhoI	This work
3350	pET15b_6xHis-Jps1	UP510 x UP511 on pUMa3257 (1.84 kb) inserted into pUMa1951 with BamHI/NdeI	This work
3523	pET22b_Jps1DCLD-6xHis (w/o <i>peIB</i> leader)	UP489 x UP490 on pUMa3059 (1.59 kb) inserted into pUMa3257 with NdeI/XhoI	This work
4285	pET15b_Jps1-eGfp_AmpR	UM987 x UM988 on pUMa3293 (2.6 kb) inserted into pUMa2154 with BamHI/NdeI	This work
4286	pET15b_Jps1DCLD-eGfp_AmpR	UM989 x UM980 on pUMa3294 (2.3 kb) inserted into pUMa2154 with BamHI/NdeI	This work

4.1.4 *U. maydis* expression strains

All *U. maydis* strains used and generated in the course of this thesis are listed below (Table 6). For cultivation purposes, cells were incubated at 28°C on shaking devices at 200 rpm. Cultures were grown in complete medium (CM) supplemented with 1% (w/v) glucose under aerobic conditions.

Table 6: Overview of *U. maydis* strains used and generated in this work.

Strain	Relevant genotype	UMa number	locus	plasmid transformed (pUMa)	Progenit or (UMa)	reference
AB33	<i>a2 Pnar: bW2bE1 PhleoR</i>	133	<i>B</i>	/		Brachmann et al., 2001
AB33_cts1Δ	<i>umag10419Δ NatR</i>	387	<i>umag_10419</i>	/	133	Koepke et al., 2011
AB33_Cts1G_NatR	<i>umag10419-egfp NatR</i>	388	<i>umag_10419</i>	/	133	Koepke et al., 2011
AB33_jps1Δ_Cts1G_HygR	<i>umag03776Δ HygR/ umag10419-egfp_NatR</i>	1846	<i>umag_03776</i>		388	Reindl and Stock et al., 2020
AB33_Jps1G_HygR	<i>Umag03776-egfp_HygR</i>	1847	<i>umag_03776</i>		133	Reindl and Stock et al., 2020
AB33_Poma:Gus-Jps1_CbxR	<i>ip'[Poma:gus-shh-jps1] ip^s CbxR</i>	2007	<i>cbx</i>	3012	133	This work
AB33_cts1Δ_Poma:Gus-Jps1_CbxR	<i>umag10419Δ NatR/ ip'[Poma:gus-shh-jps1] ip^s CbxR</i>	2008	<i>cbx</i>	3012	387	This work
AB33_cts1Δ_Jps1G_HygR	<i>umag10419Δ NatR/ umag03776-egfp HygR</i>	2009	<i>umag_03776</i>	2779	387	This work
AB33_cts1Δ_Poma:Gus_CbxR	<i>umag10419Δ NatR/</i>	2013	<i>cbx</i>	2335	387	This work

4. Material and Methods

	<i>ip</i> '[Poma:gus-shh] <i>ip</i> ^s CbxR					
AB33_Poma:Gus_CbxR	<i>ip</i> '[Poma:gus-shh] <i>ip</i> ^s CbxR	2014	<i>cbx</i>	2335	133	This work
AB33_Cts1G_NatR_Jps1C_HygR	<i>umag</i> 10419- <i>egfp</i> NatR/ <i>umag</i> 03776- <i>mcherry</i> HygR	2048	<i>umag</i> _104 19 <i>umag</i> _037 76	3034	388	This work
AB33_Poma:Jps1-Gus_CbxR	<i>ip</i> '[Poma:jps1- shh-gus] <i>ip</i> ^s CbxR	2059	<i>cbx</i>	3054	133	This work
AB33_Cts1G_jps1Δ_Poma:Gus-Jps1 (1-1441)_CbxR	<i>umag</i> 10419- <i>egfp</i> NatR/ <i>umag</i> 03776Δ HygR <i>ip</i> '[Poma:gus-shh- jps1(1-1441)] <i>ip</i> ^s CbxR	2062	<i>cbx</i>	3057	1846	This work
AB33_Cts1G_jps1Δ_Poma:Gus-Jps1 (61-1830)_CbxR	<i>umag</i> 10419- <i>egfp</i> NatR/ <i>umag</i> 03776Δ HygR <i>ip</i> '[Poma:gus- shh-jps1(61- 1830)] <i>ip</i> ^s CbxR	2063	<i>cbx</i>	3058	1846	This work
AB33_Cts1G_jps1Δ_Poma:Gus-Jps1 (261-1830)_CbxR	<i>umag</i> 10419- <i>egfp</i> NatR/ <i>umag</i> 03776Δ HygR <i>ip</i> '[Poma:gus-shh- jps1(261-1830)] <i>ip</i> ^s CbxR	2064	<i>cbx</i>	3059	1846	This work
AB33_Cts1G_jps1Δ_Poma:Gus-Jps1 (1-1830)_CbxR	<i>umag</i> 10419- <i>egfp</i> NatR/ <i>umag</i> 03776Δ HygR <i>ip</i> '[Poma:gus-shh- jps1(1-1830)] <i>ip</i> ^s CbxR	2094	<i>cbx</i>	3012	1846	This work
AB33_Cts1G_jps1Δ_Poma:Gus_CbxR	<i>umag</i> 10419Δ NatR/ <i>umag</i> 03776Δ HygR <i>ip</i> '[Poma:gus-shh- jps1] <i>ip</i> ^s CbxR	2115	<i>cbx</i>	2335	1846	This work
AB33_Cts1G_jps1Δ_Poma:Gus-Jps1 (61-1441)_CbxR	<i>umag</i> 10419- <i>egfp</i> NatR/ <i>umag</i> 03776Δ HygR <i>ip</i> '[Poma:gus-shh- jps1(61-1441)] <i>ip</i> ^s CbxR	2117	<i>cbx</i>	3113	1846	This work
AB33_cdc3Δ_Jps1G_NatR	<i>umag</i> 10503Δ HygR/ <i>umag</i> 03776-eGfp NatR	2163	<i>umag</i> _037 76	3147	442	Zander et al., 2016
AB33_don1Δ_Jps1G_NatR	<i>umag</i> 10152Δ HygR/ <i>umag</i> 03776-eGfp NatR	2164	<i>umag</i> _037 76	3147	1666	Aschenbroich et al., 2019
AB33_Jps1G_NatR	<i>umag</i> 03776- <i>egfp</i> NatR	2173	<i>umag</i> _037 76	3147	133	This work
AB33_Poma:Jps1G_CbxR	<i>ip</i> '[Poma:jps1- egfp] <i>ip</i> ^s CbxR	2093	<i>cbx</i>	3095	133	This work
AB33_don3Δ_Jps1G_NatR	<i>Umag</i> 05543Δ HygR/ <i>umag</i> 03776-eGfp NatR	2240	<i>umag</i> _037 76	3147	2028	Aschenbroich et al., 2019
AB33_jps1Δ_Pjps1-Jps1G_CbxR	<i>umag</i> 03776Δ	2274	<i>cbx</i>	3293	2092	This work

	<i>HygR/ ip'[Pjps1:jps1-egfp] ip^s CbxR</i>					
AB33_jps1Δ_Pjps1-Jps1ΔCLD-G_CbxR	<i>umag03776Δ HygR/ ip'[Pjps1:jps1Δcld-egfp] ip^s CbxR</i>	2275	<i>cbx</i>	3294	2092	This work
AB33_Pjps1-Jps1G_CbxR	<i>ip'[Pjps1:jps1-egfp] ip^s CbxR</i>	2299	<i>cbx</i>	133	3293	This work
AB33_Pjps1:Jps1ΔCLD-G_CbxR	<i>ip'[Pjps1:jps1Δcld-egfp] ip^s CbxR</i>	2314	<i>cbx</i>	133	3294	This work
AB33_jps1Δ_Poma:Jps1G_CbxR	<i>umag03776Δ HygR/ ip'[Poma:jps1-egfp] ip^s CbxR</i>	2335	<i>cbx</i>	2092	3095	This work
AB33_jps1Δ_Poma:Jps1ΔCLD-G_CbxR	<i>umag03776Δ HygR/ ip'[Poma:jps1Δcld-egfp] ip^s CbxR</i>	2337	<i>cbx</i>	2092	3349	This work
AB33_jps1Δ_NatR-Cdc10G_HygR	<i>umag03776Δ HygR/ umag10644-egfp NatR</i>	2527	<i>umag_10644</i>	2092	1499	Zander et al., 2016; this work
AB33_cdc10Δ_HygR_Jps1G_NatR	<i>umag10644Δ HygR/ umag03776 NatR</i>	2528	<i>umag_03776</i>	3147	834	Zander et al., 2016, this work
AB33_cdc10Δ_HygR_Poma:Jps1G_CbxR	<i>Umag10644Δ HygR/ ip'[Poma:jps1-egfp] ip^s CbxR</i>	2529	<i>umag_03776</i>	3147	834	Zander et al., 2016, this work
AB33_Jps1mKate2_HygR	<i>umag03776-mkate2 HygR</i>	2629	<i>umag_03776</i>	3634	133	This work
AB33_Cts1G-NatR_Jps1mKate2-HygR	<i>umag10419-egfp NatR/ umag03776-mkate2 HygR</i>	2630	<i>umag_03776</i>	3634	388	This work
AB33_jps1Δ_G418R	<i>umag03776Δ G418R</i>	2710	<i>umag_03776</i>	3111	133	This work
AB33_jps1Δ_G418R-anx1Δ_HygR	<i>umag03776Δ G418R/ umag03580 HygR</i>	3143	<i>umag_03580</i>	3006	2710	This work

4.1.5 *E. coli* expression strains

E. coli strain BL21 (DE3) was used for protein expression. Cells were grown shaking (180 rpm) at 37°C (Table 7).

Table 7: Overview of *E. coli* strains used and generated in this work.

Strain	Relevant genotype	UMa number	Plasmid transformed (pUMa)	Progenitor (UMa)	Reference
<i>E. coli</i> _BL21 (DE3)_pET22b)-Jps1-6xHis	<i>F- ompT gal dcm_(DE3)_pET22b)- Jps1-6xHis_AmpR</i>	2329	3257	<i>E. coli</i> _BL21 (DE3)	This work

<i>E. coli</i> _BL21 (DE3)_pET22b)- Jps1ΔCLD- 6xHis	<i>F- ompT gal</i> <i>dcm_(DE3)_pET22b)-</i> <i>Jps1ΔCLD-</i> <i>6xHis_AmpR</i>	2486	3523	<i>E. coli</i> _BL21 (DE3)	This work
<i>E. coli</i> _BL21 (DE3)_pET15b)- 6xHis- Jps1- eGfp	<i>F- ompT gal</i> <i>dcm_(DE3)_pET15b)-</i> <i>6xHis-Jps1-</i> <i>eGfp_AmpR</i>	3059	4285	<i>E. coli</i> _BL21 (DE3)	This work
<i>E. coli</i> _BL21 (DE3)_pET15b)- 6xHis- Jps1ΔCLD-eGfp	<i>F- ompT gal</i> <i>dcm_(DE3)_pET15b)-</i> <i>6xHis-Jps1ΔCLD-</i> <i>eGfp_AmpR</i>	3060	4286	<i>E. coli</i> _BL21 (DE3)	This work
<i>E. coli</i> _BL21 (DE3)_pET15b)- 6xHis- eGfp	<i>F- ompT gal</i> <i>dcm_(DE3)_pET15b)-</i> <i>6xHis- eGfp_AmpR</i>	3113	2156	<i>E. coli</i> _BL21 (DE3)	This work

4.1.6 Enzymes

Enzymes used in this work are listed below (Table 8).

Table 8: Overview of enzymes used in this work and producing companies.

Name	Application	Company
Lysozyme	Plasmid isolation	Merck
Glucanex	Protoplast preparation of <i>U. maydis</i>	Merck
Phusion DNA polymerase	DNA amplification	Finnzymes
Restriction enzymes	DNA restriction	New England Biolabs
RNAse A	Plasmid isolation, gDNA isolation	Boehringer Ingelheim
T4-DNA ligase	DNA ligation	Roche

4.1.7 Kits and substrates for detection purposes

Kits and substrates used in this work are listed below (Table 9).

Table 9: Overview of Kits and substrates used in this work and producing companies.

Name	Application	Company
CDP-Star® (chemiluminescent substrate for alkaline phosphatase)	Southern blot analysis	Invitrogen

Amersham™ ECL™ Prime Western blotting detection kit (chemiluminescent substrate for horseradish peroxidase, HRP)	Western blot analysis	GE Healthcare Life Sciences
Aceglow™ Ultrasensitive chemiluminescence substrate (for horseradish peroxidase, HRP)	Western blot analysis	PeqLab
QuantaRed Enhanced Fluoro-chemiluminescent HRP substrate	Fluoro-chemiluminescence based microtiter plate assay	ThermoFisher Scientific
High Pure plasmid isolation kit	Preparation of plasmid DNA	GE Healthcare Life Sciences
High Pure PCR product purification kit	PCR product clean-up	GE Healthcare Life Sciences
Monarch gel extraction kit	DNA fragment isolation from agarose gels	New England Biolabs
Monarch DNA purification kit	Clean-up of plasmid	New England Biolabs
PCR DIG Labeling Mix	Digoxigenin-labelling of PCR products (for DNA probes used in Southern blots)	Roche
SureClean	Clean-up of PCR products	Bioline
Mini-plasmid prep	Extraction of plasmid DNA from <i>E. coli</i>	Macherey und Nagel

4.1.8 Bioinformatic tools and computer programs

Bioinformatic tools and computer programs used in this work are listed below (Table 10).

Table 10: Overview of bioinformatic tools and computer programs used in this work.

Programm	Company	Application
Word 2010	Microsoft	Text generation
Excel 2010	Microsoft	Evaluation of data
PowerPoint 2010	Microsoft	Image editing /presentations
Clone Manager 9.0	Sci-Ed	Virtual planing of genetic modifications/ Alignment of protein and DNA sequences
Canvas 15.0	ACD Systems	Image editing, Figure generation
IrfanView 4.36	Irfan Skiljan	Image editing
JaView	(Waterhouse et al., 2009)	Alignment visualization
SignalP 5.0	(Nielsen et al., 2019)	Signal peptide prediction
PEDANT	Munich information center for protein sequences	Genome database
Prism5	GraphPad	Generation of graphs, evaluation of data
Metamorph	ImagXCell	Image editing after microscopy
ImageJ	Worldwide contributors (imagej.net)	Image editing after microscopy
TargetP 2.0	(Armenteros et al., 2019)	Prediction of intracellular protein localization
BLAST N	NCBI	Identification of orthologues nucleotide sequences
BLAST P	NCBI	Identification of orthologues amino acid sequences
BLAST P PSI (position specific iterativ)	NCBI	Identification of distantly related orthologues amino acid sequences
FUGUE	Mizuguchi Lab	Identification of structural orthologues according to a predicted secondary structure
PredictProtein	(Yachdav et al., 2014)	Secondary structure prediction of proteins

RaptorX	(Källberg et al., 2012)	Secondary structure prediction of proteins
Phyre2	(Kelley et al., 2016)	Secondary structure prediction of proteins
HeliQuest	(Gautier et al., 2008) ^b .	Prediction of amphipathic helices

4.2 Methods

4.2.1 Molecular biology methods

All standard techniques of cloning including preparation, purification, restriction digestion and electrophoretic separation of DNA were followed according to Ausubel et al. (1987) and Sambrook et al. (1989). If kits were used, preparation and purification of DNA was performed according to instructions.

4.2.1.1 Polymerase chain reaction (PCR)

For amplification of DNA fragments, PCR was used. PCR programs, especially elongation times, were adapted for each amplified fragment depending on its size. In most cases, 65°C served as annealing temperature. If amplified DNA fragments should be used for cloning purposes, Phusion polymerase (NEB; Frankfurt am Main) was used for PCR. PCR cyclers used in this thesis were purchased from SensoQuest (Germany).

DNA fragment:	1 µL (10 - 50 ng)
Primer 1:	0.5 µL (1 µM)
Primer 2:	0.5 µL (1 µM)
dNTPs:	0.25 µL
DMSO:	0.75 µL
10x Phusion-buffer:	5 µL
Phusion polymerase:	0.5 µL (1 U)
ddH ₂ O	41,5 µL

Example of a standard PCR program:

98°C:	1 min
98°C:	10 sec
55-70°C:	20 sec
72°C:	30 sec
	x34 cycles
4°C	∞

4.2.1.2 Restriction analysis

Enzymes used in this work were purchased from NEB (Darmstadt, Germany) and Roche (Mannheim, Germany). Depending on the restriction enzyme, restriction mixtures were incubated at suitable temperatures for one to four hours. Restriction-derived products were analysed by agarose gel electrophoresis.

Example of a standard restriction reaction:

Restriction enzyme:	0.5 µL
Plasmid DNA:	1 - 3 µL
Enzyme specific buffer:	4 µL
	ad 20 µL ddH ₂ O

4.2.1.3 Ligation of DNA fragments

T4 DNA ligase (Roche; Mannheim, Germany) was used for ligation reactions. For the reaction, insert and vector DNA were used in a molar ratio of 5:1, 3:1 or 1:1. The ligations were incubated overnight at 16°C or at room temperature (~22°C) for 4 h.

Example of a standard ligation reaction:

Vector backbone-DNA:	50-250 ng
Insert-DNA:	3 x molar excess of ligatable ends
T4 DNA Ligase buffer (10X):	1 µL
T4 DNA Ligase:	1 µL
	ad 10 µL with ddH ₂ O

4.2.1.4 Golden Gate cloning

Golden Gate cloning was conducted according to the protocol published in (Terfrüchte et al., 2014). It is based on the application of type II S restriction enzymes, like Bsal and SapI, which are able to hydrolyse DNA fragments outside their recognition sequence. This allows to conduct restriction and ligation reactions in a single reaction tube. Golden Gate cloning was used for the generation of vectors for gene replacements or *in locus* gene fusions, e.g. fluorescence marker genes. For gene deletions, the flanking regions of ~ 1 kb upstream and downstream of the annotated ORF were amplified by PCR. Genomic DNA of wildtype *U. maydis* strain UM521 was used as a template. In a OnePot reaction, containing a combination of restriction enzymes and T4 DNA ligase, the generated PCR fragments were mixed with receiving sites of storage and destination vectors. Storage vectors harboured the resistance cassettes for the gene replacements (Hyg, Nat, G418). The PCR generated upstream and downstream flanks carried compatible restriction sites (Bsal or SapI) to ligate with the resistance cassettes from the storage vectors and the backbones of the destination vectors. *In locus* fusions were conducted in a similar way. Here flanking regions were amplified upstream and downstream of the stop codon of the respective ORF, to generate a 3'-insertion of the fluorescence marker gene. Again, Bsal and SapI compatible storage and destination vectors were used and ligated with the amplified upstream and downstream flanks in a OnePot reaction. A list of storage and destination vectors used in this work, can be found below (Table11/12).

Example of a OnePot reaction mix:

Components	Thermocycler reaction
Upstream flank (40 ng)	Cycle 1: 37°C 2 min
Downstream flank (40 ng)	Cycle 2: 16°C 5 min
Storage vector (75 ng)	Cycle 3: 37°C 5 min
Destination vector (75 ng)	Cycle 4: 50°C 5 min
0.5 µL Bsal-HF/SapI	Cycle 5: 80°C 5min
0.75 µL T4 DNA ligase	Cycle 6: 16°C ∞
1.5 µL 10x T4 DNA ligase buffer	
ad ddH ₂ O 15 µL	

Table 11: Overview of Golden Gate storage vectors used in this work.

pUMa number	Genotype	Insert amplification and backbone insertion	Linearization	Insertion locus	Reference
1694	pStor_NatR_Bsal	/	/	/	Carl Haag
2778	pStor_HygR_SapI	/	/	/	Reindl and Stock et al., 2020
3035	pStor_mCherry_HygR_SapI	MB449 x MB450 on pUMa1557 (0.74 kb) inserted into pUMa2778 with AscI/SapI (4 fragment OnePot with 3 backbone parts: 2.4 kb, 0.28 kb, 2.2 kb)	/	/	This work
3632	pStor_mKate2_SapI	UP832 x UP833 on pUMa2983 (0.72 kb) inserted into pUMa3035 with AscI/EcoRI (4.8 kb)	/	/	This work

Table 12: Overview of Golden Gate destination vectors used in this work.

pUMa number	Genotype	Insert amplification and backbone insertion	Linearization	Insertion locus	Reference
2074	pDest_SapI_HygR	/	SspI	To choose	This work
2779	pDest_UMAG_03776-egfp_HygR (Golden Gate with SapI)	/	SspI	<i>umag_03776</i>	Reindl and Stock et al., 2020
3034	pDest_UMAG_03776-mCherry (Golden Gate with SapI)	UF: DD824 x DD825 on gDNA of UMa521 (1.0 kb). DF: DD819 x DD820 on gDNA of UMa521 (0.92 kb) One Pot reaction with	SspI	<i>umag_03776</i>	This work

		pStor3035 and pDest2074			
3111	pDest_UMAG_03776_G41 8 (Golden Gate with SapI)	/	Sspl	<i>umag_03776</i>	Kai Hussnaette r
3634	pDest_mKate2- Jps1_HygR (Golden Gate with SapI)	UF: DD824 x DD825 on gDNA of UMa521 (1.0 kb). DF: DD819 x DD820 on gDNA of UMa521 (0.92 kb) One Pot reaction with pStor3632 and pDest2074	Sspl	<i>umag_03776</i>	This work

4.2.1.5 Sequencing

All plasmids generated in this thesis were verified by sequencing. Plasmid DNA was purified using the Monarch DNA Clean Up Kit (New England Biolabs) for the sequencing reaction. The reaction mixture additionally contained sequencing oligonucleotides. Sequencing was conducted at Eurofins (Germany).

Example of a standard sequencing reaction:

Plasmid-DNA:	250 ng
Oligonucleotide:	3.2 pmol
	ad 15 µl with ddH ₂ O

4.2.1.6 Separation and detection of nucleic acid

Nucleic acids were analysed using agarose gel electrophoresis. In most cases, an agarose concentration of 0.8% (w/v) was used. The agarose was solved in 1x TAE buffer and boiled in a microwave.

After the gel cooled down to about 60°C, Ethidium bromide was added to a final concentration of 0.25 µg/mL. The liquid gel was poured into a chamber with comb to generate loading wells. After polymerization, (ca. 20 min) the gel was transferred into a running chamber. 1x TAE was used as running buffer. An appropriate amount of 5x

DNA loading buffer was added to each sample before loading into the sample wells. A constant voltage from 80 to 120 V was applied for migration of the poly-anionic DNA fragments from cathode to anode. UV irradiation at 254 nm allowed visualization of separated DNA fragments. For documentation of the gels, the Infinity gel documentation system (Peqlab, Erlangen, Germany) was used.

<u>50x TAE-buffer:</u>	2 mM Tris-Base
	2 mM acetic acid
	10% (v/v) 0.5 M EDTA, pH
	8.0, prepared in ddH ₂ O
<u>5x DNA-loading buffer:</u>	30% (v/v) glycerol
	0.4% (w/v) bromphenol blue,
	prepared in ddH ₂ O

4.2.1.7 Determination of DNA concentration

The concentration of DNA samples was determined by spectrophotometric analysis with NanodropR (Schwerte, Germany). For the measurement, 1 µL of the DNA solution was used. 1 µL of ddH₂O served as blank. A layer thickness of 1 cm corresponds to OD₂₆₀ = 1, at a concentration of 50 µg/ml double-stranded DNA. To determine purity of the DNA, a quotient of A₂₆₀ to A₂₈₀ was used. For pure DNA, a value of 1.8 was expected. Lower values can be related to contamination with proteins, higher values to contamination with salts or sugars.

4.2.1.8 Southern blot analysis

This method was modified according to (Southern, 1975). gDNA isolated from *U. maydis* was prepared as described by (Hoffman and Winston, 1987). First, samples were enzymatically hydrolysed into smaller fragments by type II restriction enzymes and separated by gel electrophoresis. An agarose concentration of 0.8% and a voltage of 100 V were used. After approximately 4-5 h, the agarose gel was incubated in 0.25 M HCl, DENAT and RENAT solutions for 20 min, respectively. During these steps the DNA was depurinated, generating smaller pieces for an efficient transfer from the gel to a nylon membrane during the capillary blot. Here, the transfer solution (20x SSC)

(from a buffer reservoir) migrates through the gel by capillary forces. This allows the elution of DNA fragments and their binding to an overlying nylon membrane (Hybond-N+, Amersham GE Healthcare). The blotting procedure was performed for 4-6 h with or overnight. DNA transferred to the membrane was crosslinked by UV irradiation in a UV-Crosslinker (Cleaver Scientific) at 120 J.

<u>0.25 M HCL:</u>	3.26% (v/v) HCl (25%)
<u>DENAT solution:</u>	1.5 M NaCl 0.4 M NaOH
<u>RENAT solution:</u>	1.5 M NaCl 282 mM Tris-HCl 218 mM Tris-Base
<u>SSPE buffer (20x):</u>	3 mM NaCl 227 mM NaH ₂ PO ₄ *H ₂ O 20 mM Na ₂ -EDTA*2H ₂ O adjust to pH 7.4 with NaOH

Gene-specific probes were labelled by incorporation of Digoxigenin-labelled dNTPs during PCR. PCR mixture contained 10 to 100 pg plasmid DNA, 10 µL PCR buffer, 5 µL PCR DIG labelling mix (Roche), 20 pmol each of the two oligonucleotides and 0.5 µL Phusion polymerase. The reaction was performed in a thermocycler similar to a standard PCR reaction.

The blotted nylon membranes were pre-incubated with Southern hybridization buffer for 30 min at 65°C to saturate nonspecific binding sites. Before application, probes were denatured at 95°C for 5 min and added to 30 mL of pre-warmed hybridization buffer (37°C).

<u>Southern hybridisation buffer:</u>	26% (v/v) SSPE (20x) 5% (v/v) Denhardt solution 5% (v/v) SDS (10%)
---------------------------------------	--

<u>Southern wash buffer I:</u>	10% (v/v) SSPE (20x) 1% (v/v) SDS (10%)
<u>Southern wash buffer II:</u>	5% (v/v) SSPE (20x) 1% (v/v) SDS (10%)
<u>Southern wash buffer III:</u>	0.5% (v/v) SSPE (20x) 1% (v/v) SDS (10%)
<u>DIG-1:</u>	0.1 M malic acid 0.15 M NaCl
<u>DIG-2:</u>	90% (v/v) DIG-1 10% (w/v) skimmed milk powder
<u>DIG-3:</u>	0.1 M Tris-HCL 0.1 M NaCl adjust to pH 9.5 with NaOH
<u>DIG-wash buffer</u>	0.3% (v/v) Tween 20 9.7% (v/v) DIG-1
<u>CDP star solution:</u>	100 µl-CDP star in 10 ml DIG3
<u>Denhard solution:</u>	2% (w/v) BSA fraction V 2% (w/v) Ficoll 2% (w/v) PVP (polyvinylpyrrolidone)

4.2.2 Microbiological methods for *E. coli*

4.2.2.1 Transformation of competent *E. coli* cells

Chemically competent *E. coli* Top10 cells were prepared according to the modified protocol of (Cohen et al., 1972) and stored at -80°C in 50 µL aliquots until use. For transformation, competent cells were thawed on ice (10 min) and 0.5

(retransformation) to 10 μL of a plasmid DNA or ligation mixture were added to the cell suspension. After addition of DNA, cells were further incubated on ice for 30 min, subjected to a heat shock (42°C , 45 s) and again incubated on ice for 2 min. Next, cells were mixed with 300 μL of dYT medium and incubated for 30 min at 37°C for regeneration. In case of a retransformation (plasmid reproduction) the 30 min' time of incubation was shortened to an incubation period of two minutes. In both cases the transformation was plated on dYT solid medium containing Ampicillin for selection and incubated overnight at 37°C .

4.2.2.2 Isolation of plasmid DNA from *E. coli*

Isolation of plasmids for restriction analysis was performed according to protocols of Sambrook et al. (1989). Single colonies of *E. coli* transformants were cultivated in 3 ml dYT liquid medium, supplemented with Ampicillin, overnight at 37°C . On the next day 2 mL culture was pelleted by centrifugation (2 min/ 13000 rpm). The cell pellet was resuspended in 200 μL STET buffer and 20 μL lysozyme solution and boiled for one minute at 95°C . After boiling, the suspension was centrifuged for ten minutes at 13000 rpm. The slimy pellet containing cell debris and genomic DNA was removed with a sterile toothpick. Next, 20 μL sodium acetate solution and 500 μL of isopropanol were added. To precipitate plasmid DNA, the sample was inverted several times and then again centrifuged ten minutes at 13000 rpm. The supernatant was discarded. The pellet was washed in 200 μL of 70% (v/v) ethanol and centrifuged for one minute at 13000 rpm. Supernatant was removed and the pellet dried at 37°C for about 15 minutes. The plasmid DNA was dissolved in 100 μL TE-RNase at 50°C , shaking (500 rpm).

STET-buffer:

0.1 M NaCl
10 mM Tris-HCl, pH 8.0
1 mM EDTA
5% (v/v) Triton-X-100
in ddH₂O, autoclaved

Lysozyme solution:

1.0% (w/v) lysozyme (muraminidase)
10 mM Tris-HCl, pH 8.0
in ddH₂O, filter sterile

<u>Sodium acetate:</u>	3.0 M Sodium acetate in ddH ₂ O, autoclaved
<u>TE-buffer:</u>	8.69 mM Tris-HCl, pH 8,0 10 mM Na ₂ -EDTA*2H ₂ O 1.31 mM Tris-Base in ddH ₂ O, adjust pH to 8.0, autoclave
<u>TE-RNase:</u>	50 µL RNaseA (10 mg/mL) in 50 mL TE

DNA isolated by this method was purified for cloning and sequencing purposes as well as *U. maydis* transformation using the DNA purification Kit from Monarch® (NEB).

4.2.3 Microbiological methods for *U. maydis*

4.2.3.1 Generation of competent cells of *U. maydis* (protoplasts)

The preparation of competent *U. maydis* cells was performed according to the modified protocol by (Schulz et al., 1990) and (Gillissen et al., 1992). A pre-culture was inoculated in 3-10 mL CM-glucose medium and incubated overnight at 28°C on a rotary wheel (3 mL) or on a shaker (10 mL) (200 rpm). On the next morning, a main culture was prepared in 20 or 50 ml CM-glucose medium, adjusting OD₆₀₀ to 0.2. The main culture was grown until an OD₆₀₀ of 0.8 was reached. Cells were pelleted at 3000 rpm for five minutes at room temperature. Next, the pellet was washed with 25 mL SCS buffer (pH 5.8) and centrifuged again at 3000 rpm for five minutes. To degrade the cell wall, the pellet was resuspended in 5 mL of Glucanex solution (30 mg/ ml SCS buffer) and incubated for about five to ten minutes, until the appearance of cone-head-like structures was observed under the microscope. The reaction was stopped adding 50 mL of ice-cold SCS buffer. Cells were then centrifuged at 2400 rpm for 5 min at 4°C. Latter step was repeated. In the last step the pellet was dissolved in 1mL STC buffer. Aliquots of 100 µL were prepared and stored at -80°C until use.

<u>SCS buffer:</u>	20 mM sodium citrate, pH 5.8 1 M sorbitol (Sigma S-1876) in ddH ₂ O, autoclaved
--------------------	--

<u>STC buffer:</u>	10 mM Tris-Cl, pH 7.5
	100 mM CaCl ₂
	1 M sorbitol
	in ddH ₂ O, filtered sterile

4.2.3.2 Transformation of *U. maydis*

A 100 µL aliquot of competent cells of *U. maydis* (protoplasts) was used for the transformation reaction. Cells were thawed on ice for about ten minutes and mixed with 1 to 5 µg of linearized plasmid DNA. 1 µL of heparin solution was added additionally. After ten minutes of incubation on ice, 500 µL of STC/PEG solution were mixed to the suspension and incubated for another 15 min on ice. Next, the entire transformation mixture was plated on a two-layered regeneration agar plate (Bottom layer with appropriate antibiotic, top layer without antibiotic (both need to have the same volume of Reg-light!) that was freshly prepared for each transformation. Plates were incubated for five to seven days at 28°C. Grown colonies were singled on CM agar plates containing the respective antibiotic for selection.

<u>STC/PEG solution:</u>	15 mL STC
	10 g PEG4000

<u>Agar for regeneration</u> <u>(Schulz et al., 1990):</u>	<u>top:</u>
	1.5% (w/v) bacto agar
	8.22% (w/v) 1 M sorbitol
	1.0% (w/v) yeast extract
	0.4% (w/v) bacto pepton
	0.4% (w/v) sucrose
	<u>bottom:</u>
	Prepared like top agar,
	double concentrate antibiotic
	was added here: e.g.
	carboxin 80 µg/100 mL

4.2.3.3 Preparation of *U. maydis* gDNA for Southern blot analysis

The isolation of genomic DNA was performed by a modified protocol published by Hoffman and Winston (1987). A culture of a singled transformant, selected on an antibiotic-containing plate, was inoculated in 3 mL of CM-glucose medium and incubated for two days at 28°C and 200 rpm in a rotatory wheel. After one day of cultivation, 10 µl of the culture were spotted onto a CM-glucose agar plate, to rescue the candidate strain for future use. After two days, cells from 2 mL culture were pelleted by centrifugation at 13000 rpm for 2 min. ~200 µL glass beads were added to the pellet. For cell disruption, the suspension was shaken for 10 min at 1200 rpm on a Vibrax. To further destabilize cell wall and membrane components, the suspension was incubated for 15 min in a heating block at 65°C. Before separating cell components and genomic DNA by centrifugation (15 min/ 13000 rpm), the suspension was incubated on ice for 5 min and mixed with 200 µL of 8 M potassium acetate solution (invert 8-10 times). Centrifugation results in the formation of a lower organic phase, containing cell components such as proteins, and an upper aqueous phase, containing the genomic DNA. 400 µL of this aqueous phase were transferred into a new reaction tube. Genomic DNA was precipitated by addition of 500 µL Isopropanol and centrifugation (15 min/ 13000 rpm). The resulting whitish pellet was again washed with 200 µL of 70% Ethanol (15 min/ 13000 rpm). Ethanol was removed and the pellet was dried at 50°C for 3 minutes (or at 37°C for 15 min). The dry pellet was dissolved in 50 µl TE-RNase at 50°C, shaking (400 rpm).

<u>Lysis-buffer:</u>	10 mM Tris-HCl, pH 8.0
	100 mM NaCl
	1% (w/v) SDS
	1 mM EDTA
	in ddH ₂ O
<u>8M potassium acetate:</u>	prepared in ddH ₂ O

4.2.3.4 Growth analysis of *U. maydis* yeast-like cells with BioLector

To follow cell growth of *U. maydis* yeast-cells online, over a long period of time, the BioLector from m2plabs was used. This device is able to measure the backscattered light of the growing cells over time. In combination with a calibration curve the units of

backscattered light can be correlated with the OD of the cells. Moreover, the BioLector is able to measure fluorescence over time. This can be used to correlate the growth stage of the cells to the expression initiation of a Gfp-tagged protein.

For analysis, a pre-culture of yeast-like cells was grown over night in 10 mL CM-glucose medium (28°C/ 200 rpm). On the next morning cultures were adjusted to an OD₆₀₀ of 0.05. 1.5 mL of the diluted cultures were pipetted into 48-well round-well plates (m2plabs) as technical triplicate. CM-glucose medium was used as blank. The BioLector 2 software was used to programme the setup of the plate and to follow cell growth online. Cell growth was followed for 48 h.

Calculation of growth rate

$$r = \frac{\log(OD_{600}[tx]) - \log(OD_{600}[t0])}{\log(2) * (tx - t0)}$$

Calculation of doubling time from growth rate

$$g = \frac{\ln(2)}{r}$$

4.2.4 Protein biochemical methods

4.2.4.1 Sodium dodecyl sulfate polyacrylamide gel electrophoresis

To separate proteins according to their molecular weight, protein extracts were denatured adding and appropriate amount of sodium dodecylsulfate (SDS) and β-mercaptoethanol (Laemmli buffer). Samples were boiled for five minutes at 95°C. Before loading on a SDS PAGE gel, samples were centrifuged for 5 min at 13000 rpm. To determine protein sizes, PageRuler Prestained Protein Ladder (Thermo Fisher Scientific) was used as size marker. Separation of proteins during SDS PAGE was conducted at 40 mA/gel for 1 h in 1x SDS running buffer. Coomassie Brilliant blue staining of the gels allowed visualization of separated proteins. The staining was performed for 10 min, followed by another 10 to 30 min incubation in destaining solution and ddH₂O.

Stacking gel (for 4 gels): 2.4 mL Tris-HCl pH 6.8
 1.6 mL (v/v) acrylamide
 5.5 mL H₂O
 48 µL 20% (w/v) SDS
 9.6 µL TEMED
 48 µL 10% APS

Running gel (for 4 gels): 10.1 mL Tris-HCl pH 8.8
 6.9 mL H₂O
 135 µL (v/v) 20% (w/v) SDS
 135 µL (v/v) APS
 27 µL (v/v) TEMED

SDS running buffer: 25 mM Tris pH 8.4
 192 mM glycine
 0.1% (v/v) SDS

Laemmli buffer: 150 mM Tris-HCl pH 6.8
 6% (v/v) SDS
 30% (v/v) glycerine
 15% (w/v) β-mercaptoethanol
 0.003% (w/v) bromphenolblue

4.2.4.2 Coomassie brilliant blue staining

For visualization of proteins, the SDS-polyacrylamide gels were stained in Coomassie Brilliant Blue (CBB) staining solution for 1 h. In this case, the CBB binds to the separated proteins. To remove unbound CBB, the gels were then shaken three times for 20 min in CBB destaining solution.

CBB staining solution: 0.05% (w/v) Coomassie Brilliant-Blue R250
 9% (v/v) acetic acid
 45% (v/v) methanol
 in ddH₂O

<u>CBB destaining solution:</u>	10% (v/v) acetic acid
	10% (v/v) methanol
	80% (v/v) ddH ₂ O

4.2.4.3 Western blot analysis

10 µg of denatured protein extracts or protein precipitated from defined volumes of culture supernatants were used for SDS-PAGE and transferred to a PVDF membrane (Amersham, Hybond-P), activated in 100% methanol. Blotting was performed at 75 mA per gel for 1 h in semi-dry blot device (Biometra). For the transfer, Whatman papers were soaked in Anode I, Anode II and Cathode buffer.

Assembly of the Blot:

Cathode of the chamber

SDS gel

1x PVDF membrane

(activated in 100% MeOH)

1x Whatman paper in Anode buffer II

2x Whatman paper in Anode buffer I

Anode of the chamber

A blocking step in TBS-T buffer, supplemented with 3% skimmed milk powder, was conducted for 30 min to 1 h after the blotting procedure. For detection of Jps1 fusion proteins in cell extracts and supernatants of *U. maydis*, α-HA (monoclonal-mouse), α-Gfp (monoclonal-mouse) or α-tRFP (polyclonal-rabbit) primary antibodies (Roche; 1:3000/ Sigma, 1:3000/ Evrogen, 1:2000) were used. For detection of Jps1 fusion proteins in cell extracts of *E. coli*, α-His (monoclonal-mouse) or α-Gfp (monoclonal-mouse) (Roche; 1:1000/ Sigma, 1:3000) were used as primary antibodies. α-mouse or α-rabbit IgG HRP conjugates (Promega; 1:10.000/ NEB 1:10.000) served as secondary antibodies. HRP activity was detected incubating membranes with 150 µL of ECL Prime Western Blotting Detection Reagent (GE Healthcare, Amersham) for 1 min and LAS4000 chemiluminescence imager (GE Healthcare).

<u>Anode buffer I:</u>	300 mM Tris-HCl (pH 10.4)
	15 % (v/v) MeOH
	ad 1 L ddH ₂ O

<u>Anode buffer II:</u>	30 mM Tris-HCl (pH 10.4) 15 % (v/v) MeOH ad 1 L ddH ₂ O
<u>Cathode buffer:</u>	25 mM Tris-HCl (pH 9.4) 15 % (v/v) MeOH 40 mM 6-aminohexanoic acid ad 1 L ddH ₂ O
<u>TBS:</u>	20 mM Tris-HCl 136 mM NaCl in ddH ₂ O, pH 7.4
<u>TBST:</u>	add 0.05 % Tween-20

4.2.4.4 Bradford Assay for determination of protein concentrations

Protein concentrations were determined according to the protocol of (Bradford, 1976). This method is based on a shift in absorption of the triphenylmethane dye Coomassie Brilliant Blue. The dye is able to form complexes with cationic and non-polar side chains of proteins in acidic solution. In its unbound form the absorption maximum is at 470 nm and shifted to 595 nm in the bound form. To determine protein concentrations of the sample, a bovine serum albumin (BSA) standard with known concentrations (0, 50, 100, 125 and 250 µg/mL) was used. Concentration plotted against the absorption value determined for each BSA concentration gives a calibration curve to estimate the protein concentration present in the sample. Therefore, the sample was diluted (1:10) with H₂O. 10 µL of this dilution were incubated with 200 µL 1:5 diluted Bradford reagent (Bio-Rad, Hercules, USA) in a 96 well plate (Sarstedt, Germany) for ten minutes in the dark. Absorbance was measured at 595 nm in a microplate reader (TECAN 200, Männedorf, Switzerland) in duplicates.

4.2.4.5 Protein extraction from yeast like cells in steel cups and reaction tubes

Yeast-like cells were grown to an OD₆₀₀ of 0.75 in 50 mL CM-glucose medium. Cells were harvested by centrifugation at 5000 rpm for 3 min at 4°C. Pelleted cells were either resuspended in 2 mL denaturing or native extraction buffer. The cell suspension

was added to pre-cooled steel cups and shock frozen in liquid nitrogen. Cells were disrupted using a pebble mill (Retsch) for ten minutes at 30 Hz and 4°C. A final centrifugation step (30 min/ 13000 rpm/ 4°C) allowed to pellet cell debris. Protein concentrations in the extracts were determined by Bradford assay (Bradford, 1976).

Alternatively, cell extracts were prepared in reaction tubes. Therefore, 10 mL of the culture were harvested (3 min/ 5000 rpm/ 4°C). The pellet was resuspended in 2 mL TBS-buffer and transferred to a 2 mL reaction tube. The centrifugation step was repeated, and the pellet was shock frozen in liquid nitrogen and stored at -80°C. For protein extraction, the pellet was resuspended in 500 µL native or denaturing extraction buffer. The Retsch Mill was used for cell disruption (30 Hz/ 1 min). To enhance disruption of the fungal cell wall, the reaction tubes were directly incubated in liquid nitrogen. After defrosting at 4°C (5-20 min), the samples were transferred to the Vibrax (5 min/ 1200 rpm/ 4°C). The extraction cycle was repeated after pelleting yet undisrupted cells (3 min/ 5000 rpm/ 4°C). After the second extraction cycle, samples were centrifuged (30 min/ 14.800 rpm/ 4°C). Cell extracts were transferred to fresh reaction tubes. Native cell extracts should be directly used for analysis (e.g. determination of enzyme activity), denatured cell extracts could be stored for several uses (e.g. expression analysis via Western Blot analysis) at -20°C.

Denaturing extraction buffer:

Prepared as stock solution:

0.1 M Na₂PO₄/NaH₂PO₄ (pH 8.0)

8 M urea

0.01 M Tris-HCl (pH 8.0)

Added for protein extraction (for 10 mL):

100 µL 0.1 M PMSF

100 µL Protease inhibitor cocktail (Roche)

50 µL 0.5 mM Benzamidine

Native extraction buffer (for 10 mL): 10 mL 1x PBS (pH 7.0/7.2)

100 µL 0.1 M PMSF

100 µL Protease inhibitor cocktail (w/o EDTA)
(Roche)

50 µL 0.5 mM Benzamidine

4.2.4.6 Protein enrichment from culture supernatants

For the enrichment of Jps1 fusion proteins from culture supernatants yeast-like cells were grown to an OD_{600} of 0.75 in 50 mL CM-glucose medium or Verduyn minimal medium. Supernatants were harvested by centrifugation (3 min/ 5000 rpm/ 4°C) and filtered (MN 615¼ filter paper, Macherey-Nagel). 10% of TCA were added to 40 mL of supernatant. The suspension was inverted at least ten times and incubated for 4 h or overnight at 4°C. Next, precipitated proteins were pelleted by centrifugation (30 min/ 8000 rpm/ 4°C) and repetitive washing with acetone. In the first washing step, 20 mL ice-cold acetone were added and centrifuged for 20 min at 8000 rpm. In the second washing step, pellets were resuspended in 2 mL ice-cold Acetone and transferred to a 2 ml reaction tube for the final centrifugation step (table centrifuge, 20 min/ 13.000 rpm/ 4°C). Resulting pellets were dried and finally dissolved (stepwise) in minimal amounts of 3x Laemmli buffer (~ 50 µL). pH was adjusted using minimal amounts 1M NaOH (2 µL, stepwise) until the colour of the suspension turned from yellow to blue. Before loading on SDS PAGE gels, samples were boiled for five minutes and centrifuged (5 min/ 13000 rpm).

4.2.4.7 Protein enrichment from culture supernatants for MS analysis

In contrast to the protocol for standard TCA precipitation, cells were cultivated in Verduyn minimal medium for mass spectrometry. In addition to TCA solution, 10% N-lauryl sarcosine (f.c. 0.1 %) were added to the harvested culture supernatant and inverted immediately. Also here, precipitation was incubated overnight on ice at 4 C. For application see p. 127.

Verduyn minimal medium:

Prepared as stock solution:

0.1 M Na_2PO_4/NaH_2PO_4 (pH 8.0)

8 M Urea

0.01 M Tris-HCl (pH 8.0)

Added for protein extraction

(for 10 ml):

100 µL 0.1 M PMSF

100 µL Protease inhibitor cocktail
(Roche)

50 µL 0.5 mM Benzamidine

4.2.4.8 Purification of His-tagged proteins from cell extracts of *U. maydis*

4.2.4.8.1 Tabletop purification:

His-tagged Jps1 fusion proteins were purified by immobilized metal affinity chromatography (IMAC) from culture supernatants or native cell extracts of *U. maydis*. To this end, yeast-like cells were inoculated in 10 ml CM-medium (supplemented with 1% glucose) and incubated for 24 hours at 28°C. On the next afternoon a main culture was inoculated in 200 mL CM medium (supplemented with 1% glucose) and set to an OD₆₀₀ of 0.004. The culture was incubated overnight at 28°C. In the next morning supernatant and cells were separated by centrifugation (10 min/ 5000 rpm/ 4°C) when an OD₆₀₀ of approximately 0.8 was reached. Supernatants were filtered (MN 615¼ filter paper, Macherey-Nagel) and cell pellets were resuspended in 2 ml native lysis buffer (further protocol for native cell extract procedure see pp. 112). Cell-free supernatant was adjusted to pH 8.0 with 10x lysis buffer and one complete protease inhibitor cocktail tablet was added (Roche). Ni²⁺-NTA matrix (Macherey-Nagel) was equilibrated with ten column volumes of 1x His lysis buffer supplemented with 10 mM imidazole. 2 mL of equilibrated matrix were added to 200 mL cell-free supernatant and stirred for one hour at 4°C in a batch procedure. For purification of native cell extracts 2 mL equilibrated matrix were added to the extract and incubated on a rotatory wheel for one hour in batch purification at 4°C. Each suspension was then passed through a column and washed with two column volumes each of lysis buffer supplemented with 10 mM and 20 mM imidazole. Bound protein was eluted stepwise with 2 mL of 1x His lysis buffer supplemented with 250 mM imidazole and 1 mL 1x His lysis buffer supplemented with 500 mM imidazole. Fractions were checked by Western blot analysis or by procedures listed below to check for presence of full-length Jps1 fusion proteins.

His-lysis buffer:

50 mM Tris buffered saline (pH 7.4)*

150 mM NaCl

100 µL 0.1 M PMSF

in ddH₂O, set pH to 8.0, add different
conc. of imidazole (1 M stock)

*purchased from Thermo Fisher Scientific

4.2.4.9 Purification of His-tagged proteins from cell extracts of *E. coli*

4.2.4.9.1 Tabletop purification

His-tagged Jps1 fusion proteins were purified by immobilized metal affinity chromatography (IMAC) from native cell extracts of *E. coli*. To this end, one colony of the corresponding *E. coli* strain was inoculated in 10 mL dYT-medium (supplemented with an antibiotic for selection) and incubated over night at 37°C. On the next morning a main culture was inoculated in 200 mL dYT-medium (supplemented with an antibiotic for selection) with 1 ml of the overnight culture. The culture was incubated at 37°C until an OD₆₀₀ of 0.6 was reached. Expression of the Jps1 fusion protein was induced by addition of 0.05M IPTG. Expression was conducted over night at 28°C. On the next morning cells were harvested by centrifugation (10 min/ 7000 rpm/ 4°C). The resulting pellet was resuspended in 30 mL His lysis buffer with 10 mM Imidazole. Cells were lysed by sonication: Five cycles of one-minute sonication steps (continuous; duty cycle: 80%; output control: 8) alternated with 2 min of chilling were applied. Cell debris were separated by centrifugation (30 min/ 11.500 rpm/4°C). Resulting supernatant was used for IMAC. Ni²⁺-NTA matrix (Machery-Nagel) was equilibrated with ten column volumes of 1x His lysis buffer supplemented with 10 mM imidazole. 2 mL of equilibrated matrix were added to the supernatant and batched for two hours at 4°C. The batch was added to a tabletop purification column. After the flow through has passed the column the matrix was washed with two column volumes of lysis buffer supplemented with 10 mM and 20 mM imidazole. Bound protein was eluted stepwise with 2 mL of 1x His lysis buffer supplemented with 100 mM imidazole, 1 mL of 1x His lysis buffer supplemented with 250 mM imidazole and finally with 2 ml of 500 mM His lysis buffer. Fractions were checked by SDS PAGE and Western blot analysis for the presence of full-length Jps1 fusion proteins.

4.2.4.9.2 Purification of proteins from *E. coli* using the ÄTKA Prime plus system

A culture of the respective *E. coli* BL21 DE3 expression strain was grown to an OD₆₀₀ of 0.6 in 300 mL dYT-Amp liquid medium. To induce protein expression IPTG was added to a final concentration of 0.5 mM. The culture was further incubated over night at 28 °C. On the next day the culture was harvested (10 min/ 7000 rpm/ 4°C) and the cell pellet was lysed by sonication. The pellet was resuspended in 10 mL/ 100 mL culture 10 mM His lysis buffer. Sonication was conducted in intervals (5x 1 min) with a

continuous, pulsed duty mode of 80% on ice, with chilling pauses of two min between each cycle. Cell debris and lysate were separated by a centrifugation step (30 min, 11.000 rpm/ 4°C). The generated cell lysate was loaded on a five ml Ni-NTA column, pre-equilibrated in five column volumes (CV) of 10 mM His lysis buffer.

The cell lysate was loaded onto the column. The column was washed with another 5 CV of 10 mM His lysis buffer until the UV spectrum was back down to the equilibration level. Absorption of tryptophan is measured at 280 nm by the ÄKTA indicating protein loading onto or leaving the column. Next 10 CV of 20 mM His Wash buffer were used to remove unbound and unspecifically bound proteins from the column. To avoid contaminations of the purified protein with the host-specific chaperone DnaK in the Elution fractions 20 CV of 20 mM His Wash buffer supplemented with 10 mM ATP and 20 mM MgCl₂ were applied to the column. It is recommended to conduct this washing step with a slow flow rate (0.5 mL/min). Note that the UV spectrum will increase due to absorption of ATP at 280 nm. Again another 10 CV of 20 mM of His Wash buffer were used to bring the UV spectrum down to baseline before elution of the recombinant protein was initiated. 10 CV of 100 mM His Elution buffer were used to elute the recombinant protein from the column matrix.

4.2.4.10 Desalting of Elution fractions after ÄKTA purification

Desalting was conducted to avoid unspecific interactions of the purified proteins and imidazole. First, elution fractions of the IMAC purification were pooled. A maximum of 15 mL can be loaded onto the desalting column. After connecting the column to the system, it needed to be washed with water (5 CV ~ 100 mL) and equilibrated with 1xTBS (5 CV). Next, the sample was loaded onto the column. The column was again washed with 1xTBS until the UV absorption spectrum increased (protein on column). The system was stopped, and the waste tube was placed into a fresh 50 mL reagent tube. The flow of the system was restarted, collecting the eluting protein. After the UV absorption spectrum went back to zero (all protein left the column), the waste tube was placed into the waste bottle to elute the separated salt molecules. In general, the total elution volume of the desalted protein fraction was around 30-35 mL.

4.2.5 Biochemical characterization of Jps1

4.2.5.1 Size exclusion chromatography

To separate aggregates and different oligomeric stages of Jps1, size exclusion using Superdex 200 GL 10/30 (GE Healthcare) was used. The column was connected to the ÄKTA prime plus and washed with two CV (60 mL) of water at a flow rate of 0.1 mL/min overnight. On the next day the column was equilibrated with two CV of 1xTBS buffer (pH 7.4). Importantly, also the feeding loop had to be washed with water and TBS-buffer. Therefore, the ÄKTA was set into the mode “inject” right from the start of the washing procedure. If the measured UV-spectrum of the chromatogram was above baseline-level (0 mAU) the system was manually set to zero (“Autozero”).

In general, 3 mg/mL of the purified protein were loaded onto the column, again using the “injection” mode. Importantly, the size of the sample should not be higher than $\frac{1}{4}$ of the injection loops volume (here: 500 μ L). First, the sample was concentrated before analysis using Amicon Ultra 50K (for Jps1) centrifugal filters (Merck Millipore). Therefore, the protein amount of the whole sample (e.g. 5 mL of elution fraction or 30 mL of desalting fraction) was determined in a Bradford assay. The concentration volume was calculated, determining the quotient of 6 mg/mL (to achieve 3 mg/mL in 500 μ L) and the whole protein amount of the sample.

Example: Bradford assay: **611 μ g/mL** (total volume: **35 mL** after desalting)

$$\frac{6000 \mu g}{611 \mu g} = 10$$

$$\frac{35 mL}{10} = 3,5 mL$$

→ The sample has to be concentrated from 35 mL to 3,5 mL to load approximately 500 μ L of 3 mg/mL protein onto the SEC column

Next, the concentrated protein sample was injected carefully via the injection loop, without any air bubbles in the syringe.

Sampling of the fractions was started when the volume of TBS-buffer passed the dead volume of the column (here: 8 mL). 500 μ L elution fractions were collected as long the chromatogram indicated protein leaving the column.

For size estimation of eluting proteins from the SEC column, elution volumes were compared to a molecular weight standard with proteins of known molecular weight (Table 13).

Table 13: Overview of proteins used for calibration of Superdex 200 GL 10/30, molecular sizes and expected elution volumes.

Protein	Size (kDa)	Elution volume (mL)
Thyroglobulin	669	9.2
Apoferrin	443	10.3
Beta amylase	200	11.6
Alcohol dehydrogenase	150	12.6
Bovine serum albumine	66	14.0
Bovine carbonic anhydrase	29	16.5

4.2.5.2 Multi Angle Light Scattering analysis

(performed in coop. with the Institute for Biochemistry I.HHU, Prof. Lutz Schmitt and Olivia Spitz)

This method was used to determine the approximate molecular weight of Jps1. MALS was performed after SEC of Jps1. The collected sample was applied onto another SEC column (here: Superdex 200 GL 10/30; GE Healthcare) which was directly connected to a triple-light scattering detector (miniDAWN TREOS, Wyatt Technology Europe GmbH, Dernbach, Germany) and a differential refractive index detector (OPTILab T-rEX, Wyatt Technology). Astra7 (Wyatt Technology) was used for evaluation of the collected data.

4.2.5.3 Blue Native PAGE

Blue Native polyacrylamide gel electrophoresis (PAGE) was performed to determine the native conformation of Jps1 (monomer, dimer etc.). Therefore, Jps1 was expressed and purified from *E. coli* cell extracts. In contrast to standard SDS-PAGE, native PAGE allows migration of proteins in their native state without breaking intramolecular bonds. Coomassie Brilliant Blue (CBB) binds to hydrophobic amino acid side chains is conferring a negative charge to the proteins surface (Wittig et al., 2006). This enables migration of the protein through the PAGE from the negative to the plus pole.

NativePAGE Running buffer (20x stock) 50 mM BisTris
50 mM Tricine
ad 1 L ddH₂O
Adjust pH 6.8

Buffer is diluted (1x) with ddH₂O for native PAGE. (1x) native PAGE running buffer is in the following referred to as **Anode buffer**.

For preparation of the **Cathode buffer**, 0.4% Coomassie G-250 is added to 1 L of (1x) Anode buffer. The (20x) buffer stock, the Cathode and the Anode buffer are stable at RT for six months.

NativePAGE Sample buffer (4x) 50 mM BisTris
6 N HCl
50 mM NaCl
10% w/v Glycerol
0.001% Ponceau S
ad 10 mL ddH₂O
adjust to pH 7.2

The buffer is used in a (1x) concentration. Store (4x) sample buffer at 4°C. The buffer is stable for six months at 4°C.

Samples were treated with the NativePAGE Sample buffer and analysed on 4-16% NativePAGE Bis Tris gels. Gels were purchased at "Life Technologies™". A XCell SureLock® Mini-Cell gel running tank was used for gel electrophoresis. Samples were separated at a constant voltage of 150 V for 105-120 minutes at 4°C. The inner chamber of the gel tank was filled with Cathode buffer to the very edge. Anode buffer was filled into the outer chamber of the tank. After 30 minutes, the blue Cathode buffer was exchanged with Anode buffer to be capable of seeing the protein bands separating in the gel. Use a 20 mL glass pipet and a pipet boy to soak the buffer from the inner chamber of the gel tank. Novex™ NativeMARK™ from Thermo Fisher Scientific was used as a molecular size standard.

4.2.6 Lipid biochemical methods

4.2.6.1 Lipid binding analysis on PtdInsP strips

To analyse lipid binding of Jps1 initial analysis was performed using “Membrane Lipid Strips” and “PIP Lipid Strips” from Echelon (Figure 4.1). Before use, the lipid strips were blocked for one hour in 1x TBS buffer with 0.05 % Tween 20 (TBS-T) and 3% BSA. 5 µg of purified Jps1 protein were incubated with the pre-blocked strips in TBS-T buffer supplemented with 3% BSA (total volume 15 ml, shaking box, keep dark). After 1 h incubation at room temperature, unbound protein was removed in three 10 min washing steps with TBS-T. A His- primary antibody (Sigma, 1:2000, anti-mouse) was incubated with the protein-treated lipid strips to detect Jps1 bound via its C-terminal sextuple His-tag. After one hour unbound His-antibody was again removed in three TBS-T washing steps and one with TBS only. AceGlow Western Blot detection solution was used to detect chemiluminescent signals on the lipid membrane.

The PtdIns(4,5)P₂-grip protein (2.5 µg) provided by the kit was used as positive control. The lyophilized protein was resuspended in 12 µL of TBS buffer and added to 5 ml of TBS-T/3%BSA blocking solution to make a final concentration of 0.5 µg. The solution was added to another PIP-strip and incubated for 1 h at room temperature. Washing steps were conducted as mentioned above. Here, a primary anti-GST (Sigma, 1:3000, anti-rabbit) was used to detect bound PtdIns(4,5)P₂-grip protein.

PIP Strips[™] catalog P-6001

Lysophosphatidic Acid (LPA cat # L-0200)	<input type="radio"/>	<input type="radio"/>	Sphingosine-1-phosphate (S1P cat # S-2000)
Lysophosphocholine (LPC cat # L-1518)	<input type="radio"/>	<input type="radio"/>	PtdIns(3,4)P ₂ (cat # P-3416)
PtdIns (cat # P-0016)	<input type="radio"/>	<input type="radio"/>	PtdIns(3,5)P ₂ (cat # P-3516)
PtdIns(3)P (cat # P-3016)	<input type="radio"/>	<input type="radio"/>	PtdIns(4,5)P ₂ (cat # P-4516)
PtdIns(4)P (cat # P-4016)	<input type="radio"/>	<input type="radio"/>	PtdIns(3,4,5)P ₃ (cat # P-3916)
PtdIns(5)P (cat # P-5016)	<input type="radio"/>	<input type="radio"/>	Phosphatidic Acid (PA cat # L-4116)
Phosphatidylethanolamine (PE cat # L-2116)	<input type="radio"/>	<input type="radio"/>	Phosphatidylserine (PS cat # L-3116)
Phosphatidylcholine (PC cat # L-1116)	<input type="radio"/>	<input checked="" type="radio"/>	Blue Blank

Figure 4.1: Schematic overview of PIP Strips (Echelon).

4.2.6.2 Preparation of Giant Unilamellar Vesicles

All lipids were purchased from Cayman Chemicals or Avanti Lipids. Lipids and chloroform were pipetted using individual Hamilton pipets only. All stock solutions were prepared with chloroform in a concentration of 0.2 mg/mL except for the cholesterol stock with 10 mg/mL. Stocks were kept in amber screw vials with Teflon caps (Supelco), which were cleaned with chloroform before use. In addition, Parafilm was wrapped around the caps to avoid evaporation of the lipid stocks during storage. Stocks had to be layered with nitrogen or Argon for storage at -20°C. Before use, lipid stock solutions had to be incubated over night at -20°C. Nitrogen or Argon layering had to be repeated after every opening of the stock.

GUVs were produced using the “PVA-assisted swelling” method published by Weinberger et al., 2013. Therefore, two microscopy object slides were cleaned with chloroform under the fume hood. 100 µL of the 5% PVA were spread equally on the front of one object slide within an area marked on its backside (e.g. a circle). For drying, the PVA coated slide was placed on a thermoblock heated to 50°C.

In the meantime, lipid mixes could be prepared in amber screw vials. Stock solutions needed to reach room temperature (25°C) for pipetting. Lipids were mixed in ratios as listed below (Table 14).

Table 14: Overview of lipid ratios used for PtdIns(4,5)P₂- containing GUVs

Lipid (mol%)	Volume (µL)
DOPC (74,75 mol%)	8.7
Cholesterol (20 mol%)	1.1
PtdInsP (5 mol%)	39.7
Texas Red (0.25 mol%)	0.5
Chloroform	163.4
	Total: 213.4

Table 15: Overview of lipid ratios used for PtdIns(4,5)P₂- containing GUVs

Lipid (mol%)	Volume (µL)
DOPC (74,75 mol%)	8
Cholesterol (20 mol%)	1
PtdInsP (5 mol%)	40.5

Texas Red (0.25 mol%)	0.5
Chloroform	147.5
	Total: 197.5

Of note, it is crucial to also store these lipid mixes overnight at -20°C before use. Prepared lipid mixes could be stored for several uses. They need to be layered with nitrogen after every opening. Screw caps need to be sealed additionally with parafilm for storage. After formation by the swelling method GUVs could be stored for five days at 4°C .

10 μL of the lipid mixes were spread equally onto the PVA coated slides. Another 10 μL of the lipid mix were added after the first layer of lipids had dried. Marked areas of PVA+dried lipids were surrounded by Vitrex on the slides in a “U”-shape. The second cleaned object slide was squeezed onto the Vitrex, generating a sealed chamber. Approx. 500 μL of 10% sucrose solution (e.g. 1g of sucrose solved in 10 mL of H_2O) were filled carefully into the chamber. In case of leakage the sucrose filling was stopped immediately and the Vitrex sealing was corrected. The sucrose-filled chamber needs to be sealed at the top with another layer of Vitrex. Swelling is performed at room temperature ($\sim 25^{\circ}\text{C}$) for one hour. GUVs are harvested from the incubation chamber with microcapillary-tips (VWR) and transferred into fresh reaction tubes. Avoid touching or soaking the PVA-coat during the harvesting process.

Harvested GUVs can now be used for microscopy. If GUVs were not labelled beforehand, they can be visualized by adding 1 μL of FM-64. Ibidi® uncoated μ -angiogenesis slides were used for confocal microscopy. They can be filled with a GUV-protein-buffer mixture up to 50 μL . For experiments in this thesis, 10 μL of GUVs were used and mixed with different amounts of protein. 1xTBS-buffer was added to adjust the required total protein concentration in the well. To immobilize GUVs and to avoid interaction of Jps1 with the negatively charged surface of the wells, wells were coated with 30 μL of β -casein solution for five minutes at room temperature. β -casein was discarded and wells washed with 50 μL of 1xTBS-buffer three-times.

4.2.7 Microscopy

4.2.7.1 Microscopes used in this thesis

1) Basic microscopic analysis of *U. maydis* cells was performed with a wide-field microscope from Visitron Systems (Munich, Germany), Zeiss (Oberkochen, Germany), Axio Imager M1 equipped with a Spot Pursuit CCD camera (Diagnostic Instruments, Sterling Heights, MI) and objective lenses Plan Neofluar (40x, NA 1.3) and Plan Neofluar (63x, NA 1.25). An HXP metal halogen lamp (LEJ, Jena, Germany) in combination with filter sets for mCherry (ET560/40BP, ET585LP, ET630/75BP, Chroma, Bellow Falls, VT), DAPI (HC387/11BP, BS409LP, HC 447/60BP; AHF Analysentechnik, Tübingen, Germany) and Gfp (ET470/40BP, ET495LP, ET525/50BP), was used to excite fluorescence proteins. The programme MetaMorph (Molecular Devices, version 7, Sunnyvale, CA) was used to control the microscope and to adjust the individual settings. MetaMorph, ImageJ and IrfanView served as programmes for image processing, including the adjustment of brightness and contrast as well as the calculation and insertion of scale bars.

2) **Inverted laser scanning confocal microscopy with Airy Scan module:** Zeiss, LSM 880, property of the Centre for Advanced Imaging (CAi), Heinrich Heine University, Düsseldorf. Operated by Sebastian Hänsch. The 32-element AiryScan detector was used, to optimize resolution and signal to noise ratio.

4.2.7.2 Widefield and fluorescence microscopy

For microscopic analysis of *U. maydis* cells, a 20 mL CM-glucose medium overnight culture was inoculated. On the next morning cells had an OD₆₀₀ of ~0.5. A patch of 3% water-agarose was used to fix the cells on the object slide. Therefore ~200 µL water-agarose were spotted on an object slide. 2 µL of *U. maydis* culture were placed on the dried agarose spot. When the culture was dried as well, a thin cover glass was placed on top. Depending on the magnification used, a drop of immersion oil had to be added on the cover glass to allow visualization of the cells with the respective objective.

4.2.7.3 AiryScan confocal microscopy of GUVs

ibidi[®] plates either coated with casein or uncoated were used for inverted laser scanning confocal microscopy with an AiryScan module (Zeiss). To immobilize GUVs and to avoid interaction of Jps1 with the negatively charged surface of the wells, wells

were coated with 30 μL of β -casein solution for five minutes at room temperature. β -casein was discarded, and wells washed with 50 μL of 1xTBS-buffer three times. 30-300 μg of 1mg/mL purified Jps1-eGfp protein from *E. coli* were used for the GUV binding studies. Total protein concentration in the well was adjusted with 1x TBS buffer (max. volume of plate wells: 50 μL).

4.2.8 Determination of enzyme activities

4.2.8.1 Gus activity assay in culture supernatants and native cell extracts

Gus activity in culture supernatants of *U. maydis* was determined using a modified protocol (Stock et al., 2012). Therefore, *U. maydis* strains expressing the Gus-reporter construct were grown to an OD_{600} of 0.8. 2 mL of the culture were pelleted (3 min/ 5000 rpm) and the supernatant was transferred to a fresh reaction tube. For the activity measurement, supernatants were diluted 1:10 (90 μL ddH₂O and 10 μL supernatant). 100 μL of each diluted sample were transferred to a black 96-well plate (96 Well, PS, F-Bottom, μCLEAR , black, CELLSTAR). The reaction was started by adding 100 μL of MUG working solution, containing the fluorogenic substrate 4-methylumbelliferyl β -D-glucuronide hydrate (MUG, bioWORLD) (Mead et al., 1967), solved in 2xGus-buffer, to the samples. Fluorescence was determined for 90 min at 365 nm/ 465 nm in a kinetic measurement using the Tecan Infinite M200 plate reader (Männedorf, Switzerland). The gain of the measurement was adjusted to 60. For calculations, a fluorescence standard was prepared using different concentrations (ranging from 0.1 to 1000 μM) of the product 4-methylumbelliferone (MU).

For determination of Gus activity in native cell extracts, cell extracts of Gus reporter construct expressing strains were prepared according to the protocol "Protein extraction from yeast-like cells". Whole protein concentration was determined using Bradford assay. Samples were adjusted to 10 $\mu\text{g}/\text{mL}$. For the measurement samples were diluted 1:10 (90 μL ddH₂O and 10 μL of 10 $\mu\text{g}/\text{mL}$ cell extract). 100 μL 2x Gus assay buffer were added to each sample to start the reaction. Fluorescence was determined for 90 min at 365 nm/ 465 nm in a kinetic measurement using the Tecan Infinite M200 plate reader (Männedorf, Switzerland). The gain of the measurement was adjusted to 60. For calculations, a fluorescence standard was prepared using different concentrations (ranging from 0.1 to 1000 μM) of the product 4-methylumbelliferone (MU).

2x Gus extraction buffer

28 μ M β -mercaptoethanol
 0.8 mM EDTA (1 M stock, pH 8.0)
 10 mM Na₂PO₄ (1 M stock, pH 7.0)
 0,004 % (v/v) Lauryl-sarcosine
 0.004% (v/v) Triton-X-100
 In ddH₂O

2x Gus assay buffer

1x Gus extraction buffer
 0.2 mg/mL BSA
 2 mM MUG

4.2.8.2 Cts1 activity assay on the cell surface and in native cell extracts

Cts1 activity on the cell surface of *U. maydis* was determined using a modified protocol (Stock et al., 2012). Therefore, *U. maydis* strains were grown to an OD₆₀₀ 0.5. 2 mL of the culture were pelleted (3 min/ 5000 rpm) and the supernatant was discarded. For the activity measurement, cells were resuspended in 1 mL KHM buffer (measure OD₆₀₀ for calculation). 30 μ L of each sample were transferred to a black 96-well plate (96 well, PS, F-Bottom, μ CLEAR, black, CELLSTAR). The reaction was started by adding 70 μ L of MUC working solution, containing the fluorogenic substrate 4-methylumbelliferyl- β -D-N, N', N''-triacetylchitotrioside (MUC, Sigma) (Langner et al., 2015), solved in KHM buffer, to the samples. Fluorescence was determined at a wavelength of 360/450 nm after 1 h incubation at 37 °C using the Tecan Infinite M200 plate reader (Männedorf, Switzerland). The reaction was stopped by adding 200 μ L of 1M Na₂CO₃ solution to the samples in each well. The gain of the measurement was adjusted for each measurement (gain optimal). Obtained fluorescence values were adjusted to OD₆₀₀.

KHM buffer

110 mM Potassium acetate
 20 mM HEPES
 2 mM MgCl₂
 In ddH₂O

MUC working solution

2 mg/mL MUC (dissolved in DMSO), 1:10
 diluted in KHM buffer

4.2.9 Interactome studies

4.2.9.1 Gfp pull-down analysis for interactome studies of Jps1

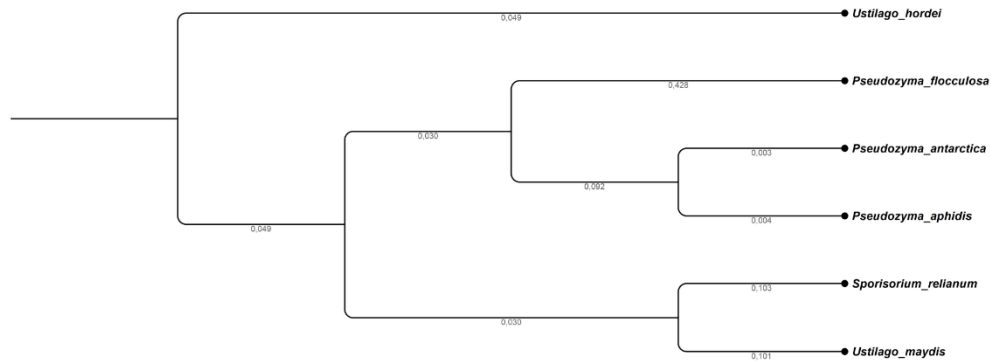
For the pull-down assay native cell extracts of the strains of interest needed to be prepared freshly in pull-down lysis buffer. Gfp-coupled magnetic dynabeads (Chromotech) were equilibrated by washing them twice with 500 μ L of washing buffer. 30 μ L of the beads were added to the native cell extracts and mixed by vortexing. Native cell extract and beads were incubated for 1 h at 4°C on a wheel. Next, samples were shortly pelleted in the centrifuge to separate beads from cell extract. The supernatant was removed with the help of a magnetic stand to avoid any loss of the protein-coupled magnetic beads. Beads were washed trice with 500 μ L of washing buffer. After the washing steps, beads were resuspended in 21 μ L HPLC-grade H₂O. 7 μ L of 4x Laemmli buffer were added additionally and samples were incubated for 5 min at 95°C to denature proteins and to uncouple proteins from the magnetic beads. Samples were again transferred into the magnetic stand to harvest the supernatant for MS-analysis. MS-analysis was performed in cooperation with Gereon Poschmann (BMFZ, HHU Duesseldorf). Orbitrap Fusion Lumos (Thermo Fisher) was used for mass spectrometric analysis.

<u>Lysis buffer</u>	<u>100 mL</u>
50 mM Tris/HCl pH 7.4 (Stock 1 M)	5 mL
150 mM NaCl (Stock 5M)	3 mL
0.5 mM EDTA (Stock 0.5 M)	0.1 mL
0.5 % NP40 (Stock 10%)	5 mL
ddH ₂ O	86.9 mL

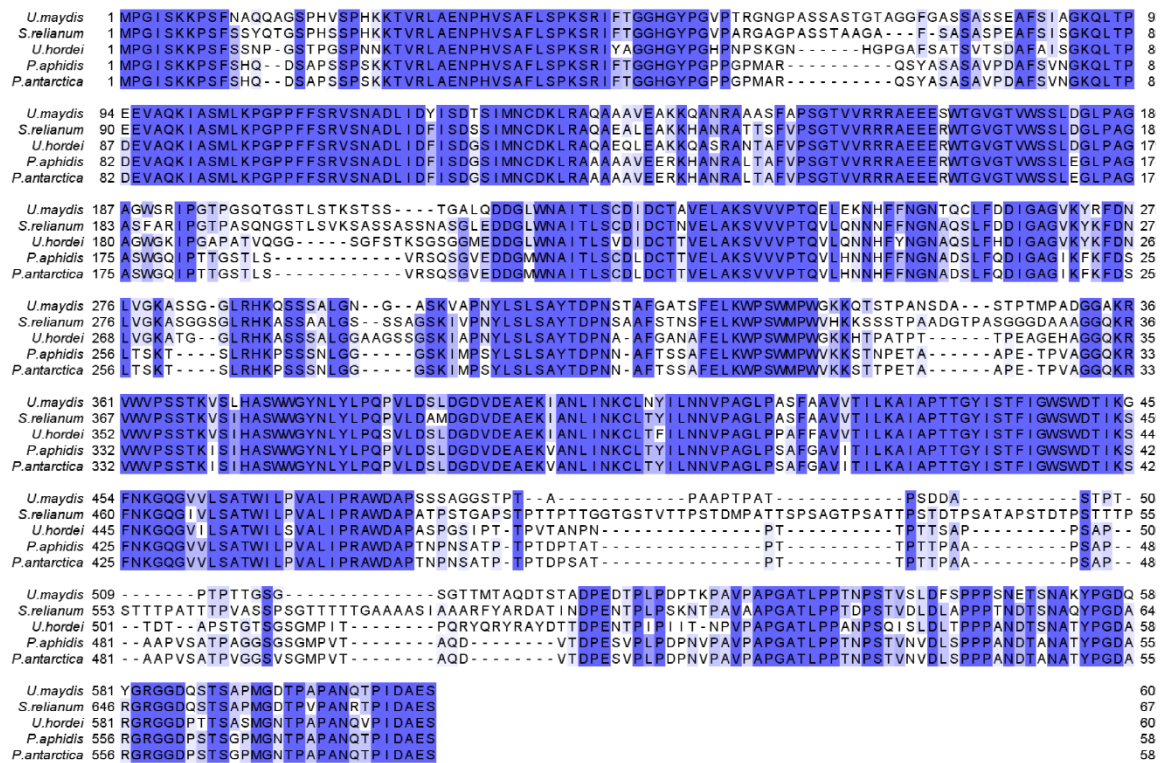
<u>Washing buffer</u>	<u>100 mL</u>
10mM Tris/HCl pH 7.4 (Stock 1M)	1 mL
150mM NaCl (Stock 5M)	3 mL
0.5mM EDTA (Stock 0.5M)	0.1 mL
ddH ₂ O	91.9 mL

5. Supplementary Material

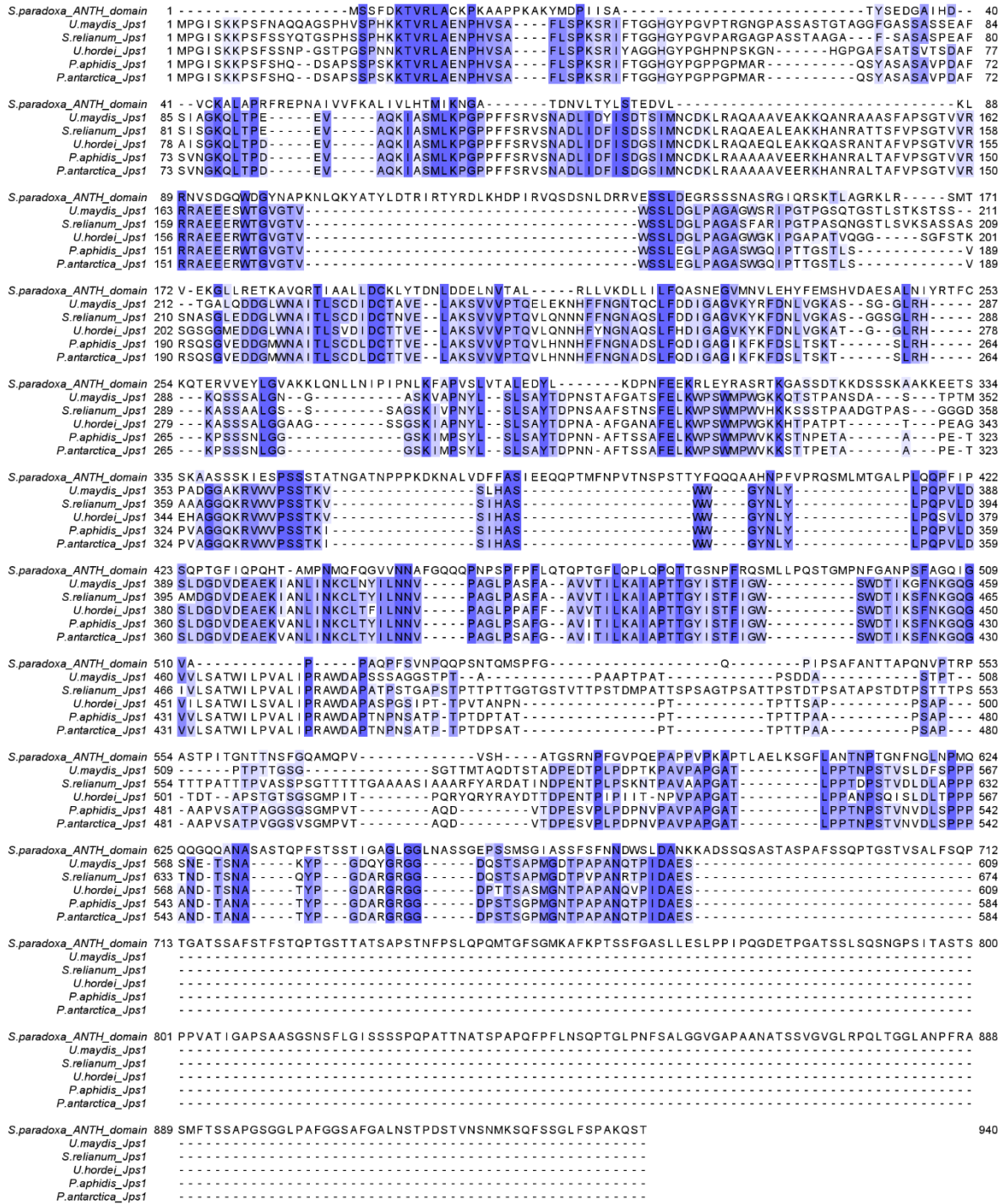
A



B



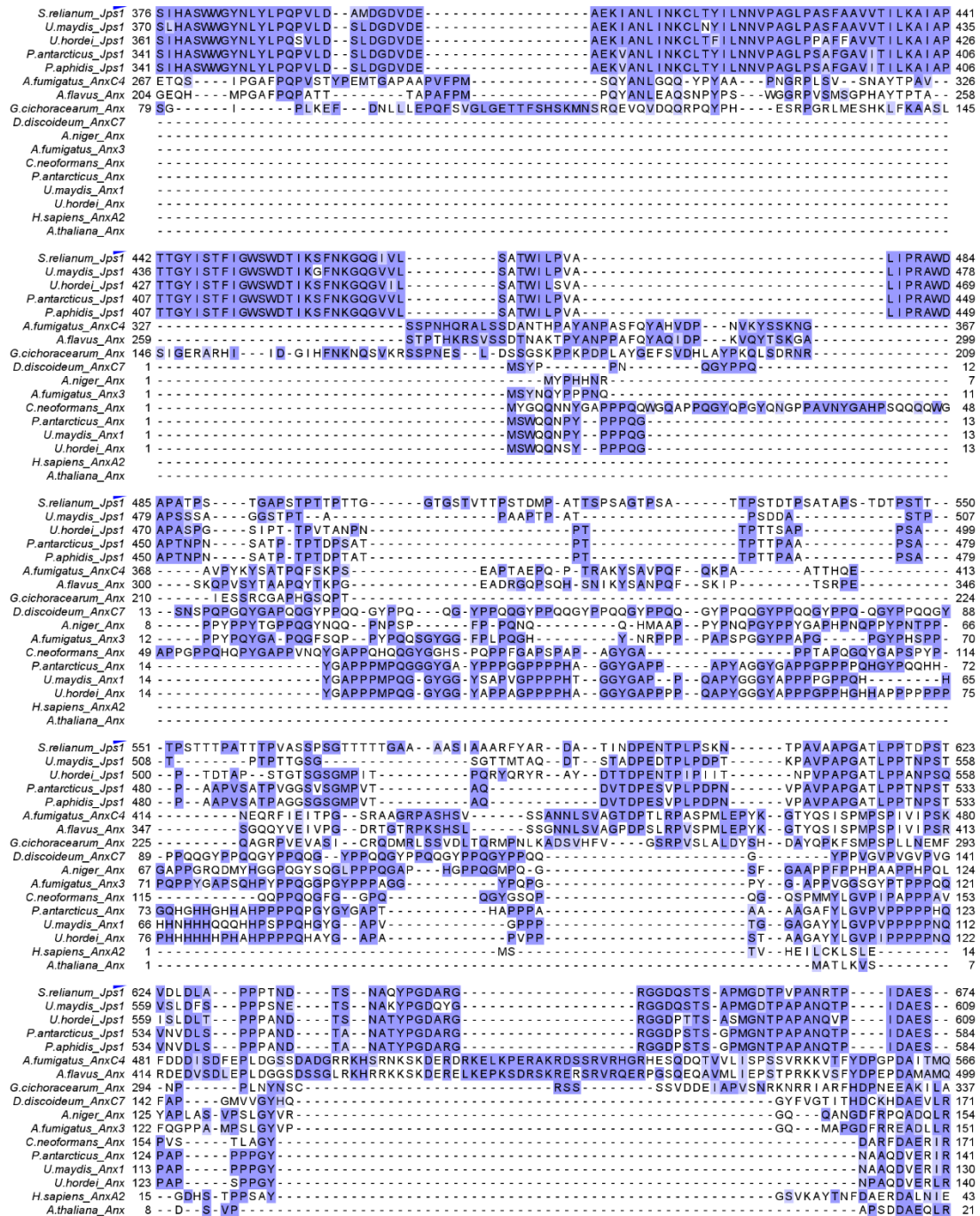
Supplementary Figure 1: (A) Phylogenetic tree displaying the lineage of basidiomycete relatives of *U. maydis* according to the conservation of the protein sequence of Jps1. **(B)** Alignment of Jps1 and close basidiomycete relatives. Highly conserved parts within the amino acid sequence are marked in dark blue, more variable ones in light blue. Conserved regions stretch all over the protein. Alignment and tree generated with ClustalOmega and JalView.



Supplementary Figure 2: Alignment of an ANTH-domain containing protein from *Schizopora paradoxa* vs. Jps1 and orthologs from close basidiomycete relatives. Highly conserved parts within the amino acid sequence are marked in dark blue, regions of lower conservation in lighter shades of blue. Alignment generated with ClustalOmega and JalView.

5. Supplementary Material

<i>S.reliantum</i> _Jps1	1	MPGI SKKPSFSSYQTGSPHSSPHKKTVRLAENPHVSAFLSPKSRIFTGGHGYPGVPARGAGPASSTAAGA---F-SASASPEAFSI	82
<i>U.maydis</i> _Jps1	1	MPGI SKKPSFNAQAGSPHVSPHKKTVRLAENPHVSAFLSPKSRIFTGGHGYPGVPTRGNGPASSASTGTAGFGASSASSEAFSI	86
<i>U.hordei</i> _Jps1	1	MPGI SKKPSFSSNP-GSTPGSPNNKTVRLAENPHVSAFLSPKSRITYAGGHGYPGHPNPSKGN-----HGGGAFSATSVTSDAFI	79
<i>P.antarcticus</i> _Jps1	1	MPGI SKKPSFSSHQ--DSAPSSPKKTVRLAENPHVSAFLSPKSRIFTGGHGYPGPPGPMAR-----QSYASASAVPDAFSV	74
<i>P.aphidis</i> _Jps1	1	MPGI SKKPSFSSHQ--DSAPSSPKKTVRLAENPHVSAFLSPKSRIFTGGHGYPGPPGPMAR-----QSYASASAVPDAFSV	74
<i>A.fumigatus</i> _AnxC4	1	MSLQVKDPR-----SRGRSKSPSGRIFDRSKSRD-----SRLPSTAPDAARS	42
<i>A.flavus</i> _Anx	1	MSLQADDPR-----SRGRSKSRGRSSSHA-----SA	26
<i>G.cichoracearum</i> _Anx			
<i>D.discoideum</i> _AnxC7			
<i>A.niger</i> _Anx			
<i>A.fumigatus</i> _Anx3			
<i>C.neoformans</i> _Anx			
<i>P.antarcticus</i> _Anx			
<i>U.maydis</i> _Anx1			
<i>U.hordei</i> _Anx			
<i>H.sapiens</i> _AnxA2			
<i>A.thaliana</i> _Anx			
<i>S.reliantum</i> _Jps1	83	SGK-QLTPEEVAQKI ASMLKPGPPFFSRVSNADLI DFI SDGSI MNCDKLRQAQEALEAKKHANRATTSFV-----	151
<i>U.maydis</i> _Jps1	87	AGK-QLTPEEVAQKI ASMLKPGPPFFSRVSNADLI DFI SDGSI MNCDKLRQAQAAVEAKKQANRAAASFA-----	155
<i>U.hordei</i> _Jps1	80	SGK-QLTPEEVAQKI ASMLKPGPPFFSRVSNADLI DFI SDGSI MNCDKLRQAQEALEAKKQASRANTAFV-----	148
<i>P.antarcticus</i> _Jps1	75	NGK-QLTPEEVAQKI ASMLKPGPPFFSRVSNADLI DFI SDGSI MNCDKLRQAQAAVEERKHANRALTAFV-----	143
<i>P.aphidis</i> _Jps1	75	NGK-QLTPEEVAQKI ASMLKPGPPFFSRVSNADLI DFI SDGSI MNCDKLRQAQAAVEERKHANRALTAFV-----	143
<i>A.fumigatus</i> _AnxC4	43	SERKYLATDARDHLLRSRSG--G--PRDSINTSVSS-----H--RSRSRYDVSDSASERDDRKDRYL	97
<i>A.flavus</i> _Anx	27	RGNTYLSSEPADEYLRARSRSRG--YRTSAGHL-----	57
<i>G.cichoracearum</i> _Anx			
<i>D.discoideum</i> _AnxC7			
<i>A.niger</i> _Anx			
<i>A.fumigatus</i> _Anx3			
<i>C.neoformans</i> _Anx			
<i>P.antarcticus</i> _Anx			
<i>U.maydis</i> _Anx1			
<i>U.hordei</i> _Anx			
<i>H.sapiens</i> _AnxA2			
<i>A.thaliana</i> _Anx			
<i>S.reliantum</i> _Jps1	152	-----PSGTV---VRRRA-----EEERWTGVTWSSLDGLPAGASFARI PGT PASQNGSTLSVKSASSASS	210
<i>U.maydis</i> _Jps1	156	-----PSGTV---VRRRA-----EEESWTGVTWSSLDGLPAGAGWSRI PGT PGSQTGSLSTKSTSS--	211
<i>U.hordei</i> _Jps1	149	-----PSGTV---VRRRA-----EEERWTGVTWSSLDGLPAGAGWGI P G A P A T V Q G G-----S G F S T K S	202
<i>P.antarcticus</i> _Jps1	144	-----PSGTV---VRRRA-----EEERWTGVTWSSLDGLPAGASWGI P T T G S T L S-----V R	190
<i>P.aphidis</i> _Jps1	144	-----PSGTV---VRRRA-----EEERWTGVTWSSLDGLPAGASWGI P T T G S T L S-----V R	190
<i>A.fumigatus</i> _AnxC4	98	RSERRRDHYIQSDSGESKLAKRDRDKDYARSPNLRPVITYE SPS--DDSYSDT--DDEALAYGDAPS D L E R D F Y G Y R K P A R A S S--	176
<i>A.flavus</i> _Anx	58	-----PSGPD LGHYTYLRDNTDPSRSPNLRPVRYDAPP--DDVYSES--DDEGLAYGDFP G G L E R D Y Y G Y M A T P R T S S--	126
<i>G.cichoracearum</i> _Anx			
<i>D.discoideum</i> _AnxC7			
<i>A.niger</i> _Anx			
<i>A.fumigatus</i> _Anx3			
<i>C.neoformans</i> _Anx			
<i>P.antarcticus</i> _Anx			
<i>U.maydis</i> _Anx1			
<i>U.hordei</i> _Anx			
<i>H.sapiens</i> _AnxA2			
<i>A.thaliana</i> _Anx			
<i>S.reliantum</i> _Jps1	211	NASGLEDDGLWNAITLSCDIDCTNVELAKSVVPTQVLQNNHFFNGNAQSLFDDIGAGVKYKFDNLVKGASGGSLRHKASSAALG	296
<i>U.maydis</i> _Jps1	212	TGALODDGLWNAITLSCDIDCTAVELAKSVVPTQELKNNHFFNGNTQCLFDDIGAGVKYRFDNLVKGASSG-GLRHKQSSSALG	295
<i>U.hordei</i> _Jps1	203	GSGMEDDGLWNAITLSDVIDCTTVELAKSVVPTQVLQNNHFFNGNAQSLFHDIGAGVKYKFDNLVKGATG--GLRHKASSSALG	286
<i>P.antarcticus</i> _Jps1	191	SQSGVEDDGMWNAITLSCDIDCTTVELAKSVVPTQVLHNNHFFNGNADSLFQDIGAGIKFKFDSLTSKT---SLRHKPSSSNIKG	272
<i>P.aphidis</i> _Jps1	191	SQSGVEDDGMWNAITLSCDIDCTTVELAKSVVPTQVLHNNHFFNGNADSLFQDIGAGIKFKFDSLTSKT---SLRHKPSSSNIKG	272
<i>A.fumigatus</i> _AnxC4	177	-----PRVDGP-----VM-----SGALNGAPP-----AKHD-----SRSRHAASEDIPG	211
<i>A.flavus</i> _Anx	127	-----SQVNGA-----MM-----SGALNGDRR-----VGKE-----PTS--GRSSEELG	159
<i>G.cichoracearum</i> _Anx			
<i>D.discoideum</i> _AnxC7	1	-----MR-----MRIQNDPE-----MDLS-----NS-----LD--T	20
<i>A.niger</i> _Anx			
<i>A.fumigatus</i> _Anx3			
<i>C.neoformans</i> _Anx			
<i>P.antarcticus</i> _Anx			
<i>U.maydis</i> _Anx1			
<i>U.hordei</i> _Anx			
<i>H.sapiens</i> _AnxA2			
<i>A.thaliana</i> _Anx			
<i>S.reliantum</i> _Jps1	297	S--SSA-----GSKI VPNYLSLSAYTDPNSAAFSTNSFELKWP SWMPWVHKSSSTPAADGTPASGGGDA AAGGQKRWWPSSSTKV	375
<i>U.maydis</i> _Jps1	296	N--G-----ASKVAPNYLSLSAYTDPNSTAFGATSFELKWP SWMPWGKKTSTPANSDA--STPTMPADGGAKRWWPSSSTKV	369
<i>U.hordei</i> _Jps1	287	GAAGSS-----GSKI APNYLSLSAYTDPNA-AFGANAFELKWP SWMPWGKKTTPATPT-----TPEAGEHAGGQKRWWPSSSTKV	360
<i>P.antarcticus</i> _Jps1	273	G-----GSKI MPSYLSLSAYTDPNN-AFTSSAFELKWP SWMPWVKKSTTPETA-----APE-TPVAGGQKRWWPSSSTKI	340
<i>P.aphidis</i> _Jps1	273	G-----GSKI MPSYLSLSAYTDPNN-AFTSSAFELKWP SWMPWVKKSTTPETA-----APE-TPVAGGQKRWWPSSSTKI	340
<i>A.fumigatus</i> _AnxC4	212	HHPYSYARPGGFYAMP SQYG--QFQP-----SYPTTS-APQSNWAFIPECERF-----GFVPPSSQA	266
<i>A.flavus</i> _Anx	160	GHPSYAKPGAWKYATPGQYL--HA-----QPDWAT IPECERF-----GFVPPSSQA	203
<i>G.cichoracearum</i> _Anx			
<i>D.discoideum</i> _AnxC7	21	AIEKNSRSQSWEMETQHDSSMTFMN-----GINELEQKIKVQRVTANAHI ERK-----NTIPATSRH	78
<i>A.niger</i> _Anx			
<i>A.fumigatus</i> _Anx3			
<i>C.neoformans</i> _Anx			
<i>P.antarcticus</i> _Anx			
<i>U.maydis</i> _Anx1			
<i>U.hordei</i> _Anx			
<i>H.sapiens</i> _AnxA2			



Supplementary Figure 3: Alignment of Jps1 and orthologs with annexins of other basidiomycetes. Highly conserved parts within the amino acid sequence are marked in dark blue, regions of lower conservation in lighter shades of blue. Alignment generated with ClustalOmega and JalView.

```

Um Anx1/1-430 1 MSWQQNPYP P P P P P Q G Y G A P P P M P Q G G Y G G Y S A P V G P P P P H T G G Y G A P P Q A P Y G G G Y A P P P P 56
Jps1/1-609 1 . . . . . M P . . . . . G I S K . . . . . K P S F N A Q Q A 11

Um Anx1/1-430 60 G P P Q H H H H N H H H H Q Q Q H H P S P P Q H G Y G A P V G P P P T G G A G A Y Y L G V P V P P P P N Q . . . . . 116
Jps1/1-609 16 G S P H V S P H K K T V R . . L A E N P H V S A F L S P K S R I F T G G H . . G Y P G V P T R G N G P A S S A S T G T 71

Um Anx1/1-430 113 . . . . . P A P P P P G Y N A A Q D V E R I R K A T K G F G T 139
Jps1/1-609 71 A G G F G A S S A S S E A F S I A G K Q L T P E E V A Q K I A S M L K P G P P F F S R V S N A D L . . . . . 118

Um Anx1/1-430 139 D E G A L I A T L A P L D A W Q V D A L R H T F K A S V G K . . . . . D L L T V L E K E T S G W F E A 185
Jps1/1-609 120 . . . . . I D Y I S D T S I M N C D K L R A Q A A A V E A K Q A N R A A A S F A P S G T V V R R R A E E E S W T G V 176

Um Anx1/1-430 185 A L R A K . V L G P V L Y D C W L I K R . . . . . A C Q G A G 201
Jps1/1-609 174 G T V W S S L D G L P A G A G W S R I P G T P G S Q T G S T L S T K S T S S T G A L Q D D G L W N A I T L S C D I D C 231

Um Anx1/1-430 210 T H E D L L N E V L L G R T N S . E M H I L K Q A Y Q A T Y G K N M E K V V E E L S F K T K R M F V M A . M Q G V R 266
Jps1/1-609 233 T A V E L A K S V V V P T Q E L E K N H F F N G N T Q C L F D . . . . . D I G A G V K Y R F D N L V G K A S S G G L R 288

Um Anx1/1-430 267 Q E D N I P V D P R A V E A D V A A L H G A A R G A G T D E I A I C G I L I Q . R S S P H L A . . . . . 313
Jps1/1-609 287 H K Q . . . . . S S S A L G N G A S K V A P N Y L S L S A Y T D P N S T A F G A T S F E L K W P 321

Um Anx1/1-430 313 . . . . . A V A Q A Y Q Q R H R R P L S K 329
Jps1/1-609 330 S W M P W G K K Q T S T P A N S D A S T P T M P A D G G A K R V W V P S S T K V S L H A S W W G Y N L Y L P Q P V L D 388

Um Anx1/1-430 329 M I D A E F . . . . . S G H M Q D A L R F I V D G A E H D G Q G I T R D A R L L E D S M K G M G T K D E R L I Y R V 385
Jps1/1-609 389 S L D G D V D E A E K I A N L I N K C L N Y I L N N V P A . . . . . G L P A S F A A V V T I L K A I A . . . . . P T T G Y I S 444

Um Anx1/1-430 382 A R L H W N K P R F E G Q I K P A Y A Q L . . . . . F H K K G L K N R V E G . . . . . E T S G D Y K R M . . . . . 428
Jps1/1-609 442 T F I G W S W D T I K G F N K G Q G V V L S A T W I L P V A L I P R A W D A P S S S A G G S T P T A P A A P T P A T P 500

Um Anx1/1-430 424 . . . . . L S A M I G S . . . . . 430
Jps1/1-609 501 S D D A S T P T P T P T T G S G S G T T M T A Q D T S T A D P E D T P L P D P T K P A V P A P G A T L P P T N P S T V 551

Um Anx1/1-430 . . . . .
Jps1/1-609 560 S L D F S P P P S N E T S N A K Y P G D Q Y G R G G D Q S T S A P M G D T P A P A N Q T P I D A E S 606

```

Supplementary Figure 4: Alignment of Jps1 and Anx1 from *U. maydis*. Highly conserved parts within the amino acid sequence are marked in dark blue, regions of lower conservation in lighter shades of blue. Alignment generated with ClustalOmega and JalView.

References

- Aichinger, C., Hansson, K., Eichhorn, H., Lessing, F., Mannhaupt, G., Mewes, W., Kahmann, R.** (2003). Identification of plant-regulated genes in *Ustilago maydis* by enhancer-trapping mutagenesis. *Molecular Genetics and Genomics*, **270(4)**, 303–314. <https://doi.org/10.1007/s00438-003-0926-z>
- Abrahamson, H., Stenmark, H.** (2010). Protein Secretion: Unconventional exit by exophagy. *Current Biology*, **20(9)**, 415–418. DOI: 10.1016/j.cub.2010.03.011
- Akerblom, L., Ehrenberg, A., Gräslund, A., Lankinen, H., Reichard, P., Thelander, L.** (1981). Overproduction of the free radical of ribonucleotide reductase in hydroxyurea-resistant mouse fibroblast 3T6 cells. *Proceedings of the National Academy of Sciences of the United States of America*, **78(4)**, 2159–2163. <https://doi.org/10.1073/pnas.78.4.2159>
- Altamirano, S., Chandrasekaran, S., Kozubowski, L.** (2017). Mechanisms of cytokinesis in basidiomycetous yeasts. *Fungal Biology Reviews*, **31(2)**, 73–87. <https://doi.org/10.1016/j.fbr.2016.12.002>
- Alvarez-Tabarés, I., Pérez-Martín, J.** (2010). Septins from the phytopathogenic fungus *Ustilago maydis* are required for proper morphogenesis but dispensable for virulence. *PLoS ONE*, **5(9)**, 1–17. <https://doi.org/10.1371/journal.pone.0012933>
- Andrei, C., Dazzi, C., Lotti, L., Torrisi, M. R., Chimini, G., Rubartelli, A.** (1999). The secretory route of the leaderless protein interleukin 1 β involves exocytosis of endolysosome-related vesicles. *Molecular Biology of the Cell*, **10(5)**, 1463–1475. <https://doi.org/10.1091/mbc.10.5.1463>
- Armenteros, J. J. A., Salvatore, M., Emanuelsson, O., Winther, O., Von Heijne, G., Elofsson, A., Nielsen, H.** (2019). Detecting sequence signals in targeting peptides using deep learning. *Life Science Alliance*, **2(5)**, 1–14. <https://doi.org/10.26508/lsa.201900429>
- Aschenbroich, J.** (2019). Analyse des unkonventionellen Sekretionsmechanismus der Chitinase Cts1 aus *Ustilago maydis*. *PhD Thesis*, Heinrich-Heine-Universität Düsseldorf.
- Aschenbroich, J., Hussnaetter, K. P., Stoffels, P., Langner, T., Zander, S., Sandrock, B., Bölder, M., Feldbrügge, M., Schipper, K.** (2018). The germinal centre kinase Don3 is crucial for unconventional secretion of chitinase Cts1 in *Ustilago maydis*. *Biochimica et Biophysica Acta - Proteins and Proteomics*, *October*. <https://doi.org/10.1016/j.bbapap.2018.10.007>
- Ast, T., Cohen, G., Schuldiner, M.** (2013). A network of cytosolic factors targets SRP-independent proteins to the endoplasmic reticulum. *Cell*, **152(5)**, 1134–1145. <https://doi.org/10.1016/j.cell.2013.02.003>
- Ausubel, F., Brent, R., Kingston, R., Moore, D., Seidman, J. G., Smith, J., Struhl, K.** (1991). No Title. *Current Protocols in Molecular Biology*, **66(2)**.
- Backhaus, R., Zehe, C., Wegehngel, S., Kehlenbach, A., Schwappach, B., Nickel, W.** (2004). Unconventional protein secretion: Membrane translocation of FGF-2 does not require protein unfolding. *Journal of Cell Science*, **117(9)**, 1727–1736.

<https://doi.org/10.1242/jcs.01027>

- Banuett, F.** (1991). Identification of genes governing filamentous growth and tumor induction by the plant pathogen *Ustilago maydis*. *Proceedings of the National Academy of Sciences of the United States of America*, **88(9)**, 3922–3926. <https://doi.org/10.1073/pnas.88.9.3922>
- Banuett, F., Quintanilla, R. H., Reynaga-Peña, C. G.** (2008). The machinery for cell polarity, cell morphogenesis, and the cytoskeleton in the Basidiomycete fungus *Ustilago maydis*—A survey of the genome sequence. *Fungal Genetics and Biology*, **45(SUPPL. 1)**. <https://doi.org/10.1016/j.fgb.2008.05.012>
- Begerow, D., Kellner, R., Vollmeister, E., Feldbrügge, M.** (2011). Interspecific Sex in Grass Smuts and the Genetic Diversity of Their Pheromone-Receptor System. *PLoS Genetics*, **7(12)**, 1–17. <https://doi.org/10.1371/journal.pgen.1002436>
- Bertolotti, A., Zhang, Y., Hendershot, L. M., Harding, H. P., Ron, D.** (2000). Dynamic interaction of BiP and ER stress transducers in the unfolded-protein response. *Nature Cell Biology*, **2(6)**, 326–332. <https://doi.org/10.1038/35014014>
- Beychok, S.** (1966). Circular dichroism of biological macromolecules. *Science*, **154(3754)**, 1288–1299. <https://doi.org/10.1126/science.154.3754.1288>
- Bhavsar-Jog, Y. P., Bi, E.** (2017). Mechanics and regulation of cytokinesis in budding yeast. *Seminars in Cell and Developmental Biology*, **66**, 107–118. <https://doi.org/10.1016/j.physbeh.2017.03.040>
- Bianco, F., Pravettoni, E., Colombo, A., Schenk, U., Möller, T., Matteoli, M., Verderio, C.** (2005). Astrocyte-Derived ATP Induces Vesicle Shedding and IL-1 β Release from Microglia. *The Journal of Immunology*, **174(11)**, 7268–7277. <https://doi.org/10.4049/jimmunol.174.11.7268>
- Blobel, G., Dobberstein, B.** (1981). Presence of Proteolytically Processed and Unprocessed Nascent Immunoglobulin Light Chains On Membrane-Bound Ribosomes of Murine Myeloma. *Annual Review of Biochemistry*, **67**, 835–851. <http://www.annualreviews.org/doi/pdf/10.1146/annurev.bi.50.070181.001533>
- Böhmer, C., Böhmer, M., Bölker, M., Sandrock, B.** (2008). Cdc42 and the Ste20-like kinase Don3 act independently in triggering cytokinesis in *Ustilago maydis*. *J Cell Sci*, **121(Pt 2)**, 143–148. <https://doi.org/10.1242/jcs.014449>
- Böhmer, C.** (2009). Septin- und Aktomyosindynamik während der Zellteilung von *Ustilago maydis*. *PhD thesis*. Philipps-Universität Marburg.
- Böhmer, C., Ripp, C., Bölker, M.** (2009). The germinal centre kinase Don3 triggers the dynamic rearrangement of higher-order septin structures during cytokinesis in *Ustilago maydis*. *Molecular Microbiology*, **74(6)**, 1484–1496. <https://doi.org/10.1111/j.1365-2958.2009.06948.x>
- Bölker, M.** (2001). *Ustilago maydis* A valuable model system for the study of fungal dimorphism and virulence. *Microbiology*, **1435(147)**, 24–1395. <http://www.microbiologyresearch.org/docserver/fulltext/micro/147/6/1471395a.pdf?expires=1529333365&id=id&acname=guest&checksum=DCE6345E9CA312FC011995FE1C022330>

- Boll, A., Jatho, A., Czudnochowski, N., Geyer, M., Steinem, C.** (2011). Mechanistic insights into the translocation of full length HIV-1 Tat across lipid membranes. *Biochimica et Biophysica Acta - Biomembranes*, **1808(11)**, 2685–2693. <https://doi.org/10.1016/j.bbamem.2011.07.030>
- Bouzenzana, J., Pelosi, L., Briolay, A., Briolay, J., Bulone, V.** (2006). Identification of the first Oomycete annexin as a (1→3)- β -D- glucan synthase activator. *Molecular Microbiology*, **62(2)**, 552–565. <https://doi.org/10.1111/j.1365-2958.2006.05389.x>
- Boyce, K. J., Chang, H., D'Souza, C. A., Kronstad, J. W.** (2005). An *Ustilago maydis* septin is required for filamentous growth in culture and for full symptom development on maize. *Eukaryotic Cell*, **4(12)**, 2044–2056. <https://doi.org/10.1128/EC.4.12.2044-2056.2005>
- Braakman, I., Bulleid, N. J.** (2011). Protein Folding and Modification in the Mammalian Endoplasmic Reticulum. *Annual Review of Biochemistry*, **80(1)**, 71–99. <https://doi.org/10.1146/annurev-biochem-062209-093836>
- Brachmann, A., König, J., Julius, C., Feldbrügge, M.** (2004). A reverse genetic approach for generating gene replacement mutants in *Ustilago maydis*. *Molecular Genetics and Genomics*, **272(2)**, 216–226. <https://doi.org/10.1007/s00438-004-1047-z>
- Brachmann, Andreas.** (2001). Die frühe Infektionsphase von *Ustilago maydis*: Genregulation durch das bW/bE-Heterodimer. *PhD Thesis*, Ludwig-Maximilians-Universität München.
- Bradford, M.** (1976). A rapid and sensitive method for the quantification of microgram quantities of protein utilizing the principle of protein-dye binding. *Analytical Biochemistry*, **72**, 248–254.
- Brough, D., Pelegrin, P., Nickel, W.** (2017). An emerging case for membrane pore formation as a common mechanism for the unconventional secretion of FGF2 and IL-1 β . *Journal of Cell Science*, **130(19)**, 3197–3202. <https://doi.org/10.1242/jcs.204206>
- Brough, D., Rothwell, N. J.** (2007). Caspase-1-dependent processing of pro-interleukin-1 β is cytosolic and precedes cell death. *Journal of Cell Science*, **120(5)**, 772–781. <https://doi.org/10.1242/jcs.03377>
- Brown, J. C. S., Nelson, J., Vandersluis, B., Deshpande, R., Butts, A., Kagan, S., Polacheck, I., Krysan, D. J., Myers, C. L., Madhani, H. D.** (2014). Unraveling the biology of a fungal meningitis pathogen using chemical genetics. *Cell*, **159(5)**, 1168–1187. <https://doi.org/10.1016/j.cell.2014.10.044>
- Burgoyne, R. D., Geisow, M. J.** (1989). The annexin family of calcium-binding proteins. Review article. *Cell Calcium*, **10(1)**, 1–10. [https://doi.org/10.1016/0143-4160\(89\)90038-9](https://doi.org/10.1016/0143-4160(89)90038-9)
- Burke, T., Christensen, J., Barone, E., Suarez, C., Sirotkin, V., Kovar, D.** (2014). Homeostatic Actin Cytoskeleton Networks Are Regulated by Assembly Factor Competition for Monomers. *National Institutes of Health (NIH)*, **24(5)**, 579–585. <https://doi.org/10.1016/j.cub.2014.01.072.Homeostatic>
- Cánovas, D., Pérez-Martín, J.** (2009). Sphingolipid biosynthesis is required for polar growth in the dimorphic phytopathogen *Ustilago maydis*. *Fungal Genetics and Biology*, **46(2)**, 190–200. <https://doi.org/10.1016/j.fgb.2008.11.003>
- Carbó, N., Pérez-Martín, J.** (2010). Activation of the cell wall integrity pathway promotes

- escape from G2 in the Fungus *Ustilago maydis*. *PLoS Genetics*, **6(7)**, 1–18. <https://doi.org/10.1371/journal.pgen.1001009>
- Casamayor, A., Snyder, M.** (2002). Bud-site selection and cell polarity in budding yeast. *Current Opinion in Microbiology*, **5(2)**, 179–186. [https://doi.org/10.1016/S1369-5274\(02\)00300-4](https://doi.org/10.1016/S1369-5274(02)00300-4)
- Casselton, L., Feldbrügge, M.** (2010). Mating and Sexual Morphogenesis in Basidiomycete Fungi. *Cellular and Molecular Biology of Filamentous Fungi - ASM Fungi*, **Ch. 34**, 536–557.
- Chan, F. Y., Silva, A. M., Saramago, J., Pereira-Sousa, J., Brighton, H. E., Pereira, M., Oegema, K., Gassmann, R., Carvalho, A. X.** (2019). The ARP2/3 complex prevents excessive formin activity during cytokinesis. *Molecular Biology of the Cell*, **30(1)**, 96–107. <https://doi.org/10.1091/mbc.E18-07-0471>
- Chang, F., Drubin, D., Nurse, P.** (1997). Cdc12P, a Protein Required for Cytokinesis in Fission Yeast, Is a Component of the Cell Division Ring and Interacts With Profilin. *Journal of Cell Biology*, **137(1)**, 169–182. <https://doi.org/10.1083/jcb.137.1.169>
- Chant, J.** (1999). Cell polarity in yeast. *Annu. Rev. Cell Dev. Biol.*, **15**, 365–391.
- Chirico, W. J., Waters, M. G., Blobel, G.** (1988). 70K heat shock related proteins stimulate protein translocation into microsomes. *Nature*, **332(6167)**, 805–810. <https://doi.org/10.1038/332805a0>
- Ciobanasu, C., Siebrasse, J.-P., Kubitscheck, U.** (2010). Cell-penetrating HIV1 TAT peptides can generate pores in model membranes. *Biophysical Journal*, **99(1)**, 153–162. <https://doi.org/10.1016/j.bpj.2010.03.065>
- Cohen, S. N., Chang, A. C., Hsu, L.** (1972). Nonchromosomal antibiotic resistance in bacteria: genetic transformation of *Escherichia coli* by R-factor DNA. *Proceedings of the National Academy of Sciences of the United States of America*, **69(8)**, 2110–2114. <https://doi.org/10.1073/pnas.69.8.2110>
- Colman-Lerner, A., Chin, T. E., Brent, R.** (2001). Yeast Cbk1 and Mob2 activate daughter-specific genetic programs to induce asymmetric cell fates. *Cell*, **107(6)**, 739–750. [https://doi.org/10.1016/S0092-8674\(01\)00596-7](https://doi.org/10.1016/S0092-8674(01)00596-7)
- Creutz, C. E.** (1992). The annexins and exocytosis. *Science*, **258(5084)**, 924–931. <https://doi.org/10.1126/science.1439804>
- Curwin, A. J., Brouwers, N., Adell, M. A. Y., Teis, D., Turacchio, G., Parashuraman, S., Ronchi, P., Malhotra, V.** (2016). ESCRT-III drives the final stages of CUPS maturation for unconventional protein secretion. *ELife*, **5**, 1–25. <https://doi.org/10.7554/eLife.16299>
- DeMarini, D. J., Adams, A. E. M., Fares, H., De Virgilio, C., Valle, G., Chuang, J. S., Pringle, J. R.** (1997). A septin-based hierarchy of proteins required for localized deposition of chitin in the *Saccharomyces cerevisiae* cell wall. *Journal of Cell Biology*, **139(1)**, 75–93. <https://doi.org/10.1083/jcb.139.1.75>
- Deshaies, R. J., Sanders, S. L., Feldheim, D. A., Schekman, R.** (1991). Assembly of yeast Sec proteins involved in translocation into the endoplasmic reticulum into a membrane-bound multisubunit complex. *Nature*, **349(6312)**, 806–808.

<https://doi.org/10.1038/349806a0>

- Di Paolo, G., De Camilli, P.** (2006). Phosphoinositides in cell regulation and membrane dynamics. *Nature*, **443(7112)**, 651–657. <https://doi.org/10.1038/nature05185>
- Ding, Y., Wang, J., Wang, J., Stierhof, Y. D., Robinson, D. G., Jiang, L.** (2012). Unconventional protein secretion. *Trends in Plant Science*, **17(10)**, 606–615. <https://doi.org/10.1016/j.tplants.2012.06.004>
- Dobbelaere, J., Barral, Y.** (2004). Spatial coordination of cytokinetic events by compartmentalization of the cell cortex. *Science*, **305(5682)**, 393–396. <https://doi.org/10.1126/science.1099892>
- Doehlemann, G., Wahl, R., Vranes, M., de Vries, R. P., Kämper, J., Kahmann, R.** (2008). Establishment of compatibility in the *Ustilago maydis*/maize pathosystem. *Journal of Plant Physiology*, **165(1)**, 29–40. <https://doi.org/10.1016/j.jplph.2007.05.016>
- Drücker, P., Pejic, M., Galla, H. J., Gerke, V.** (2013). Lipid segregation and membrane budding induced by the peripheral membrane binding protein annexin A2. *Journal of Biological Chemistry*, **288(34)**, 24764–24776. <https://doi.org/10.1074/jbc.M113.474023>
- Dupont, N., Jiang, S., Pilli, M., Ornatowski, W., Bhattacharya, D., Deretic, V.** (2011). Autophagy-based unconventional secretory pathway for extracellular delivery of IL-1 β . *EMBO Journal*, **30(23)**, 4701–4711. <https://doi.org/10.1038/emboj.2011.398>
- Duran, J. M., Anjard, C., Stefan, C., Loomis, W. F., Malhotra, V.** (2010). Unconventional secretion of Acb1 is mediated by autophagosomes. *Journal of Cell Biology*, **188(4)**, 527–536. <https://doi.org/10.1083/jcb.200911154>
- Durzyńska, J., Goździcka-Józefiak, A.** (2015). Viruses and cells intertwined since the dawn of evolution Emerging viruses. *Virology Journal*, **12(1)**. <https://doi.org/10.1186/s12985-015-0400-7>
- Ebert, A. D., Laußmann, M., Wegehangel, S., Kaderali, L., Erfle, H., Reichert, J., Lechner, J., Beer, H. D., Pepperkok, R., Nickel, W.** (2010). Tec-Kinase-Mediated Phosphorylation of Fibroblast Growth Factor 2 is Essential for Unconventional Secretion. *Traffic*, **11(6)**, 813–826. <https://doi.org/10.1111/j.1600-0854.2010.01059.x>
- Eilers, M., Schatz, G.** (1986). Binding of a specific ligand inhibits import of a purified precursor protein into mitochondria. *Nature*, **322(17)**, 1–5.
- Ellgaard, L., Ruddock, L. W.** (2005). The human protein disulphide isomerase family: Substrate interactions and functional properties. *EMBO Reports*, **6(1)**, 28–32. <https://doi.org/10.1038/sj.embor.7400311>
- Evangelista, M., Blundell, K., Longtine, M. S., Chow, C. J., Adames, N., Pringle, J. R., Peter, M., Boone, C.** (1997). Bni1p, a yeast formin linking Cdc42p and the actin cytoskeleton during polarized morphogenesis. *Science*, **276(5309)**, 118–122. <https://doi.org/10.1126/science.276.5309.118>
- Evangelista, M., Zigmond, S., Boone, C.** (2003). Formins: Signaling effectors for assembly and polarization of actin filaments. *Journal of Cell Science*, **116(13)**, 2603–2611. <https://doi.org/10.1242/jcs.00611>
- Fang, X., Luo, J., Nishihama, R., Wloka, C., Dravis, C., Travaglia, M., Iwase, M., Vallen, E.**

- A., Bi, E.** (2010). Biphasic targeting and cleavage furrow ingression directed by the tail of a myosin II. *Journal of Cell Biology*, **191(7)**, 1333–1350. <https://doi.org/10.1083/jcb.201005134>
- Feldbrügge, M., Bölker, M., Steinberg, G., Kämper, J., Kahmann, R.** (2006). Regulatory and structural networks orchestrating mating, dimorphism, cell shape, and pathogenesis in *Ustilago maydis*. *The Mycota I*, **18**.
- Feldbrügge, Michael, Kellner, R., Schipper, K.** (2013). The biotechnological use and potential of plant pathogenic smut fungi. *Applied Microbiology and Biotechnology*, **97**, 3253–3265. <https://doi.org/10.1007/s00253-013-4777-1>
- Fields, S., Song, O.** (1989). A novel genetic system to detect protein-protein-interactions. *Nature*, **43(6230)**, 245–246. <https://doi.org/10.1038/340245a0>
- Fischer, T., Lu, L., Haigler, H. T., Langen, R.** (2007). Annexin B12 is a sensor of membrane curvature and undergoes major curvature-dependent structural changes. *Journal of Biological Chemistry*, **282(13)**, 9996–10004. <https://doi.org/10.1074/jbc.M611180200>
- Ford, M. G. J., Mills, I. G., Peter, B. J., Vallis, Y., Praefcke, G. J. K., Evans, P. R., McMahon, H. T.** (2002). Curvature of clathrin-coated pits driven by epsin. *Nature*, **419(6905)**, 361–366. <https://doi.org/10.1038/nature01020>
- Freitag, J., Lanver, D., Böhmer, C., Schink, K. O., Bölker, M., Sandrock, B.** (2011). Septation of infectious hyphae is critical for appressoria formation and virulence in the smut fungus *Ustilago maydis*. *PLoS Pathogens*, **7(5)**. <https://doi.org/10.1371/journal.ppat.1002044>
- Friesen, H., Lunz, R., Doyle, S., Segall, J.** (1994). Mutation of the SPS1-encoded protein kinase of *Saccharomyces cerevisiae* leads to defects in transcription and morphology during spore formation. *Genes and Development*, **8(18)**, 2162–2175. <https://doi.org/10.1101/gad.8.18.2162>
- Futter, C. E., White, I. J.** (2007). Annexins and endocytosis. *Traffic*, **8(8)**, 951–958. <https://doi.org/10.1111/j.1600-0854.2007.00590.x>
- Gautier, R., Douguet, D., Antonny, B., Drin, G.** (2008). HELIQUEST: A web server to screen sequences with specific α -helical properties. *Bioinformatics*, **24(18)**, 2101–2102. <https://doi.org/10.1093/bioinformatics/btn392>
- Geiser, E., Reindl, M., Blank, L. M., Feldbrügge, M., Wierckx, N.** (2016). Activating Intrinsic Carbohydrate-Active Enzymes of the Smut Fungus. *Applied and Environmental Microbiology*, **82(17)**, 5174–5185. <https://doi.org/10.1128/AEM.00713-16.Editor>
- Gerke, V., Moss, S. E.** (2002). Annexins: From structure to function. *Physiological Reviews*, **82(2)**, 331–371. <https://doi.org/10.1152/physrev.00030.2001>
- Gillissen, B., Bergemann, J., Sandmann, C., Schroerer, B., Bölker, M., Kahmann, R.** (1992). A two-component regulatory system for self/non-self recognition in *Ustilago maydis*. *Cell*, **68(4)**, 647–657. [https://doi.org/10.1016/0092-8674\(92\)90141-X](https://doi.org/10.1016/0092-8674(92)90141-X)
- Grant, S. G. N., Jessee, J., Bloom, F. R., Hanahan, D.** (1990). Differential plasmid rescue from transgenic mouse DNAs into *Escherichia coli* methylation-restriction mutants. *Proceedings of the National Academy of Sciences of the United States of America*,

- 87(12)**, 4645–4649. <https://doi.org/10.1073/pnas.87.12.4645>
- Guo, Y., Sirkis, D. W., Schekman, R.** (2014). Protein Sorting at the trans -Golgi Network . *Annual Review of Cell and Developmental Biology*, **30(1)**, 169–206. <https://doi.org/10.1146/annurev-cellbio-100913-013012>
- Hoffman, C. S., Winston, F.** (1987). A ten-minute DNA preparation from yeast efficiently releases autonomous plasmids for transformiaon of *Escherichia coli*. *Gene*, **57(2–3)**, 267–272. [https://doi.org/10.1016/0378-1119\(87\)90131-4](https://doi.org/10.1016/0378-1119(87)90131-4)
- Holliday, R.** (1974). *Ustilago maydis*. *Handbook of Genetics*, 575–595.
- Hom, R. A., Vora, M., Regner, M., Subach, O. M., Cho, W., Verkhusha, V. V., Stahelin, R. V., Kutateladze, T. G.** (2007). pH-dependent Binding of the Epsin ENTH Domain and the AP180 ANTH Domain to PI(4,5)P2-containing Bilayers. *Journal of Molecular Biology*, **373(2)**, 412–423. <https://doi.org/10.1016/j.jmb.2007.08.016>
- Hussnaetter, Kai Philipp** (2016). Studiyng the role of the novel factor Jps1 during unconventional secretion of the chitinase Cts1. *Master thesis*. Heinrich-Heine-Universität Düsseldorf.
- Jacob, R., Heine, M., Eikemeyer, J., Frerker, N., Zimmer, K. P., Rescher, U., Gerke, V., Naim, H. Y.** (2004). Annexin II Is Required for Apical Transport in Polarized Epithelial Cells. *Journal of Biological Chemistry*, **279(5)**, 3680–3684. <https://doi.org/10.1074/jbc.C300503200>
- Jaffe, A. B., Hall, A.** (2005). RHO GTPASES: Biochemistry and Biology. *Annual Review of Cell and Developmental Biology*, **21(1)**, 247–269. <https://doi.org/10.1146/annurev.cellbio.21.020604.150721>
- Jiang, S., Dupont, N., Castillo, E. F., Deretic, V.** (2013). Secretory versus degradative autophagy: Unconventional secretion of inflammatory mediators. *Journal of Innate Immunity*, **5(5)**, 471–479. <https://doi.org/10.1159/000346707>
- Jost, M., Zeuschner, D., Seemann, J., Weber, K., Gerke, V.** (1997). Identification and characterization of a novel type of annexin-membrane interaction: Ca²⁺ is not required for the association of annexin II with early endosomes. *Journal of Cell Science*, **110(2)**, 221–228.
- Juanes, M., Piatti, S.** (2016). The final cut: cell polarity meets cytokinesis at the bud neck in *S. cerevisiae*. *Cell Mol Life Sci*, **73**, 3315-3136. <https://doi.org/10.1007/s00018-016-2220-3>
- Källberg, M., Wang, H., Wang, S., Peng, J., Wang, Z., Lu, H., Xu, J.** (2012). Template-based protein structure modeling using the RaptorX web server. *Nature Protocols*, **7(8)**, 1511–1522. <https://doi.org/10.1038/nprot.2012.085>
- Kämper, J., Reichmann, M., Romeis, T., Bölker, M., Kahmann, R.,** (1990). Multiallelic recognition: Nonsself-dependent dimerization of the bE and bW homeodomain proteins in *Ustilago maydis*. *Cell*, **81(1)**, 73-83. [https://doi.org/10.1016/0092-8674\(95\)90372-0](https://doi.org/10.1016/0092-8674(95)90372-0)
- Kämper, J., Kahmann, R., Bölker, M., Ma, L. J., Brefort, T., Saville, B. J., Banuett, F., Kronstad, J. W., Gold, S. E., Müller, O., Perlin, M. H., Wösten, H. A. B., De Vries, R., Ruiz-Herrera, J., Reynaga-Peña, C. G., Snetselaar, K., McCann, M., Pérez-Martín, J.,**

- Feldbrügge, M., ... Birren, B. W.** (2006). Insights from the genome of the biotrophic fungal plant pathogen *Ustilago maydis*. *Nature*, **444(7115)**, 97–101. <https://doi.org/10.1038/nature05248>
- Karlsson, M., Stenlid, J.** (2008). Comparative evolutionary histories of the fungal Chitinase gene family reveal non-random size expansions and contractions due to adaptive natural selection. *Evolutionary Bioinformatics*, **2008(4)**, 47–60. <https://doi.org/10.4137/ebo.s604>
- Kelley, L., Mezulis, S., Yates, C., Wass, M., Sternberg, M.** (2016). The Phyre2 web portal for protein modeling, prediction and analysis. *Nature Protocols*, **10(6)**, 845–858. <https://doi.org/10.1038/nprot.2015-053>
- Kikhney, A. G., Svergun, D. I.** (2015). A practical guide to small angle X-ray scattering (SAXS) of flexible and intrinsically disordered proteins. *FEBS Letters*, **589(19)**, 2570–2577. <https://doi.org/10.1016/j.febslet.2015.08.027>
- Koenig, J., Baumann, S., Koepke, J., Pohlmann, T., Zarnack, K., Feldbrügge, M.** (2009). The fungal RNA-binding protein Rrm4 mediates long-distance transport of *ubi1* and *rho3* mRNAs. *EMBO J.*, **28**, 1855–1866. <https://doi.org/10.1038/emboj.2009.145>
- Koepke, J., Kaffarnik, F., Haag, C., Zarnack, K., Luscombe, N. M., König, J., Ule, J., Kellner, R., Begerow, D., Feldbrügge, M.** (2011). The RNA-binding protein Rrm4 is essential for efficient secretion of endochitinase Cts1. *Molecular & Cellular Proteomics: MCP*, **10(12)**, M111.011213. <https://doi.org/10.1074/mcp.M111.011213>
- Kosaka, N., Iguchi, H., Yoshioka, Y., Takeshita, F., Matsuki, Y., Ochiya, T.** (2010). Secretory mechanisms and intercellular transfer of microRNAs in living cells. *Journal of Biological Chemistry*, **285(23)**, 17442–17452. <https://doi.org/10.1074/jbc.M110.107821>
- Kozubowski, L., Heitman, J.** (2010). Septins Enforce Morphogenetic Events during Sexual Reproduction and Contribute to Virulence of *Cryptococcus neoformans*. *National Institutes of Health (NIH)*, **75(3)**, 658–675. <https://doi.org/10.1038/jid.2014.371>
- Kozubowski, L., Panek, H., Rosenthal, A., Bloecher, A., DeMarini, D., Tatchell, K.** (2003). A Bni4-Glc7 Phosphatase Complex That Recruits Chitin Synthase to the Site of Bud Emergence. *Molecular Biology of the Cell*, **14(12)**, 26–39. <https://doi.org/10.1091/mbc.E02>
- Krishna, P., Kennedy, B. P., Waisman, D. M., Van Sande, J. H. D. E., Mcghef, J. D.** (1990). Are many Z-DNA binding proteins actually phospholipid-binding proteins? *Proceedings of the National Academy of Sciences of the United States of America*, **87(4)**, 1292–1295. <https://doi.org/10.1073/pnas.87.4.1292>
- Krombach, S., Reissmann, S., Kreibich, S., Bochen, F., Kahmann, R.** (2018). Virulence function of the *Ustilago maydis* sterol carrier protein 2. *New Phytologist*, **220(2)**, 553–566. <https://doi.org/10.1111/nph.15268>
- Kuranda, M. J., Robbins, P. W.** (1991). Chitinase is required for cell separation during growth of *Saccharomyces cerevisiae*. *Journal of Biological Chemistry*, **266(29)**, 19758–19767.
- Lai, C. L., Jao, C. C., Lyman, E., Gallop, J. L., Peter, B. J., McMahon, H. T., Langen, R., Voth, G. A.** (2012). Membrane Binding and Self-Association of the Epsin N-Terminal Homology Domain. *Journal of Molecular Biology*, **423(5)**, 800–817. <https://doi.org/10.1016/j.jmb.2012.08.010>

- Langner, T.** (2015). Charakterisierung der chitinolytischen Maschinerie aus *Ustilago maydis*. *PhD Thesis*, Heinrich Heine University Düsseldorf.
- Langner, T., Öztürk, M., Hartmann, S., Cord-Landwehr, S., Moerschbacher, B., Walton, J. D., Göhre, V.** (2015). Chitinases are essential for cell separation in *Ustilago maydis*. *Eukaryotic Cell*, **14(9)**, 846–857. <https://doi.org/10.1128/EC.00022-15>
- Lee, P. R., Song, S., Ro, H.-S., Park, C. J., Lippincott, J., Li, R., Pringle, J. R., De Virgilio, C., Longtine, M. S., Lee, K. S.** (2002). Bni5p, a Septin-Interacting Protein, Is Required for Normal Septin Function and Cytokinesis in *Saccharomyces cerevisiae*. *Molecular and Cellular Biology*, **22(19)**, 6906–6920. <https://doi.org/10.1128/mcb.22.19.6906-6920.2002>
- Lehman, K., Rossi, G., Adamo, J. E., Brennwald, P.** (1999). Exocytosis and Are Associated with the Plasma Membrane SNARE , Sec9. *Journal of Cell Biology*, **146(1)**, 125–140.
- Lehmler, C., Steinberg, G., Snetselaar, K. M., Schliwa, M., Kahmann, R., Bölker, M.** (1997). Identification of a motor protein required for filamentous growth in *Ustilago maydis*. *EMBO Journal*, **16(12)**, 3464–3473. <https://doi.org/10.1093/emboj/16.12.3464>
- Lemmon, M. A.** (2008). Membrane recognition by phospholipid-binding domains. *Nature Reviews Molecular Cell Biology*, **9(2)**, 99–111. <https://doi.org/10.1038/nrm2328>
- Li, L., Dahiya, S., Kortagere, S., Aiamkitsumrit, B., Cunningham, D., Pirrone, V., Nonnemacher, M. R., Wigdahl, B.** (2012). Impact of tat genetic variation on HIV-1 disease. *Advances in Virology*, **2012**. <https://doi.org/10.1155/2012/123605>
- Machesky, L. M., Gould, K. L.** (1999). The Arp2/3 complex: A multifunctional actin organizer. *Current Opinion in Cell Biology*, **11(1)**, 117–121. [https://doi.org/10.1016/S0955-0674\(99\)80014-3](https://doi.org/10.1016/S0955-0674(99)80014-3)
- MacKenzie, A., Wilson, H. L., Kiss-Toth, E., Dower, S. K., North, R. A., Surprenant, A.** (2001). Rapid secretion of interleukin-1 β by microvesicle shedding. *Immunity*, **15(5)**, 825–835. [https://doi.org/10.1016/S1074-7613\(01\)00229-1](https://doi.org/10.1016/S1074-7613(01)00229-1)
- Mahlert, M., Leveleki, L., Hlubek, A., Sandrock, B., Bölker, M.** (2006). Rac1 and Cdc42 regulate hyphal growth and cytokinesis in the dimorphic fungus *Ustilago maydis*. *Molecular Microbiology*, **59(2)**, 567–578. <https://doi.org/10.1111/j.1365-2958.2005.04952.x>
- Maji, S., Chaudhary, P., Akopova, I., Nguyen, P., Hare, R., Gryczynski, I., Vishwanatha, J.** (2017). Exosomal annexin A2 promotes angiogenesis in breast cancer metastasis. *Mol Cancer Res*, **15(1)**, 93–105. <https://doi.org/10.1126/science.1249098.Sleep>
- Malhotra, V.** (2013). Unconventional protein secretion: an evolving mechanism. *The EMBO Journal*, **32(12)**, 1660–1664. <https://doi.org/10.1038/emboj.2013.104>
- Malkus, P., Jiang, F., Schekman, R.** (2002). Concentrative sorting of secretory cargo proteins into COPII-coated vesicles. *Journal of Cell Biology*, **159(6)**, 915–921. <https://doi.org/10.1083/jcb.200208074>
- Manjithaya, R., Anjard, C., Loomis, W. F., Subramani, S.** (2010). Unconventional secretion of *Pichia pastoris* Acb1 is dependent on GRASP protein, peroxisomal functions, and autophagosome formation. *Journal of Cell Biology*, **188(4)**, 537–546. <https://doi.org/10.1083/jcb.200911149>

- Martin, T.** (2012). Role of PI(4,5)P₂ in Vesicle Exocytosis and Membrane Fusion Thomas. *Subcell Biochem*, **59**, 111–130. <https://doi.org/10.1007/978-94-007-3015-1>
- Martinez, C., Roux, C., Jauneau, A., Dargent, R.** (2002). The biological cycle of *Sporisorium reilianum* f.sp. zeae: An overview using microscopy. *Mycologia*, **94(3)**, 505–514. <https://doi.org/10.1080/15572536.2003.11833215>
- Maryam, M., Fu, M. S., Alanio, A., Camacho, E., Goncalves, D. S., Faneuff, E. E., Grossman, N. T., Casadevall, A., Coelho, C.** (2019). The enigmatic role of fungal annexins: the case of *Cryptococcus neoformans*. *Microbiology*, **165(8)**, 852–862. <https://doi.org/10.1099/mic.0.000815>
- McLaughlin, S., Wang, J., Gambhir, A., Murray, D.** (2002). PIP₂ and proteins: Interactions, organization, and information flow. *Annual Review of Biophysics and Biomolecular Structure*, **31**, 151–175. <https://doi.org/10.1146/annurev.biophys.31.082901.134259>
- Meitinger, F., Palani, S.** (2016). Actomyosin ring driven cytokinesis in budding yeast. *Seminars in Cell and Developmental Biology*, **53**, 19–27. <https://doi.org/10.1016/j.semcdb.2016.01.043>
- Mele, A. R., Marino, J., Chen, K., Pirrone, V., Janetopoulos, C., Wigdahl, B., Klase, Z., Nonnemacher, M. R.** (2018). Defining the molecular mechanisms of HIV-1 Tat secretion: PtdIns(4,5)P₂ at the epicenter. *Traffic*, **19(9)**, 655–665. <https://doi.org/10.1111/tra.12578>
- Moss, S. E., Morgan, R. O.** (2004). The annexins. *Genome Biology*, **5(4)**, 1–8. <https://doi.org/10.1186/gb-2004-5-4-219>
- Müller, H. M., Steringer, J. P., Wegehingel, S., Bleicken, S., Münster, M., Dimou, E., Unger, S., Weidmann, G., Andreas, H., García-Sáez, A. J., Wild, K., Sinning, I., Nickel, W.** (2015). Formation of disulfide bridges drives oligomerization, membrane pore formation, and translocation of fibroblast growth factor 2 to cell surfaces. *Journal of Biological Chemistry*, **290(14)**, 8925–8937. <https://doi.org/10.1074/jbc.M114.622456>
- Müller, M. J., Stachurski, S., Stoffels, P., Schipper, K., Feldbrügge, M., Büchs, J.** (2018). Online evaluation of the metabolic activity of *Ustilago maydis* on (poly)galacturonic acid. *Journal of Biological Engineering*, **12(1)**, 1–17. <https://doi.org/10.1186/s13036-018-0128-1>
- Muralidharan-Chari, V., Clancy, J. W., Sedgwick, A., D'Souza-Schorey, C.** (2010). Microvesicles: Mediators of extracellular communication during cancer progression. *Journal of Cell Science*, **123(10)**, 1603–1611. <https://doi.org/10.1242/jcs.064386>
- Nakamura, N., Wei, J. H., Seemann, J.** (2012). Modular organization of the mammalian Golgi apparatus. *Current Opinion in Cell Biology*, **24(4)**, 467–474. <https://doi.org/10.1016/j.ceb.2012.05.009>
- Nath, A., Atkins, W. M., Sligar, S. G.** (2007). Applications of phospholipid bilayer nanodiscs in the study of membranes and membrane proteins. *Biochemistry*, **46(8)**, 2059–2069. <https://doi.org/10.1021/bi602371n>
- Nickel, W.** (2010). Pathways of unconventional protein secretion. *Current Opinion in Biotechnology*, **21(5)**, 621–626. <https://doi.org/10.1016/j.copbio.2010.06.004>
- Nielsen, H., Tsigos, K. D., Brunak, S., von Heijne, G.** (2019). A Brief History of Protein

- Sorting Prediction. *Protein Journal*, **38(3)**, 200–216. <https://doi.org/10.1007/s10930-019-09838-3>
- Palade, G.** (1975). Intracellular Aspects of the Process of Protein Synthesis. *Science*, **189(4206)**, 867–867. <https://doi.org/10.1126/science.189.4206.867-b>
- Pantano, S., Carloni, P.** (2005). Comparative analysis of HIV-1 tat variants. *Proteins: Structure, Function and Genetics*, **58(3)**, 638–643. <https://doi.org/10.1002/prot.20323>
- Parton, R. G., Hanzal-Bayer, M., Hancock, J. F.** (2006). Biogenesis of caveolae: A structural model for caveolin-induced domain formation. *Journal of Cell Science*, **119(5)**, 787–796. <https://doi.org/10.1242/jcs.02853>
- Pierce, M. M., Raman, C. S., Nall, B. T.** (1999). Isothermal titration calorimetry of protein-protein interactions. *Methods: A Companion to Methods in Enzymology*, **19(2)**, 213–221. <https://doi.org/10.1006/meth.1999.0852>
- Popa, S. J., Stewart, S. E., Moreau, K.** (2018). Unconventional secretion of annexins and galectins. *Seminars in Cell and Developmental Biology*, **83**, 42–50. <https://doi.org/10.1016/j.semcd.2018.02.022>
- Pruyne, D., Bretscher, A.** (2000). Polarization of cell growth in yeast. 1. Establishment and maintenance of polarity states. *Journal of Cell Science*, **113(3)**, 365–375.
- Rabouille, C., Malhotra, V., Nickel, W.** (2012). Diversity in unconventional protein secretion. *Journal of Cell Science*, **125(22)**, 5251–5255. <https://doi.org/10.1242/jcs.103630>
- Radisky, D. C., Stallings-Mann, M., Hirai, Y., Bissell, M. J.** (2009). Single proteins might have dual but related functions in intracellular and extracellular microenvironments. *Nature Reviews Molecular Cell Biology*, **10(3)**, 228–234. <https://doi.org/10.1038/nrm2633>
- Rana, T. M., Jeang, K. T.** (1999). Biochemical and functional interactions between HIV-1 Tat protein and TAR RNA. *Archives of Biochemistry and Biophysics*, **365(2)**, 175–185. <https://doi.org/10.1006/abbi.1999.1206>
- Raynal, P., Pollard, H. B.** (1994). Annexins: the problem of assessing the biological role for a gene family of multifunctional calcium- and phospholipid-binding proteins. *BBA - Reviews on Biomembranes*, **1197(1)**, 63–93. [https://doi.org/10.1016/0304-4157\(94\)90019-1](https://doi.org/10.1016/0304-4157(94)90019-1)
- Rédei, G. P.** (2008). Translocation Complex. *Encyclopedia of Genetics, Genomics, Proteomics and Informatics*, **367(2)**, 2016–2016. https://doi.org/10.1007/978-1-4020-6754-9_17333
- Reindl, M., Hänsch, S., Weidtkamp-Peters, S., Schipper, K.** (2019). A potential lock-type mechanism for unconventional secretion in fungi. *International Journal of Molecular Sciences*, **20(3)**. <https://doi.org/10.3390/ijms20030460>
- Reindl, M., Stock, J., Hussnaetter, K. P., Genc, A., Brachmann, A., Schipper, K.** (2020). A novel factor essential for unconventional secretion of chitinase Cts1. *BioRxiv*, 2020.02.07.938613. <https://doi.org/10.1101/2020.02.07.938613>
- Rosengarth, A., Luecke, H.** (2003). A calcium-driven conformational switch of the N-terminal and core domains of annexin A1. *Journal of Molecular Biology*, **326(5)**, 1317–1325. [https://doi.org/10.1016/S0022-2836\(03\)00027-5](https://doi.org/10.1016/S0022-2836(03)00027-5)

- Rouck, J. E., Krapf, J. E., Roy, J., Huff, H. C., Das, A.** (2017). Recent advances in nanodisc technology for membrane protein studies (2012–2017). *FEBS Letters*, **591(14)**, 2057–2088. <https://doi.org/10.1002/1873-3468.12706>
- Sambrook, J., Fritsch, E. F., Maniatis, T.** (1989). *Molecular Cloning: a laboratory manual*. In *Cold Spring Harbor Laboratory* (Vol. 2).
- Sánchez-Martínez, C., Pérez-Martín, J.** (2001). Dimorphism in fungal pathogens: *Candida albicans* and *Ustilago maydis* - Similar inputs, different outputs. *Current Opinion in Microbiology*, **4(2)**, 214–221. [https://doi.org/10.1016/S1369-5274\(00\)00191-0](https://doi.org/10.1016/S1369-5274(00)00191-0)
- Sanz, M., Castrejón, F., Durán, A., Roncero, C.** (2004). *Saccharomyces cerevisiae* Bni4p directs the formation of the chitin ring and also participates in the correct assembly of the septum structure. *Microbiology*, **150(10)**, 3229–3241. <https://doi.org/10.1099/mic.0.27352-0>
- Sarkari, P., Reindl, M., Stock, J., Müller, O., Kahmann, R., Feldbrügge, M., Schipper, K.** (2014). Improved expression of single-chain antibodies in *Ustilago maydis*. *Journal of Biotechnology*, 1–11. <https://doi.org/10.1016/j.jbiotec.2014.06.028>
- Saville, B. J., Donaldson, M. E., Doyle, C. E.** (2012). Investigating Host Induced Meiosis in a Fungal Plant Pathogen. *Meiosis - Molecular Mechanisms and Cytogenetic Diversity*, **22**, 411–460. <https://doi.org/10.5772/30032>
- Schäfer, T., Zentgraf, H., Zehe, C., Brügger, B., Bernhagen, J., Nickel, W.** (2004). Unconventional Secretion of Fibroblast Growth Factor 2 Is Mediated by Direct Translocation across the Plasma Membrane of Mammalian Cells. *Journal of Biological Chemistry*, **279(8)**, 6244–6251. <https://doi.org/10.1074/jbc.M310500200>
- Schatz, G., Dobberstein, B.** (1996). Common Principles of Protein Translocation Across Membranes. *Science*, **271(5255)**, 1519–1526.
- Schipper, K.** (2009). Charakterisierung eines *Ustilago maydis* Genclusters, das für drei neuartige sekretierte Effektoren kodiert. *PhD Thesis*, Philipps-Universität Marburg.
- Schmidt, M., Bowers, B., Varma, A., Roh, D. H., Cabib, E.** (2002). In budding yeast, contraction of the actomyosin ring and formation of the primary septum at cytokinesis depend on each other. *Journal of Cell Science*, **115(2)**, 293–302.
- Schreiber, G.** (2002). Kinetic studies of protein-protein interactions. *Current Opinion in Structural Biology*, **12(1)**, 41–47. [https://doi.org/10.1016/S0959-440X\(02\)00287-7](https://doi.org/10.1016/S0959-440X(02)00287-7)
- Schulz, B., Banuett, F., Dahl, M., Schlesinger, R., Schäfer, W., Martin, T., Ira, H., Kahmann, R.** (1990). The b alleles of *U. maydis*, whose combinations program pathogenic development, code for polypeptides containing a homeodomain-related motif. *Cell*, **60(3)**, 295–306.
- Sellers, J. R.** (2000). Myosins: A diverse superfamily. *Biochimica et Biophysica Acta - Molecular Cell Research*, **1496(1)**, 3–22. [https://doi.org/10.1016/S0167-4889\(00\)00005-7](https://doi.org/10.1016/S0167-4889(00)00005-7)
- Shirasaki, Y., Yamagishi, M., Suzuki, N., Izawa, K., Nakahara, A., Mizuno, J., Shoji, S., Heike, T., Harada, Y., Nishikomori, R., Ohara, O.** (2014). Real-time single-cell imaging of protein secretion. *Scientific Reports*, **4**. <https://doi.org/10.1038/srep04736>

- Skog, J., Wurdinger, T., VanRijn, S., Meijer, D., Gainche, L., SenaEsteves, M., William, T., Carter, R., Krichevsky, A., Breakefield, X.** (2008). Glioblastoma microvesicles transport RNA and protein that promote tumor growth and provide diagnostic biomarkers. *Nat Cell Biol.*, **10(12)**, 1470–1476. <https://doi.org/10.1038/nature22814>. Trans-kingdom
- Snetselaar, K. M., Bölker, M., Kahmann, R.** (1996). *Ustilago maydis* Mating Hyphae Orient Their Growth toward Pheromone Sources. *Fungal Genetics and Biology*, **20(44)**, 299–312.
- Southern, E. M.** (1975). Detection of specific sequences among DNA fragments separated by gel electrophoresis. *Journal of Molecular Biology*, **98**, 503–517. <https://doi.org/10.1016/b978-0-12-131200-8.50041-1>
- Spector, C., Mele, A. R., Wigdahl, B., Nonnemacher, M. R.** (2019). Genetic variation and function of the HIV-1 Tat protein. In *Medical Microbiology and Immunology (Vol. 208, Issue 2)*. Springer Berlin Heidelberg. <https://doi.org/10.1007/s00430-019-00583-z>
- Spellig, T., Bölker, M., Lottspeich, F., Frank, R. W., Kahmann, R.** (1994). Pheromones trigger filamentous growth in *Ustilago maydis*. *The EMBO Journal*, **13(7)**, 1620–1627. <https://doi.org/10.1002/j.1460-2075.1994.tb06425.x>
- Stanley, P.** (2011). Golgi glycosylation. *Cold Spring Harbor Perspectives in Biology*, **3(4)**, 1–13. <https://doi.org/10.1101/cshperspect.a005199>
- Steinberg, G., Schliwa, M., Lehmler, C., Bölker, M., Kahmann, R., McIntosh, J. R.** (1998). Kinesin from the plant pathogenic fungus *Ustilago maydis* is involved in vacuole formation and cytoplasmic migration. *Journal of Cell Science*, **111(15)**, 2235–2246.
- Steringer, J. P., Müller, H. M., Nickel, W.** (2014). Unconventional Secretion of Fibroblast Growth Factor 2-A Novel Type of Protein Translocation across Membranes? *Journal of Molecular Biology*, **427(6)**, 1202–1210. <https://doi.org/10.1016/j.jmb.2014.07.012>
- Stewart, S. E.; Ashkenazi, A.; Williamson, A.; Runbinsztein, D. E.; Moreau, K.** (2018). Transbilayer phospholipid movement facilitates the translocation of annexin across membranes. *Journal of Cell Science*, **131(14)**, 1-12. <https://doi.org/10.1242/jcs.217034>
- Stock, J., Sarkari, P., Kreibich, S., Brefort, T., Feldbrügge, M., Schipper, K.** (2012). Applying unconventional secretion of the endochitinase Cts1 to export heterologous proteins in *Ustilago maydis*. *Journal of Biotechnology*, **161(2)**, 80–91. <https://doi.org/10.1016/j.jbiotec.2012.03.004>
- Studier, F. W., Moffatt, B. A.** (1986). Use of bacteriophage T7 RNA polymerase to direct selective high-level expression of cloned genes. *Journal of Molecular Biology*, **189(1)**, 113–130.
- Szabó, Z., Tönnis, M., Kessler, H., Feldbrügge, M.** (2002). Structure-function analysis of lipopeptide pheromones from the plant pathogen *Ustilago maydis*. *Molecular Genetics and Genomics*, **268(3)**, 362–370. <https://doi.org/10.1007/s00438-002-0756-4>
- Tatu, U., Helenius, A.** (1997). Interactions between newly synthesized glycoproteins, calnexin and a network of resident chaperones in the endoplasmic reticulum. *Journal of Cell Biology*, **136(3)**, 555–565. <https://doi.org/10.1083/jcb.136.3.555>
- Terfrüchte, M., Joehnk, B., Fajardo-Somera, R., Braus, G. H., Riquelme, M., Schipper, K.,**

- Feldbrügge, M.** (2014). Establishing a versatile Golden Gate cloning system for genetic engineering in fungi. *Fungal Genetics and Biology*, **62**, 1–10. <https://doi.org/10.1016/j.fgb.2013.10.012>
- Terfrüchte, M., Wewetzer, S., Sarkari, P., Stollewerk, D., Franz-Wachtel, M., Macek, B., Schlepütz, T., Feldbrügge, M., Büchs, J., Schipper, K.** (2018). Tackling destructive proteolysis of unconventionally secreted heterologous proteins in *Ustilago maydis*. *Journal of Biotechnology*, **284(7)**, 37–51. <https://doi.org/10.1016/j.jbiotec.2018.07.035>
- Vallen, E. A., Caviston, J., Bi, E.** (2000). Roles of Hof1p, Bni1p, Bnr1p, and Myo1p in cytokinesis in *Saccharomyces cerevisiae*. *Molecular Biology of the Cell*, **11(2)**, 593–611. <https://doi.org/10.1091/mbc.11.2.593>
- VerPlank, L., Li, R.** (2005). Cell Cycle-regulated Trafficking of Chs2 Controls Actomyosin Ring Stability during Cytokinesis. *Molecular Biology of the Cell*, **16(12)**, 2529–2543. <https://doi.org/10.1091/mbc.E04>
- Volkmar, N., Fenech, E., Christianson, J. C.** (2016). New MAPS for misfolded proteins. *Nature Cell Biology*, **18(7)**, 724–726. <https://doi.org/10.1038/ncb3381>
- Vollmeister, E., Schipper, K., Baumann, S., Haag, C., Pohlmann, T., Stock, J., Feldbrügge, M.** (2012). Fungal development of the plant pathogen *Ustilago maydis*. *FEMS Microbiology Reviews*, **36(1)**, 59–77. <https://doi.org/10.1111/j.1574-6976.2011.00296.x>
- Waterhouse, A. M., Procter, J. B., Martin, D. M. A., Clamp, M., Barton, J. G.** (2009). Jalview Version 2 - a multiple sequence alignment editor and analysis workbench. *Bioinformatics*, **25(9)**, 1189–1191.
- Weinberger, A., Tsai, F., Koenderink, G.H., Schmidt, T.F., Rosangela, I., Meier, W., Schmatko, T., Schröder, A., Marques, C.** (2013). Gel-assisted formation of giant unilamellar vesicles. *Biophysical Journal*, **105(1)**, 154–164. <https://doi.org/10.1016/j.bpj.2013.05.024>
- Weinzierl, G., Leveleki, L., Hassel, A., Kost, G., Wanner, G., Bölker, M.** (2002). Regulation of cell separation in the dimorphic fungus *Ustilago maydis*. *Molecular Microbiology*, **45(1)**, 219–231. <https://doi.org/10.1046/j.1365-2958.2002.03010.x>
- Welch, M. D., DePace, A. H., Verma, S., Iwamatsu, A., Mitchison, T. J.** (1997). The human Arp2/3 complex is composed of evolutionarily conserved subunits and is localized to cellular regions of dynamic actin filament assembly. *Journal of Cell Biology*, **138(2)**, 375–384. <https://doi.org/10.1083/jcb.138.2.375>
- Welch, M., Holtzman, D., Drubin, D.** (1994). The yeast actin cytoskeleton. *Current Opinion in Cell Biology*, **6**, 110–119.
- Wesp, A., Hicke, L., Palecek, J., Lombardi, R., Aust, T., Munn, A. L., Riezman, H.** (1997). End4p/Sla2p interacts with actin-associated proteins for endocytosis in *Saccharomyces cerevisiae*. *Molecular Biology of the Cell*, **8(11)**, 2291–2306. <https://doi.org/10.1091/mbc.8.11.2291>
- White, S., Doebley, J.** (1998). Of genes and genomes and the origin of maize. *Trends in Genetics*, **14(8)**, 327–332. [https://doi.org/10.1016/S0168-9525\(98\)01524-8](https://doi.org/10.1016/S0168-9525(98)01524-8)

- Williamson, M. P.** (1994). The structure and function of proline-rich regions in proteins. *Biochemical Journal*, **297(2)**, 249–260. <https://doi.org/10.1042/bj2970249>
- Winter, D. C., Choe, E. Y., Li, R.** (1999). Genetic dissection of the budding yeast Arp2/3 complex: A comparison of the in vivo and structural roles of individual subunits. *Proceedings of the National Academy of Sciences of the United States of America*, **96(13)**, 7288–7293. <https://doi.org/10.1073/pnas.96.13.7288>
- Witkos, T. M., Lowe, M.** (2017). Recognition and tethering of transport vesicles at the Golgi apparatus. *Current Opinion in Cell Biology*, **47**, 16–23. <https://doi.org/10.1016/j.ceb.2017.02.003>
- Wittig, I., Braun, H.P., Schägger, H.** (2006). Blue Native PAGE. *Nature Protocols*, **1**, 418–428. doi:10.1038/nprot.2006.62
- Wloka, C., Nishihama, R., Onishi, M., Oh, Y., Hanna, J., Pringle, J. R., Krauß, M., Bi, E.** (2011). Evidence that a septin diffusion barrier is dispensable for cytokinesis in budding yeast. *Biological Chemistry*, **392(8–9)**, 813–829. <https://doi.org/10.1515/BC.2011.083>
- Wolf, Sabrina** (2019). Comparative analysis of unconventional chitinase secretion in *Ustilago maydis* and *Saccharomyces cerevisiae*. *Master thesis*. Heinrich-Heine-Universität Düsseldorf.
- Yachdav, G., Kloppmann, E., Kajan, L., Hecht, M., Goldberg, T., Hamp, T., Hönigschmid, P., Schafferhans, A., Roos, M., Bernhofer, M., Richter, L., Ashkenazy, H., Punta, M., Schlessinger, A., Bromberg, Y., Schneider, R., Vriend, G., Sander, C., Ben-Tal, N., Rost, B.** (2014). PredictProtein - An open resource for online prediction of protein structural and functional features. *Nucleic Acids Research*, **42(W1)**, 337–343. <https://doi.org/10.1093/nar/gku366>
- Yezid, H., Konate, K., Debaisieux, S., Bonhoure, A., Beaumelle, B.** (2009). Mechanism for HIV-1 tat insertion into the endosome membrane. *Journal of Biological Chemistry*, **284(34)**, 22736–22746. <https://doi.org/10.1074/jbc.M109.023705>
- Yin, H. L., Janmey, P. A.** (2003). Phosphoinositide Regulation of the Actin Cytoskeleton. *Annual Review of Physiology*, **65(1)**, 761–789. <https://doi.org/10.1146/annurev.physiol.65.092101.142517>
- Zander, S., Baumann, S., Weidtkamp-Peters, S., Feldbrügge, M.** (2016). Endosomal assembly and transport of heteromeric septin complexes promote septin cytoskeleton formation. *Journal of Cell Science*, **129(14)**, 2778–2792. <https://doi.org/10.1242/jcs.182824>
- Zeitler, M., Steringer, J. P., Möller, H. M., Mayer, M. P., Nickel, W.** (2015). HIV-Tat protein forms phosphoinositide-dependent membrane pores implicated in unconventional protein secretion. *Journal of Biological Chemistry*, **290(36)**, 21976–21984. <https://doi.org/10.1074/jbc.M115.667097>
- Zhang, M., Kenny, S. J., Ge, L., Xu, K., Schekman, R.** (2015). Translocation of interleukin-1 β into a vesicle intermediate in autophagy-mediated secretion. *ELife*, **4**, 1–23. <https://doi.org/10.7554/elife.11205>

Author contributions

Parts of this work were submitted for publication to *Frontiers in Microbiology* on the 9th of April 2020 (Reindl, M., Stock, J., Hussnaetter, K. P., Genc, A., Brachmann, A., Schipper, K. “A novel factor essential for unconventional secretion of chitinase Cts1”). The manuscript is already available on the BioRxiv server since the 2nd of February 2020 (2020.02.07.938613. <https://doi.org/10.1101/2020.02.07.938613>) and thus cited as “Reindl and Stock et al., 2020” in this work. M. Reindl and J. Stock contributed equally to this publication and share the first authorship.

Kerstin Schipper, Janpeter Stock and Michèle Reindl planned the experiments and analyzed results. Aycin Genc performed initial experiments for establishment of the screening strain; Janpeter Stock established the complete screening pipeline, conducted the UV mutagenesis screen and identified mutant candidates. Kai Hussnätter assisted in the laborious screening procedure and generated related figures. Andreas Brachmann performed genome sequencing and supported the evaluation of results. Michèle Reindl conducted cell biological, microscopical and biochemical experiments to characterize Jps1. Kerstin Schipper designed the study and wrote the manuscript with input of all co-authors.

Figures and sections used in this work from the above mentioned submitted manuscript:

Section 1.3: Fig. 1.4 (A/B).

Section 2.2.2: Fig. 2.4, A/B; Fig. 2.5, A-E.

Section 2.2.3: Fig. 2.6, A-E.

Section 2.2.6: Fig. 2.10, B.

This declaration is meant to clarify the use of figures and sections from this submitted manuscript.

Danksagung

Ich möchte mich zunächst bei Michael für die Möglichkeit bedanken, meine Doktorarbeit im Institut für Mikrobiologie schreiben zu dürfen. Außerdem bedanke ich mich für die kontinuierliche wissenschaftliche Unterstützung seit des Bachelorstudiums.

Auch gilt mein Dank Prof. Dr. Lutz Schmitt für die Übernahme des Zweitgutachtens meiner Arbeit.

Zusätzlich möchte ich RabXpress hervorheben: Kerstin, Tina, Peter, Magnus, Kai, Jörn und Marius – ohne euch wäre die Zeit vermutlich nur halb so schön gewesen. Ihr seid so großartige Menschen, die mir stets mit Rat und Tat zur Seite standen. Besonderer Dank gilt Kerstin, die mich seit meiner Bachelorarbeit als Betreuerin und Chefin begleitet und sowohl im wissenschaftlichen Arbeiten als auch im Schreiben geprägt hat. Jeder kann sich glücklich schätzen, dich als Betreuerin zu bekommen.

Nicht zu vergessen sind natürlich auch RabLab und RabAttack, die ebenfalls immer hilfsbereit waren und zu der freundschaftlichen Atmosphäre im Institut beigetragen haben.

Dem Sonderforschungsbereich der DFG 1208 danke ich für die Finanzierung meiner Doktorzeit, zu der lehrreiche und interessante Konferenzen im In- und Ausland zählten. Auch meine Graduiertenschule „MB Train“ hat die vielen gemeinsamen Lectures und aber vor allem die Retreats zu schönen Erlebnissen gemacht, an die ich gern zurückdenke. Die Vernetzung der Institute und Doktoranden untereinander hat es zudem ermöglicht viele neue Methoden für die eigene Forschung verwenden zu können, was ich sehr zu schätzen weiß.

Zu guter Letzt darf auch die Erwähnung meiner Familie und meiner Freunde nicht fehlen, die mir mein Studium ermöglicht haben und mich auch durch schwierige Zeiten treu begleitet haben. Ohne euren Halt und ohne eure Unterstützung wäre der Weg so viel steiniger, ja vielleicht sogar unbesiegbar gewesen.

Curriculum vitae



Personal Data

Last name: Reindl
 Surname: Michèle Sophie
 e-Mail: Michele.Reindl@hhu.de

Education

June 2010	Abitur Mataré grammar school, Meerbusch
October 2010 - October 2013	Bachelor degree program for Biology, Heinrich-Heine-University Düsseldorf
October 2013	Degree B.Sc. Biology: “Steigerung des Expressionslevels der Endochitinase Cts1 zur Optimierung der unkonventionellen Proteinsekretion in <i>Ustilago maydis</i> ” ECTS grade: A
October 2013 - January 2016	Master degree program for Biology, Heinrich-Heine-University Düsseldorf
January 2016	Degree M.Sc. Biology: “Using unconventional secretion for the export of heterologous, cofactor-dependent enzymes in <i>Ustilago maydis</i> ” ECTS grade: A
April 2016 – January 2020	PhD thesis in Biology PhD student of the Collaborative Research Centre 1208 (DFG) Institute for Microbiology, Heinrich-Heine-University Düsseldorf “A novel core factor for unconventional secretion in <i>Ustilago maydis</i> ”

List of publications

Parveen Sarkari, **Michèle Reindl**, Janpeter Stock, Olaf Müller, Regine Kahmann, Michael Feldbrügge, Kerstin Schipper (2014). “Improved expression of single-chain antibodies in *Ustilago maydis*”, *Journal of Biotechnology*, **191**, 165–175.

Elena Geiser, **Michèle Reindl**, Lars M. Blank, Michael Feldbrügge, Nick Wierckx, Kerstin Schipper (2016). “Activating Intrinsic Carbohydrate-Active Enzymes of the Smut Fungus *Ustilago maydis* for the Degradation of Plant Cell Wall Components”, *Applied and Environmental Microbiology* **82(17)**, 5174-5185.

Marius Terfrüchte, **Michèle Reindl**, Silke Jankowski, Michael Feldbrügge and Kerstin Schipper (2017). “Applying Unconventional Secretion in *Ustilago maydis* for the Export of Functional Nanobodies”, *International Journal of Molecular Science*, **18(937)**.

Michèle Reindl, Sebastian Hänsch, Stefanie Weidtkamp-Peters and Kerstin Schipper (2019). „A Potential Lock-Type Mechanism for Unconventional Secretion in Fungi”. *International Journal of Molecular Science*, **20(460)**.

Michèle Reindl, **Janpeter Stock**, Kai P. Hussnaetter, Aycin Genc, Andreas Brachmann and Kerstin Schipper (2020). “A novel factor essential for unconventional secretion of chitinase Cts1”. *Frontiers in Microbiology*, *submitted-in revision*.

Scientific contributions

Unconventional protein secretion, Lecce (Italien) (2016)	Poster
SFB1208, Membrane dynamics, Düsseldorf (2017)	Poster
SFB1208, Membrane dynamics, Kaiserswerth (2018)	Poster
Unconventional protein secretion, Assisi (Italien) (2019)	Poster
VAAM; Leipzig (2020)	Oral presentation

Qualifications

Internship and working experiences

Internship: Bacteriology, Chemisches Veterinär und Untersuchungsamt (CVUA), Krefeld (Nov-Dez,2013)

Student assistant at Institute for Microbiology, HHU Düsseldorf (Feb 2014 – Nov 2015)

GxP

Good scientific practise (GSP) (iGRAD)

Introduction to „Good manufacturing practise (GMP)“, certified

Workshops

Working with GMO (iGRAD)

Presenting in Science (iGRAD)

Basics of Teaching (iGRAD)

Leading competences (medical Research School)

Basics of project management (KUBUS)

Basics of public relations (KUBUS)

Teaching

Supervision of Bachelor and Master thesis

Supervision of Internship from DAAD

Supervision of basic and specialized annually/half-annually Bachelor degree courses

EDV

Office (Word, Excel, PowerPoint, MS Projects)

Clone Manager

CANVAS

ImageJ

MetaMorph

Prism

Languages

German (mother tongue)

English (fluent)

Latin (kleines Latinum)

Spanish (basics)

Interests

Fitness, Triathlon, Long-distance running (Marathon, Half-marathon), Reading, Cooking, Meeting friends